THE DEVELOPMENT OF CHAOTIC OSCILLATOR AND ITS APPLICATION TO SYNCHRONIZATION IN CHAOTIC – MASKING SECURE COMMUNICATION

Sura Larptawee

A Thesis Submitted in Partial Fulfillment of the Requirements
for The Degree of Master of Engineering Program in Engineering Technology
Graduate School
Thai-Nichi Institute of Technology
Academic Year 2012

Thesis Title	The Development of Chaotic Oscillator and Its Application to Synchronization in Chaotic-Masking Secure Communications
By	Sura Larptawee
Faculty	Engineering Technology
Advisor	Dr. Wimol San-um

The Graduate School of Thai-Nichi Institute of Technology has been approved and accepted as partial fulfillment of the requirement for the master's Degree

……..Dean of Graduate school
(Assoc. Prof. Dr. Pichit Sukchareonpong)
Month …….. Date……... Year …….

Thesis Committee

……..Chairman
(Assoc. Prof. Dr. Worapong Tangsrirat)

……..Member
(Asst. Prof. Dr. Warakorn Srichavengsup)

……..Member
(Dr. Thitiporn Lertrasdachakul)

……..Advisor
(Dr. Wimol San-um)

The Development of Chaotic Oscillator and Its Application to Synchronization in Chaotic-Masking Secure Communications

Sura Larptawee

A Thesis submitted in partial fulfillment of the requirements
for The Degree of Master of Engineering Technology
Thai-Nichi Institute of Technology

March 2013

Sura Larptawee: The Development of Chaotic Oscillator and Its Application to Synchronization in Chaotic-Masking Secure Communications. Advisor: Dr. Wimol San-um, 132 pp.

This thesis focuses on three chaotic systems is Rössler attractor using Diode Equation, chaotic jerk attractor and a back-to-back twisted chaotic jerk attractor using Inherent hyperbolic sine function for application to secure communications. Dynamical properties are described base including equilibrium, eigenvalue, Poincare, frequency spectrum, bifurcation, chaotic attractor and chaotic synchronization. This chapter focuses on design of chaotic oscillator and signal masking circuit using Matlab-Simulink for simulation and implement chaotic circuit for secure communication

We can design and implement circuit chaotic oscillator circuit for chaotic masking communication. Be found circuit form Rössler attractor using Diode Equation and a back-to-back twisted chaotic jerk attractor using Inherent hyperbolic sine function are low cost circuit and high stability circuit.

Graduate school Student's signature……

Field of Engineering Technology Advisor's signature……...

Academic Year 2012

Acknowledgements

The author wishes to express his profound gratitude and to respectfully dedicate this work to his parent and family members for their endless encouragements, love and sacrifices. The author is most grateful to his advisor, Dr. Wimol San-Um, for his valuable supervision, supports and encouragements throughout the study. Grateful acknowledgements are also made to Asst. Prof. Dr. Wipawadee Wongsuwan, the director of master of engineering technology program for her supports. In addition, grateful acknowledgements are made to Assoc. Prof. Dr. Worapong Tangsrirat, Asst. Prof. Dr. Warakorn Srichavengsup, Dr. Thitiporn Lertrasdachakul, members of thesis committee, for their valuable suggestions and comments. The author also wishes to acknowledge Thai-Nichi Institute of Technology for a great opportunity of master study and financial supports internships in Japan. The author sincerely appreciates all of his friends in Intelligent Electronic Systems Research laboratory for their friendships and good will.

Sura Larptawee

Table of Contents

Table of Contents (Continued)

Lists of Figures

Lists of Figures (Continued)

Lists of Figures (Continued)

Lists of Figures (Continued)

Lists of Figures (Continued)

Lists of Figures (Continued)

Lists of Table

Chapter 1

Introduction

1.1 Background

Chaos is a phenomenon that occurs in nonlinear dynamical systems. Such deterministic dynamical systems have their origin in Newtonian physics, leading to the systematic development in differential calculus. The "physical laws of nature" in the Newtonian sense propose to model all phenomena by deterministic laws describing the flow of system states [1]. Mathematicians and physicists have sought to understand the world in terms of these deterministic laws, and due to the lack of powerful computation devices, searched for closed form solutions for deterministic dynamical systems. Unfortunately, the existence of closed form solutions is essentially limited to the case of linear dynamical systems. This did, however, not limit the optimism of visionaries conjecturing that, with the knowledge of all "physical laws of nature", predictions about the however remote future of dynamical systems are feasible. In order to scope with the incompleteness of the deterministic description available about a system, the concept of randomness has been introduced to capture all behavior counters the concept of predictability. While a number of important ideas refer to Cardano, Bernoulli and, in particular Gauss and Fermat, there are mainly the results of Kolmogorov in the 1930's [2] that influenced modern probability theory. Another manifestation of randomness comes from statistics, in which by the very nature of the problem, a complete description of the underlying dynamical system is not available.

For the dynamical [3] systems approach, it was Poincare' observed that determinism does not necessarily lead to predictability without limits (though the consequences were not completely understood at his time). Indeed, Poincare' described the intrinsic nature of what has later been called "chaotic behavior", their sensitive dependence on initial conditions. An example is the computer processing evolution of a rather complex dynamical system. Despite the initial optimism it has been found unpredictable over a longer time period. However, this unpredictability need not be linked to complex systems. For the very example of the weather, Loren

found deterministic unpredictability even in a very simplified third order module. a small perturbation of the state of the system would very soon lead to a macroscopically different evolution of the system

In the past years, synchronization of chaotic systems problem has received a great deal of attention among scientists in various fields. As it is well known, the study of the synchronization problem for nonlinear systems has been very important from the nonlinear science point of view, in particular, the applications to biology, medicine, cryptography and secure data transmission. In general, synchronization research has been focused on two areas. The first one relates to the employment of state observers, where the main applications pertain to the synchronization of nonlinear oscillators. The second one is the use of control laws, which allows achieving the synchronization between nonlinear oscillators, with different structure and order. Of particular interest is the connection between the observers for nonlinear systems and chaos synchronization, which is also known as master-slave configuration. Therefore, chaos synchronization problem can be posed as an observer design procedure, where the coupling signal is viewed as output and the slave system is regarded as observer. The general idea for transmitting information via chaotic systems is that, an information signal is embedded in the transmitter system which produces a chaotic signal, the information signal is recovered when the transmitter and the receiver are identical. Since Pecora and Carroll's [1-3] observation on the possibility of synchronizing two chaotic systems, several synchronization schemes have been developed. Synchronization can be classified into mutual synchronization and master slave synchronization.

There are many applications to chaotic communication and chaotic network synchronization. The techniques of chaotic communication can be divided into three categories (1) Chaos masking; the information signal is added directly to the transmitter. (2) Chaos modulation; it is based on the master-slave synchronization, where the information signal is injected into the transmitter as a nonlinear filter. (3) Chaos shift keying; the information signal is supposed to be binary, and it is mapped into the transmitter and the receiver. In these three cases, the information signal can be recovered by a receiver if the transmitter and the receiver are synchronized. In order to reach synchronization, the receiver should be a replica of the transmitter.

1.2 Motivations

Security is an important for communication. Where of two entities are communicating in a way not susceptible to eavesdropping or interception. This is known secure communication. This includes means by which people can share information with varying degrees of certainty that third parties cannot intercept. There have been considerable interests in chaotic communications over the past several years. Synchronization caused great interest in science and technology workers. The research of the application of chaos synchronization in secret communication is the most competitive research fields in recent years. Most of the secure communication system requirements of the signal modulation, as far as possible the regular and has strong anti-interference ability to interpret.

1.3 Statement of Problems and Hypothesis

The synchronization methods have been proposed in a number of the related theories and experiment results. The existing problems encountered includes relatively high decoding errors, slow decoding of receiver processing signals, large size of circuit implementation, which may lead to the application to the communication. Various unseen result were still in which theoretical forms which have not been practically utilized in recent years. Therefore, the chaotic jerk oscillator may be a potential alternative the size and simple synchronization. Feedback reconstruction may lead to an error reduction and also perform a faster synchronization.

1.4 Objectives

1.4.1 To design and implement compact cost-effective chaotic circuits.

1.4.2 To design and implement the chaotic-masking secure communication system.

1.5 Research Scope

1.5.1 Study the dynamical system including chaos theory, nonlinear analysis through the mathematical model such as dynamic equation, time-scaling model, Eigen

value, Eigen-Vector, Jacobian-Matrix and also Stability analysis. Study chaotic indicators such as attractor, time-domain, Poincare' section, Bifurcation, Lyapunov diagram and Kaplan-York dimension [1-3]. The research will also enhance the model of chaotic function by generalizing the form of the chaotic function equation.

1.5.2 Implement chaotic circuit in secure communication systems for simulation and design including chaotic circuit by generalizing the form of the chaotic function equation.

1.5.3 Implement the chaotic-masking secure walky-talky communication system.

1.6 Expected Outcomes

1.6.1 Gain a knowledge Chaos theory and dynamics systems.

1.6.2 Gain knowledge the chaotic circuits and synchronizations in secure communication systems.

1.6.3 Achieve compact cost-effective chaotic oscillator.

1.6.4 Achieve a chaotic-masking secure walky-talky communication system.

Chapter 2

Literature Reviews

2.1 Related Theories

2.1.1 Chaos Theory and Dynamical System

2.1.1.1Definition of Chaos

Chaos is a short word describe a behavior of dynamical [2] systems which appears closely to random, however, the chaotic systems can be rewritten through the set of nonlinear equation systems. Such the chaotic systems appear normally in natural environments. Chaos and randomness are generally due to the chaotic characteristic still confused with the random behavior. Chaos can occur only in nonlinear systems and characterized by a breakdown of predictability known as sensitive dependence on initial conditions which is the most important distinguishing feature of chaos. This implies that even though chaotic systems are deterministic, even the smallest difference in initial state can cause a dramatically difference in the final state. Long term predictability of chaotic systems is impossible since all numerical calculations have a finite non-zero error which will diverge over time and the predictions unreliable. The chaotic behavior contain three majors properties , (1) chaos can occur only in deterministic nonlinear dynamical systems,(2) Chaotic behavior looks complicated and irregular but has an infinite number of unstable periodic patterns embedded in the system and (3) chaotic behavior is sensitive to initial conditions

2.1.1.2 Dynamical System

A dynamical system is one whose state changes in time. If the changes are determined by specific rules, rather than being random. The system is deterministic; otherwise it is stochastic. The changes can occur at discrete time steps or continuously. This book will be concerned with continuous-time, deterministic, dynamical systems since they arguably best approximate the real world. This view

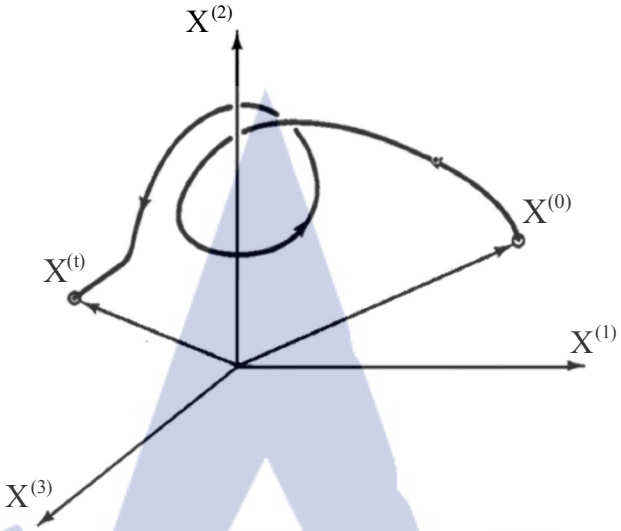

Figure 2.1 An orbit in three-dimension phase space presented by Edward Ott [2].

represents the prejudice of most physical scientists, but it is also the case that chaos is relatively too easy to achieve in discrete-time systems, and hence it is less of a challenge to find elegant examples of chaos in such systems, and those that are found have less apparent relevance to the natural world. Also, discrete-time systems have already been extensively explored, in part because they are more computationally tractable. Stochastic systems mimic many of the features of chaos, but they are not chaotic because chaos is a property of deterministic systems. Furthermore, introducing randomness into a dynamical model is a way of admitting ignorance of the underlying process and obtaining plausible behavior without a deep understanding of its cause.

A dynamical system may be defined as a deterministic mathematical prescription for evolving the state of system forward in time. Time here either may be a continuous variable, or else it may be discrete integer-valued variable. An example of a dynamic system in which time (denoted t) is a continuous variable is a system of N first-order, autonomous, ordinary differential equation,

$$\left.\begin{aligned} dx^{(1)}/dt &= F_1(x^{(1)}, x^{(2)}, \ldots, x^{(N)}, \\ dx^{(3)}/dt &= F_1(x^{(1)}, x^{(2)}, \ldots, x^{(N)}, \\ &\vdots \\ dx^{(N)}/dt &= F_1(x^{(1)}, x^{(2)}, \ldots, x^{(N)}, \end{aligned}\right\} \tag{2.1}$$

Which we shall often write in vector form as

$$dx(t)/dt = F[x(t)] \tag{2.2}$$

where x is an N-dimensional vector. This is a dynamical system because, for any initial state of the system x(0), we can in principle solve the equations to obtain the future system state x(t) for t>0. Figure 2.1 shows the path followed by the system state as it evolve with time in a case where N=3. The space ($x^{(1)}$, $x^{(2)}$, $x^{(3)}$) in the figure is referred to as phase space, and the path in phase space followed by the system as it evolves with time is referred to as an orbit or trajectory. Also, it is common to refer to a continuous time dynamical system as a flow.

In the case of discrete, integer-valued time (with n denoting the time variable, n = 0, 1, 2…), an example of a dynamical system is a map, which we write in vector form as

$$x_{n+1} = M(X_n), \tag{2.3}$$

Where x_n is N – dimensional, $x^n = (x^{(1)}, x^{(2)}, \ldots, x^{(N)})$. Given an initial state x_0, we obtain the state at time n = 1 by $x_n = M(x_0)$. Having determinedx_1, we can then determine the state at n=2 by $x_{n2} = M(x_1)$, and so on. Thus, given an initial condition x_0, we generate an orbit (or trajectory) of the discrete time system: $x_0, x_1, \ldots, x_N$As we shall see, a continuous time map of dimensionality N can often

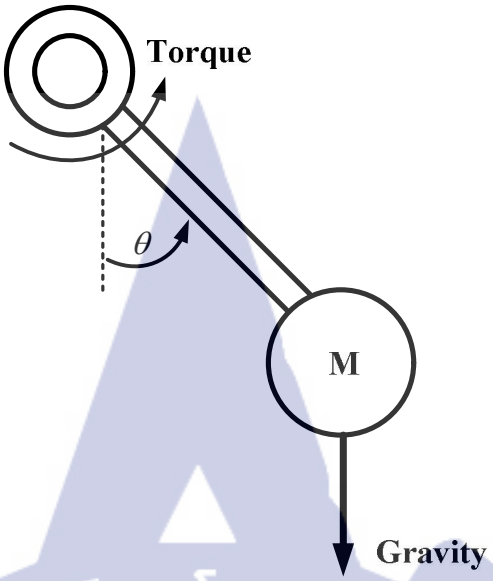

Figure 2.2 Forced, damped pendulum presented by Edward Ott [2].

profitably be reduced to a discrete time map of dimensionality $N-1$ via the Poincaré of section Technique. It is reasonable to conjecture that the complexity of the possible structure of orbits can be greater for larger system dimensionality. Thus, a natural question is how larger does N have to be in order for chaos to be possible. For the case of N first-order autonomous ordinary differential equations, the answer is that N>3 is sufficient. Thus, if one is given an autonomous first-order system with N=2, chaos can be ruled out immediately. Consider the forced damped pendulum equation. As shown in Figure 2.2.

$$\frac{d^2\theta}{dt^2} + v\frac{d\theta}{dt} + \sin\theta = T\sin(2\pi ft) \tag{2.4}$$

where the first term represents inertia, the second, friction at the pivot, the third, gravity, and the term on the right-hand side represents a sinusoidal torque applied at the pivot. (This equation also describes the behavior of a simple Josephson junction

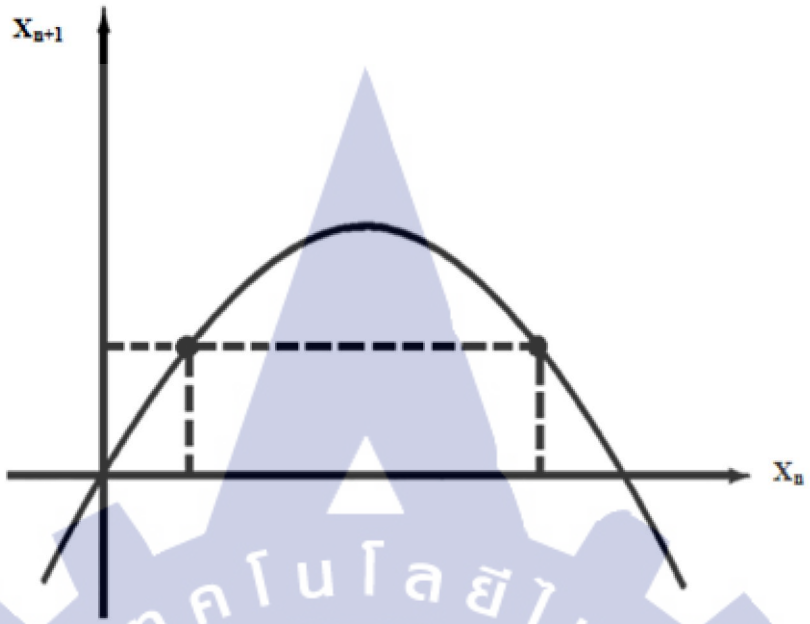

Figure 2.3 Noninvertibility of the logistic map presented by Edward Ott [2].

circuit.) We ask: is chaos rule out for the equation (which is second-order and no autonomous) into first-order autonomous form by the substitution.

$$x^{(1)} = d\theta / dt,\ x^{(2)} = \theta, \qquad (2.5)$$
$$x^{(3)} = 2\pi ft.$$

(Note that, since $x^{(1)}$ both $x^{(2)}$and appear in Eq. (2.5) as the argument of a sine function, they can be regarded as angles an may, if desired, be defined to lie between 0 and 2π.) The driven damped pendulum equation then yields the following first-order autonomous system.

$$\begin{aligned} dx^{(1)} / dt &= T \sin x^{(3)} - \sin x^{(2)} - vx^{(1)} \\ dx^{(3)} / dt &= x^{(1)} \\ dx^{(N)} / dt &= 2\pi f \end{aligned} \qquad (2.6)$$

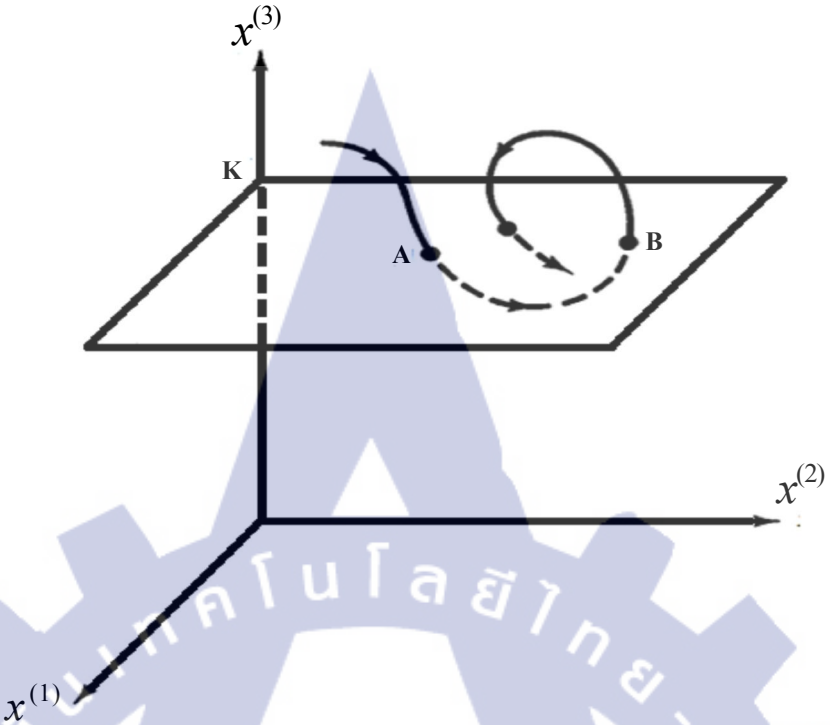

Figure 2.4 A Poincare surface of section presented by Edward Ott [2].

Since $N = 3$, chaos is not ruled out. Indeed, numerical solution shows that both chaotic and periodic solution of the driven damped pendulum equation is possible depending on the particular choice of system parameters v, T and f. We now consider the equation of the required dimensionality for chaos for the case of maps. In this case, we must distinguish between invertible and noninvertible maps. We say the map M is invertible if, given x_{n+1}we can solve x_{n+1}=M(x_n)uniquely for x_n. If this is so, we denote the solution for x_n as

$$x_n = M^{-1}(x_{n+1}) \tag{2.7}$$

and we call$M^{-1}$the inverse of M. For example, consider the one-dimensional ($N = 1$) map,

$$M(x) = rx(1-x) \tag{2.8}$$

which is commonly called the “logistic map”. As show in Figure 2.3, this map is not invertible because for a given x_{n+1} there are two possible values of x_n from which it could have come. On the other hand, consider the two-dimensional map,

$$\begin{aligned} x_{n+1}^{(1)} &= f(x_n^{(1)}) - Jx_n^{(2)}, \\ x_{n+1}^{(1)} &= x_n^{(1)}. \end{aligned} \tag{2.9}$$

This map is clearly invertible as long as $J \neq 0$

$$\begin{aligned} x_n^{(1)} &= x_{n+1}^{(2)}, \\ x_n^{(2)} &= j^{-1}[f(x_{n+1}^{(2)}) - x_{n+1}^{(1)}. \end{aligned} \tag{2.10}$$

We can now state the dimensionality on maps. If the map is invertible, then there can be no chaos unless for N>2. If the map is noninvertible, chaos is possible even in one-dimensional maps. Indeed, the logistic map Equation (2.8) exhibits chaos for large enough r.

It is often useful to reduce a continuous time system (or “flow”) to a discrete time map by a technique called the poincaré surface of section method. We consider N first-order autonomous ordinary differential Equation (2.1). The “poincaré map” represents a reduction of the N-dimensional surface flow to an (N-1)-dimensional map. For illustrative purposes, we take N=3 and illustrate the construction in Figure 2.4. Consider a solution of Equation (2.1). Now, choose some appropriate (N-1)-dimensional surface (the “surface of section”) in the n-dimension phase space, and observe the intersection of the orbit with the surface. In Figure 2.4, the surface of section is the plane $x^{(3)} = K$ but we emphasize that in general the choice of the intersections of the orbit with the surface can be tailored in a convenient way to the particular problem. Point A and B represent two successive crossing of the surface of section. Point A uniquely determines point B, because A can be used as an initial condition in (2.1) to determine B. Likewise, B uniquely determines A by reversing time in (2.1) and using B as the initial condition. Thus, the Poincaré map in this illustration represents an invertible two-dimension map transforming the coordinates

$(x_n^{(1)}, x_n^{(2)})$ of the n th piercing of the surface of section to the coordinates $(x_{n+1}^{(1)}, x_{n+1}^{(2)})$ at piercing n+1 This equivalence of an N-dimensional flow with an (N-1)-dimension invertible map show that the requirements Equation (2.11) for chaos in a map follow from Equation (2.4) for chaos in flow.

Another way to create a map form the flow generate by the system of autonomous differential equations (2.2) is to sample the flow at discrete time st_n =t_0 + *nT(n=1,2…)*,where the sampling interval T can be chosen on the basis of convenience. Thus, a continuous time trajectory x(t)yields a discrete time trajectory x_n= x (t_n).The quantity $x_{n+1}$is uniquely determined form x_n since we can use x_n as an initial condition in Eq. (2.2) and integrate the equations forward for an amount of time T to determinex_{n+1}. Thus, in principle, we have a mapx_{n+1} = M (x_n). We call this map the time T map is invisible (like the Poincare map), since the differential equation (2.2) can be integrated backward in time. Unlike the Poincare map, the dimensionality of the time T map is the same as that of the flow.

2.1.1.3 Attractor

In Hamiltonian systems such as arise in Newton's Equations for the motion of particles friction; there are choices of the phase space variables (e.g., the canonically conjugate position and momentum variables) such that phase space volumes are preserved under the time evolution. That is, if we choose an initial (t=0) closed (N-1)-dimensional surface S_0 in the N-dimensional x-phase space, and then evolve each point on the surface S_0forward in time by using them as initial condition in Eq. (2.2), then the closed surface S_0evolves to a closed surface S_1at some later time t, and the N-dimensional volumes V (0) of the region enclosed by$S_0$and V (t) of the region enclosed by S_t are the same, V (t) = V (0). We all such a volume preserving system conservative. On the other hand, if the flow does not preserve volumes, and cannot be made to do so by a change of variables, then we say that the system is non-conservative. By the divergence theorem, we have that

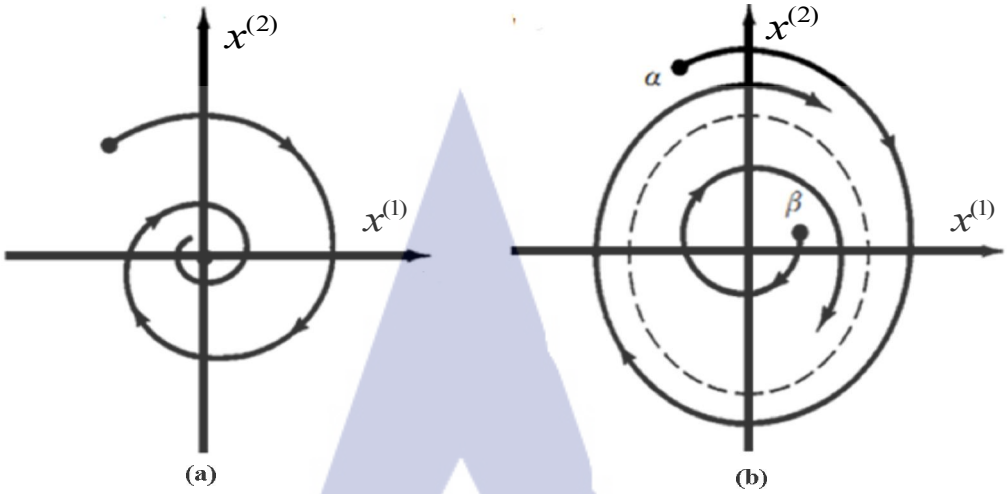

Figure 2.5 (a) The attractor is the point at original.(b) The attractor is the closed dashed curve presented by Edward Ott [2].

$$dV(t)/dt = \int_{S_t} \nabla \cdot F d^N x, \tag{2.11}$$

where signifies the integral over that volumes interior to the surface S_1, and.$\nabla \cdot \mathrm{F} \equiv \sum_{i=1}^{N} \partial \mathrm{F_i}(\mathrm{x}^{(1)}, \ldots, \mathrm{x}^{(N)}) \partial \mathrm{x}^{(i)}$ For example, for the forced damped pendulum equation written in first-order autonomous form, Eq. (2.5b), we have that $\nabla \cdot F = -v$, which is independent of the phase space position x and is negative. Form (2.11), we have$\partial \mathrm{v}(\mathrm{t})/\mathrm{dt} = -\mathrm{vV}(\mathrm{t})$ so that V decreases exponentially with time, $\mathrm{V}(\mathrm{t}) = \exp(\mathrm{vt})\,\mathrm{V}(0)$. In general$\nabla \cdot$ Fwill be a function of phase space position x. If $\nabla \cdot \mathrm{F} < 0$ in some region of phase space (signifying volume contraction in the region), then we shall refer to the system as a dissipative system. It is an important concept in dynamics that dissipative systems typically are characterized by the presence of attracting sets or attractors in the phase space. These are bounded subsets to which regions of initial condition of nonzero phase space volume asymptote as time increases. (Conservation dynamical systems do not have attractor; see the discussion of the Poincaré recurrence theorem)

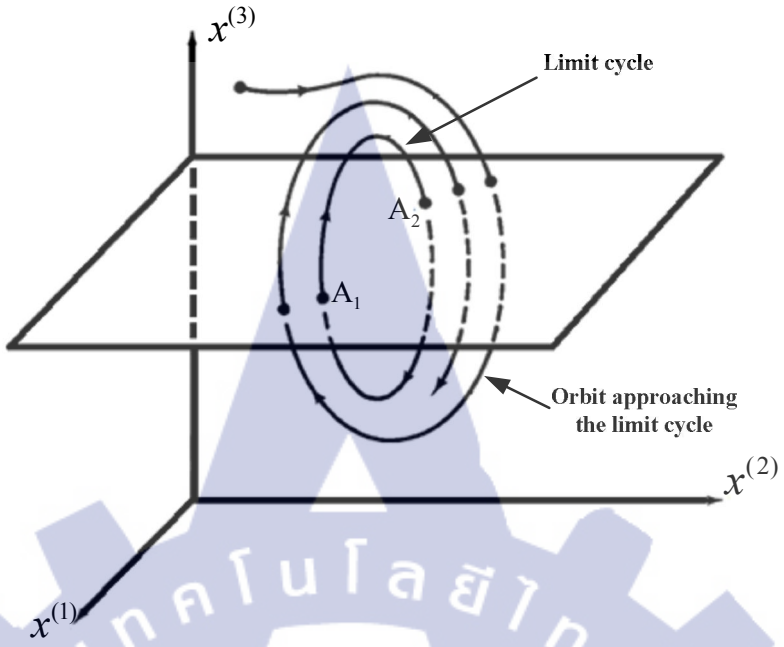

Figure 2.6 Surface of section for a three-dimensional flow with a limit cycle presented by Edward Ott [2].

As an example of an attractor, consider the damped harmonic oscillator, $d^2y/dt^2 + vdy/dt + \omega^2 y = 0$ .A typical trajectory in the phase space ($x^{(t)} = y, x^{(2)} = dy/dt$) is show in Figure 2.5(a). We see that, as time goes on, the orbit spirals into the origin, and this true for any initial condition. Thus, in this case the origin, $x^{(1)} = x^{(2)} = 0$, is said to be the "attractor" of the dynamical system. As a second example, Figure 2.5(b) shows the case of a limit cycle (the dashed curve). The initial condition (labeled α) outside the limit cycle yields an orbit which, with time, spirals into the closed dashed curve on which it circulates in periodic motion in the $t \to +\infty$ limit. Similarly, the initial condition (labeled β) inside the limit cycle yields an orbit which spirals outward, asymptotically approaching the dashed curve. Thus, in this case the dashes closed curve is the attractor. An Example of an equation displaying a limit cycle attractor as illustrate in Figure 2.5(b) is the van der Pol Equation,

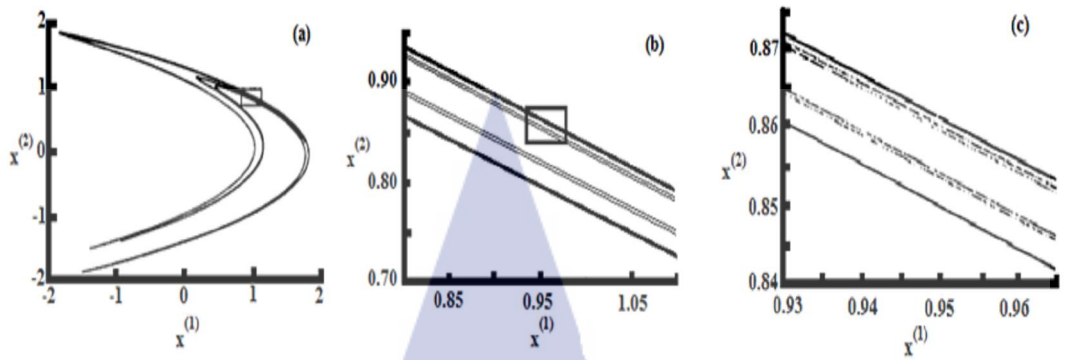

Figure 2.7(a) The Hénon attractor.(b) Enlargement of region defined by the rectangle in (a).(c) Enlargement of region defined by the rectangle in (b) presented by Grebogi et al. [3].

$$\frac{d^2y}{dt^2} + (y^2 - \eta)\frac{dy}{dt} + \omega^2 y = 0 \tag{2.12}$$

This equation was introduced in the 1920 as a model for a simple vacuum tube oscillator circuit. One can speak of conservative and dissipative maps. A conservative N-dimensional map is one which preserves N-dimensional phase space volumes on each iterate (or else can be made to do so by a suitable change of variables). A map is volume preserving if the magnitude of the determinant of its Jacobian matrix of partial derivatives is one,

$$J(x) \equiv \left|\det[\partial M(x)/\partial x\right| = 1 \tag{2.13}$$

For example, for a continuous time Hamiltonian system, a surface of section formed by setting one of the N canonically conjugate variables equal to a constant can be shown to yield a volumes preserving map in the remaining N-1 canonically conjugate variables. On the other hand, if $J(x) < 1$ in some regions, then we say the map is dissipative and, as for flows, typically it can have attractor. For example, Figure 2.6 illustrates the Poincare surface of section map for a three-dimensional flow with a limit cycle. We see that for the map, the two points $A_1$and A_2 together constitute the attractor. That is, the orbit of the two-dimensional surface of section map

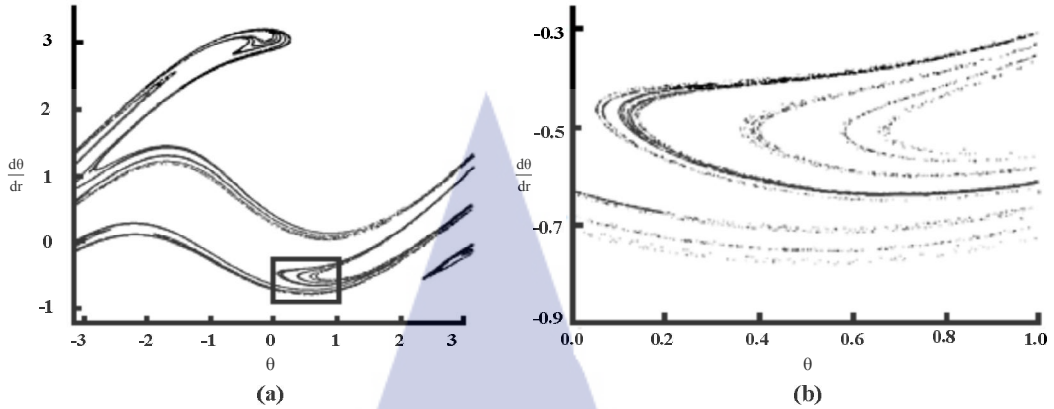

Figure 2.8 The attractor of the forced damped pendulum equation in the surface of section $x^{(3)}$ modulo $2\pi = 0$ presented by Grebogi et al. [3].

$x_{n+1} = M(x_n)$ yields a sequence $x_1, x_2, \ldots$ which converges to the set consisting of the two points A_1 and A_2, between which the map orbit sequentially alternates in the limit $n \to +\infty$.

In Figure 2.5, we have two examples, one in which the attractor of a continuous time system is a set of dimension zero (single point) and one in which the attractor is a set of dimension one (a closed curve). In Figure 2.6, the attractor of the map has dimension zero (it is the two points, A_1 and A_2). It is a characteristic of chaotic dynamic that the resulting attractors often have a much more intricate geometrical structure in the phase space than do the examples of attractors cited above. In fact, according to a standard definition of dimension, these attractors commonly have a value for this dimension which is not an integer. In the terminology of Mandelbrot, such geometrical objects are fractals. When an attractor, consider the attractor obtained for the two-dimensional Hénon map,

$$\left.\begin{aligned} x_{n+1}^{(1)} &= A - (x_n^{(1)})^2 + Bx_n^{(2)} \\ x_{n+1}^{(2)} &= x_n^{(1)} \end{aligned}\right\} \qquad (2.14)$$

For A=1.4 and B=0.3. See Hénon (1976). Note that Equation (2.14) is in the form of Equation (2.9). Figure 2.6 (a) shows the results of plotting 10^4 successive points obtained by Equation (2.14) with the initial transient before the orbit settles into the

attractor deleted. The result is essentially a picture of the attractor. Figure 2.7 (b) shows that a blow-up of the rectangle in Figure 2.7 (a) reveals that the attractor apparently has a local small-scale structure consisting of a number of parallel lines. A blow-up of the rectangle in Figure 2.7 (b) is show in Figure 2.7 (c) and reveals more lines. Continuation of this blow-up procedure would show the attractor has similar structure on arbitrarily small scale. In fact, roughly speaking, we can regard the attractor in Figure 2.7 (b) as consisting of an uncountable infinity of lines. Numerical computations show that the fractal dimension D_0 of the attractor in Figure 2.7 is a number between one and two, $D_0 \approx 1.26$. Hence, this appears to be an example of a strange attractor.

As another example of a strange attractor, consider the forced damped pendulum Equation 2.5 and Figure 2.2) with $v = 0.22$, $T = 2.7$ and $f = 1/2\pi$. Treating $x^{(3)}$ as an angle in phase space, we define

$$\bar{x}^{(3)} = x^{(3)} \text{modulo} 2\pi \tag{2.15}$$

and choose a surface of section $\bar{x}^{(3)} = 0$. The modulo operation is defined as

$$\text{y modulo K} \equiv \text{y} + \text{pK} \tag{2.16}$$

where p is a positive or negative integer chose to make $0 \le y + pK < K$. The surface of section $\bar{x}^{(3)} = 0$ is crossed at the times $t = 0, 2\pi, 4\pi, 6\pi, \ldots$ (This type of surface of section for a periodically forced system is often referred to as a stroboscopic surface of section, since it shows the system state at successive "snapshots" of the system at evenly spaced time intervals.) As seen in Figure 2.8(a) and in the blow-up of the rectangle Figure 2.8(b), the attractor again apparently consists of a number of parallel curves. The fractal dimension of the intersection of the attractor with the surface on section in this case is approximately 1.38. Correspondingly, if one considers the attracting set in the full three-dimensional phase space, it has a dimension 2.38(i.e., one greater than its intersection with the surface of section).

2.1.2. Chaotic-Based Communication

2.1.2.1 Schemes requiring for chaos synchronizations.

A large number of communication schemes that are based on chaos synchronization have been proposed during the last two decades. In this section, the phenomena of chaos synchronization will be discussed. There are many interpretations and definitions of the synchronization term. Several forms of synchronization have been proposed for the chaotic systems. A typical and most widely-used scenario of the chaotic synchronization is identical synchronization, where the state of response system converges asymptotically to the state of the drive system. Recently, two forms of synchronization, called phase synchronization and generalized synchronization have been introduced.

Identical synchronization: Two continuous-time chaotically systems given as

$$\frac{dx}{dt} = F(x) \tag{2.17}$$

$$\frac{dx'}{dt} = F(x') \tag{2.18}$$

are said to synchronize identically if $\lim_{t\to\infty}\|x'(t) - x(t)\| = 0$ For any combination of initial states $x(0)$ and $x'(0)$. From a communication point of view, we may think of system (2.17) as the transmitter and system (2.18) as the receiver. If the same initial condition is chosen for the transmitter and the receiver, i.e. $x(0) = x'(0)$, the both systems will evolve in a synchrony in the sense that, $x'(t)$ will continue being equal to $x(t)$ for all $t > 0$. The signal $s_t(t)$ which is transmitted by a communication channel is a linear combination of basic functions $g_i(t)$. We consider the case when only one basis function $g(t)$ is used and we assume that $s_i(t) \equiv g(t)$. At the receiver side, we must recover the scalar basis function $g(t) = H(x(t))$ which has been derived from the state of the drive system (2.17). The basis function $g(t)$ can be recovered by synchronizing the state of the response system identically with the drive system and applying the

same function $H(\cdot)$. In particular, if $x'(t)$ can be made to converge to $x(t)$ then the estimation $\hat{g}(t) = H(x'(t))$ will converge to $g(t)$

Phase synchronization: This scenario of the synchronization of two coupled systems occurs if the difference $|\varphi'(t) - \varphi(t)|$ between the "phases" of the two systems is bounded by a constant, where the "phases" $\varphi(t)$ is some monotonically increasing function of time suitably chosen.

Generalized synchronization: This type of synchronization occurs mainly when the coupled chaotic systems are different, although it has also been used between identical chaotic systems. Chaotic systems (2.17)and (2.18) are said to exhibit generalized synchronization if there exists transformation Φ such that $\lim_{t\to\infty}\|x'(t) - \Phi(x(t))\| = 0$ where the properties of the transformation Φ are independent of the initial conditions $x(0)$ and $x'(0)$. If the transformation Φ is invertible, then $\hat{g}(t) = H(\Phi^{-1}(x'(t)))$ approaches $g(t)$. Identical synchronization is the particular case of generalized synchronization when Φ. is the identity. A complete overview of generalized synchronization is given by K. Pyragas in. In some cases the unauthorized receiver can use a receiver with dynamics that is different from the dynamics of the transmitter, and decode the message using generalized synchronization between transmitter and receiver with different parameters. The use of generalized

2.1.2.2 Chaotic masking

Communication schemes that are based on chaos synchronization and chaotic masking of the chaotic signal with a message and illustrated in Figure 2.9. In chaotic masking communication schemes a message signal is added to a chaotic signal generated by the transmitter dynamics and the sum of the two is transmitted. At the receiver which is synchronized to the transmitter the chaotic component is

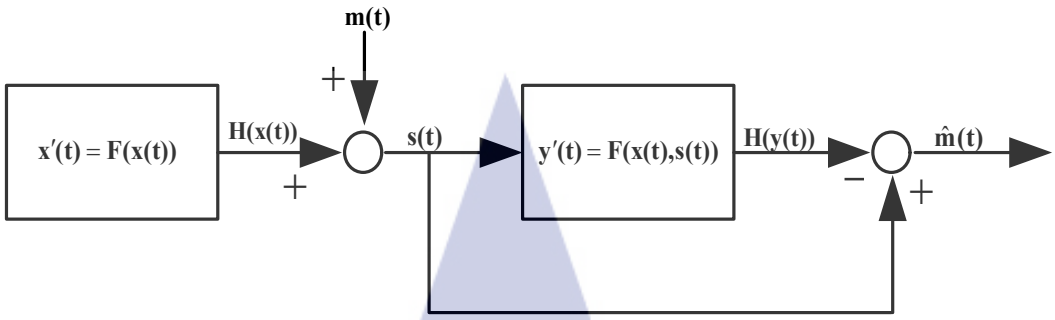

Figure 2.9 Chaotic communication schemes based on chaos synchronization and chaotic masking of a message with a chaotic component presented by Volodymyr Lynnyk [4].

subtracted from the received signal to recover the original transmitted message. In Figure 2.9 the transmitter state evolution is given by the chaotic dynamics The transmitter state x(t) synchronizes to the receiver state y(t). A scalar H(x(t)) is calculated from the transmitter state x(t). A message m(t) is added to the chaotic scalar, and the sum of the two is transmitted. At the receiver the message m(t) is reconstructed by subtracting the chaotic scalar H(y(t)) from the received signal s(t). The message magnitude |m(t)| has to be kept small compared to the chaotic scalar H(x(t)) in order to maintain synchronization between transmitter and receiver(Prague, 2010).

$$\frac{dx}{dt} = F(x(t)) \tag{2.19}$$

A chaotic scalar H(x(t)) which is a function of the transmitter state x(t)is added to the message m(t). The transmitted signal s(t) is governed by

$$s(t) = H(x(t)) + m(t) \tag{2.20}$$

The evolution of the receiver state y(t) dynamics is given by the dynamics

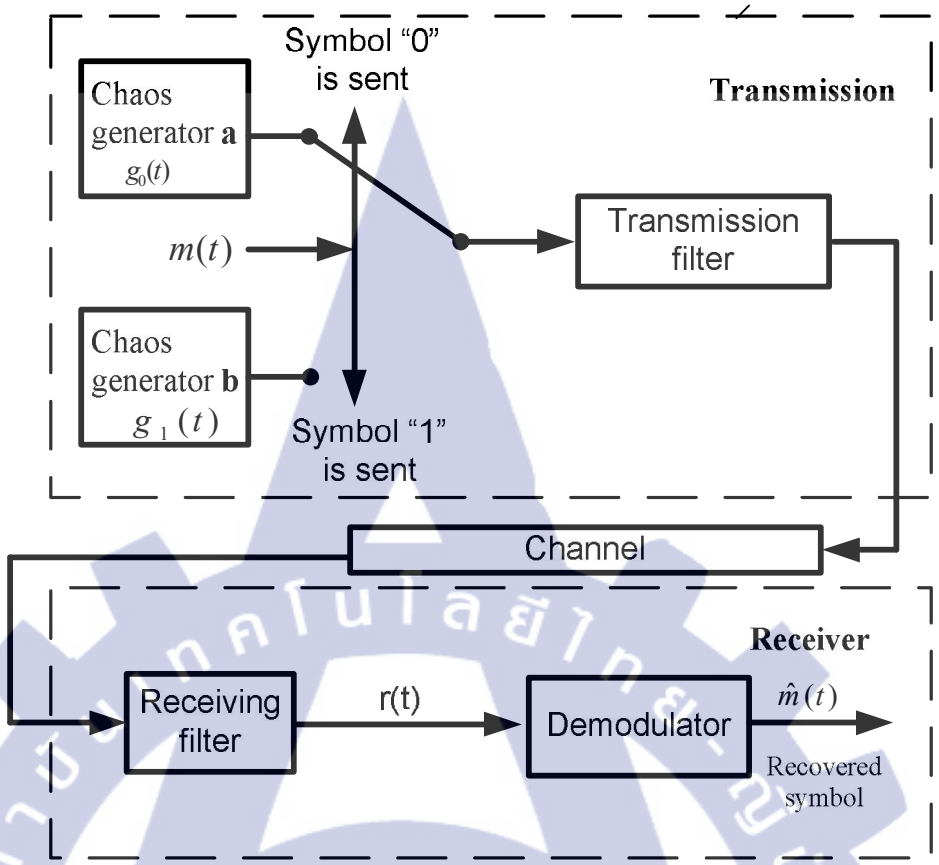

Figure 2.10 Binary chaos shifts keying digital communication system presented by Volodymyr Lynnyk [4].

$$\frac{dy}{dt} = F(y(t), s(t)) \tag{2.21}$$

The transmitter state x(t) synchronizes to the receiver state y(t) at the rate of the largest Lyapunov exponent λ, so that

$$|y(t) - x(t)| \approx e^{\lambda t} \tag{2.22}$$

At the receiver, the estimation $\hat{m}(t)$ for the message m(t) is calculated by subtracting the estimation H(y(t)) of the chaotic component H(x(t)) that was added to the message at the transmitter:

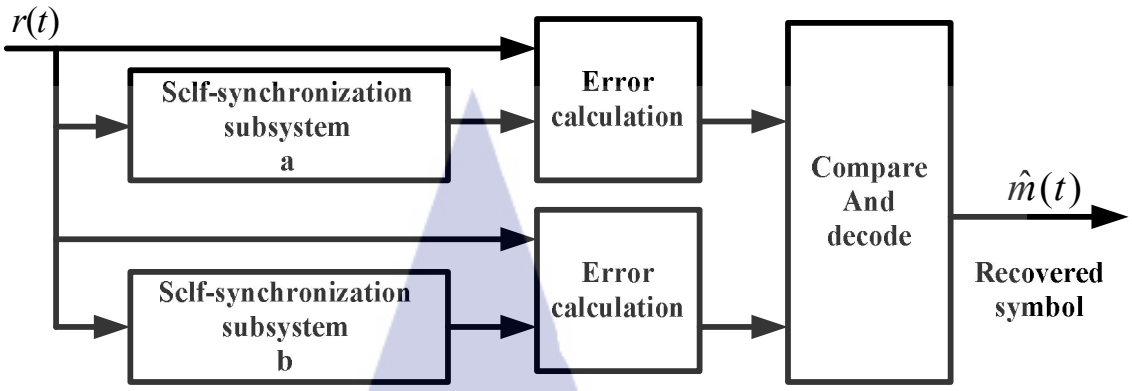

Figure 2.11 Synchronization-error-based CSK demodulator presented by Volodymyr Lynnyk [4].

$$\hat{m}(t) = s(t) - H(y(t)) \tag{2.23}$$

The addition of a message signal m(t) to the chaotic scalar H(x(t)) at the transmitter can degrade the quality of the synchronization between the transmitter and the receiver. It is assumed that for masking, the power level of massage m(t) is significantly lower than that of H(x(t)) added to the message:

$$|m(t)| << |H(x(t))| \tag{2.24}$$

2.1.2.3 Chaos Shift Keying

Chaos shift keying communication scheme, often termed as parameter modulation scheme and illustrated in Figure 2.10. In CSK the transmitter dynamics is dissipative and chaotic and the transmitter state trajectory converges to a strange attractor. A message is transmitted by changing one or more parameters of the transmitter dynamics which results in a change of the attractor dynamics. At the receiver the message is decoded by estimating to which message the received chaotic attractor corresponds. The fundamental principle of the CSK can be described in a more detail as follows. The transmitter consists of M chaos generators. In the case, when we use a binary alphabet, only two chaos generators are needed. The Figure

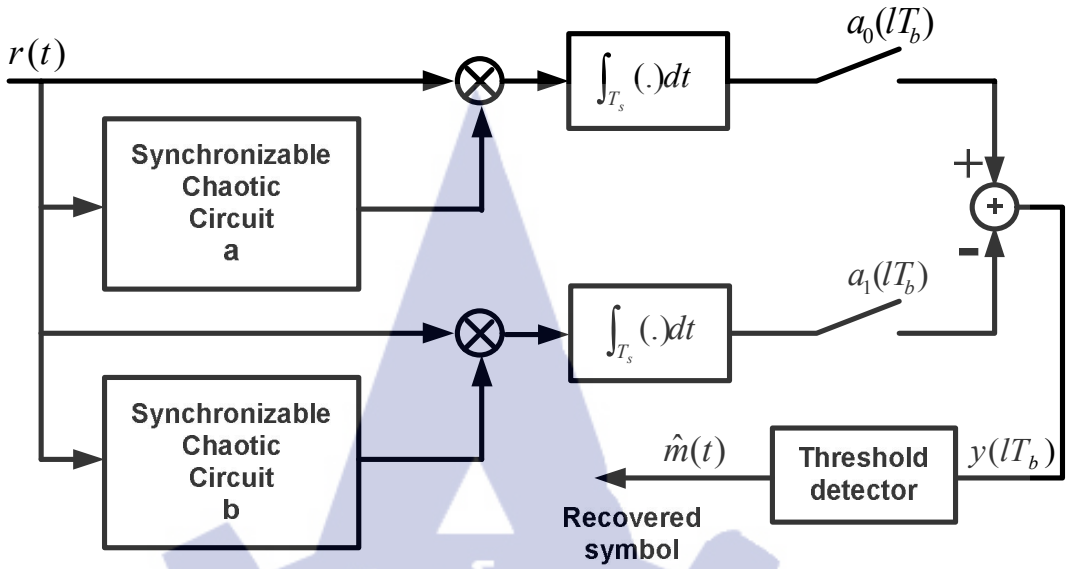

Figure 2.12 Block diagram of coherent correlation CSK receiver presented by Volodymyr Lynnyk [4].

2.10, the transmitter consists of two chaos generators a and b, producing signals $g_0(t)$ and $g_1(t)$, respectively. If a binary symbol "0"isto be sent during the interval *[(l –1)T_b, lT_b]*, g_0 is transmitted by the communication channel, and if the binary symbol "1" is to be sent, *g1* is transmitted. Here, Tb is the bit duration and l is a number of the transmitted symbol. The CSK scheme is based on the self-synchronization property of the chaotic systems. In the Figure 2.11 the receiver structure based on the Self-synchronization property is shown. The incoming signal r(t) is used for drive two self-synchronization subsystems a and b, which are matched to a and b chaos generators, respectively. When the transmitted signal is$g_o(t)$, the subsystem a will be synchronized with the incoming signal while is not, and when the transmitted signal is $g_1(t)$, the subsystem b will be synchronized with the incoming signal. Therefore, by measuring the error between the incoming signal and the output of the self-synchronization subsystems, the transmitted symbol can be recovered. In other words, the receiver needs to determine to which of the allowed attractors the transmitter dynamics converged, based on the received signal r(t). The transmitted signal s(t) is typically a scalar, while the transmitter dynamics can be of high dimension. The

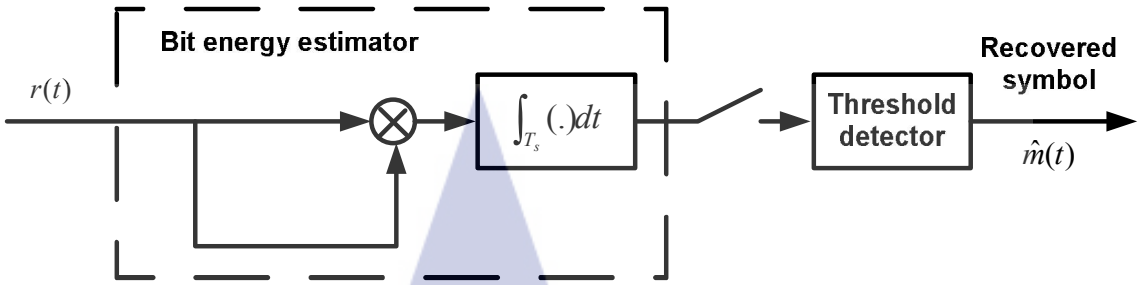

Figure 2.13 CSK receiver based on bit energy estimator presented by Volodymyr Lynnyk [4].

transmitter can use coherent detection techniques. In other words, the receiver needs to determine to which of the allowed attractors the transmitter dynamics converged, based on the received signal r(t). The transmitted signal s(t) is 3typically a scalar, while the transmitter dynamics can be of high dimension. The transmitter can use coherent detection techniques

First, the Coherent detection is investigated. In communication the term coherent detection implies that the shape of the transmitted waveforms is known to the receiver which can correlate the noisy received signal with its expected waveform, to maximize the signal to noise ratio at the output of the correlator. Coherent detection of the chaotic signals using correlator-based receivers was studied in detail. Receivers in which exact copies of all basis functions are known are called coherent receivers. The block diagram of a correlator-based receiver using binary chaos shift keying modulation is shown in the Figure 2.12.The two synchronizable chaotic circuits in the receiver attempt to reproduce the two basic functions, given the received noisy sample function r(t). An acquisition time T_s is assumed for the synchronization circuits to lock to the incoming signal. The recovered basis functions are then correlated with the received signal for the remainder of the bit duration T_b. Then, the outputs of the correlator are sampled and compared.

In the case of non-coherent demodulation the receiver does not know the shape of the transmitted chaotic basis signals. Detection has to be done based on some distinguishable property of the basis signals. Different attractors may differ in variance, meaning of the absolute value, dynamic range, and many other statistical

properties. The main advantage in the using of the non-coherent decoding methods is that the receiver is not required to synchronize with the transmitter. It only needs to determine to which one of the allowed attractors the trajectory has converged. In addition, the non-coherent receivers are often simpler than their coherent counterparts. Suppose chaotic basis signals with different bit energies are used to transmit the binary information. If a binary "0" is to be sent during the interval T_b, a chaotic basis signal $g_0(t)$ with mean bit energy E_0 is transmitted, and if binary "1" is to be sent, a chaotic basis signal $g_1(t)$ with mean bit energy E_1 is transmitted. The required chaotic signals can be generated by two chaos generators with different average bit energies. As alternative, the same chaos generator can be used to produce two signals of different bit energies by using two amplifiers of different gain. In both cases, the bit energy can be estimated by a correlator at the receiver, as shown in Fig. 2.13. Assume that only additive noise corrupts the transmitted signal and the noise power limited by the receiving filter,i.e.,

$$r(t) = s(t) + n'(t) \tag{2.25}$$

Where, s(t) denotes the transmitted signal and n′(t) is the noise component at the output of the receiving filter. For the *lth* received symbol, the energy bit $E_s(lT_b)$, is defined by

$$E_s(lT_b) = \int_{(l-1)T_b}^{lT_b} r^2(t)dt = 2\int_{(l-1)T_b}^{lT_b} s(t)n'(t)dt + \int_{(l-1)T_b}^{lT_b} [n'(t)]^2 dt \tag{2.26}$$

In the noise-free case, the second and third integrals in (2.24) are zero. Therefore, $E_s(lT_b)$ is equal to either one of the following two bit energies:

$$\begin{aligned} E_s^0(lT_b) &= \int_{(l-1)T_b}^{lT_b} g_0^2(t)dt \\ E_s^1(lT_b) &= \int_{(l-1)T_b}^{lT_b} g_1^2(t)dt \end{aligned} \tag{2.27}$$

In convectional modulation schemes, the bit energy is fixed for a given symbol.

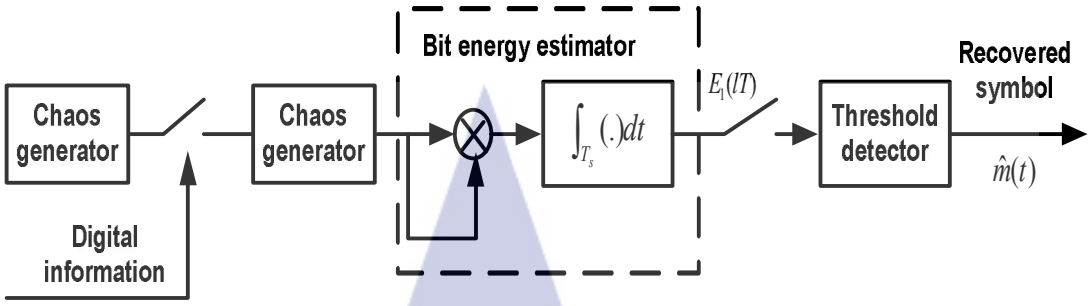

Figure 2.14 Block diagram of non-coherent COOK modulation scheme presented by Volodymyr Lynnyk [4].

2.1.2.4Chaos-On-Off-Keying

Chaos-on-off-keying (COOK) is only a special case of the chaos shift keying scheme (CSK) with non-coherent demodulator. It uses one chaos generator, which is switched “on” or “off” to transmit symbols ”1” and”0”, respectively, as shown in Fig.

2.14. The major disadvantage of the CSK system is that the threshold value of the decision circuit depends on the noise level also appears in COOK. This means that using COOK wean maximize the distance between the elements of the signal set, but the threshold level required by the decision circuit depends on the noise level. The threshold can be kept constant by applying the differential chaos shift-keying method.

2.1.2.5 Differential Chaos Shift Keying

In differential chaos shift keying scheme, every bit to be transmitted is represented by two chaotic sample functions. The first sample function serves as a reference while the second one carries the information. Bit “1” is sent by a chaos generator twice in succession, while for bit “0”, the reference chaotic signal is transmitted, followed by an inverted copy of the same signal. Thus for the *lth* symbol period, we have

$$s(t) = \begin{cases} g(t), \text{ for}(l-1)T_b \le t \le (l-1/2)T_b \\ g(t - T_b/2), \text{ for}(l-1/2)T_b \le t \le lT_b \end{cases} \quad (2.28)$$

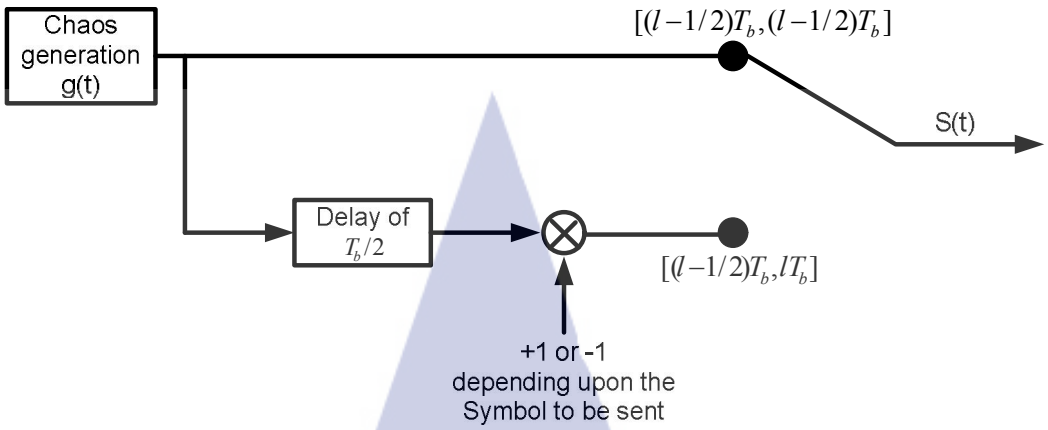

Figure 2.15 Block diagram of differential chaos shift keying modulator scheme presented by Volodymyr Lynnyk [4].

if "1" is to be transmitted, and

$$s(t) = \begin{cases} g(t), \text{ for}(l-1)T_b \le t \le (l-1/2)T_b \\ -g(t-T_b/2), \text{ for}(l-1/2)T_b \le t \le lT_b \end{cases} \quad (2.29)$$

if "0" is to be sent. Fig. 2.15 shows a block diagram of a DCSK transmitter. Since each bit is mapped to the correlation between successive segments of the transmitted signal of length $T_b/2$, the information signal can be recovered by a correlator. A block diagram of a DCSK receiver is shown in Fig. 2.15. The output of the correlator of the *lth* symbol duration is given by where $n'(t)$ is the noise component at the output of the receiving filter. The second term in Eq. (2.28) can be positive or negative, depending on whether a "1" or "0" has been transmitted. Also, all the other integral terms have a zero meaning. Thus, the threshold detector can be set optimally at zero; the decision threshold is zero independently of the noise

$$\begin{aligned} y(lT_b) &= \int_{(l-1/2)T_b}^{lT_b} r(t)r(t-T_b/2)dt \\ &= \int_{(l-1/2)T_b}^{lT_b} [s(t)+n'(t)][(t-T_b/2)+n'(t-T_b/2)] \\ &= \int_{(l-1/2)T_b}^{lT_b} [s(t)s(t-T_b/2)]dt + \int_{(l-1/2)T_b}^{lT_b} [s(t)n'(t-T_b/2)]dt + \\ &\int_{(l-1/2)T_b}^{lT_b} [n'(t)s(t-T_b/2)]dt + + \int_{(l-1/2)T_b}^{lT_b} [n'(t)n'(t-T_b/2)]dt \end{aligned} \quad (2.29)$$

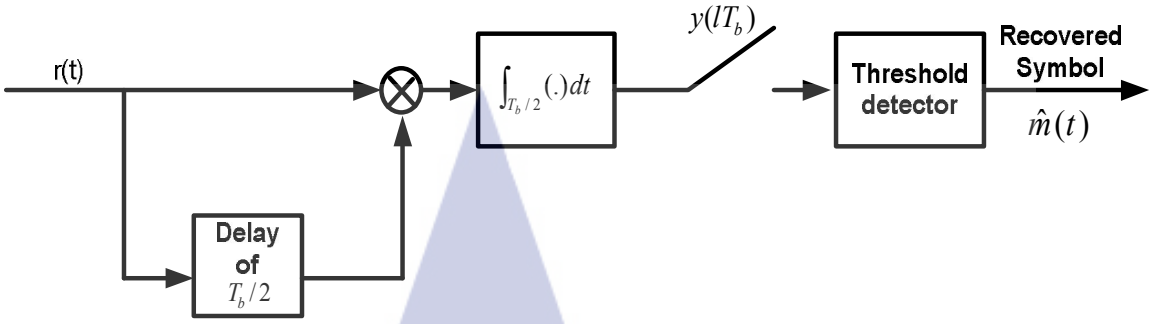

Figure 2.16 Block diagram of differential chaos shift keying demodulator presented by Volodymyr Lynnyk [4].

spectral density (E_s/N_0). By contrast with the CSK and COOK schemes discussed in Section 2.1.2.4 and Section 2.1.2.5, DCSK is an antipodal modulation scheme. The main advantage results from the fact that the reference and information-bearing sample functions pass through the same channel so they undergo the same channel distortion. DCSK can also operate over time-varying channel if the parameters of the channel remain constant for the bit duration Tb. The main drawback of DCSK, however, is that it can only transmit at half of the data rate of the other systems because it spends half of the time transmitting the non-information-bearing reference samples [49]. One way to improve the data rate is to use a multilevel modulation scheme. Alternatively, one may solve the estimation problem directly by modifying the modulation scheme such that the transmitted energy is kept constant. Frequency-modulated differential chaos shift keying scheme is an example of the latter approach.

2.1.2.6 Frequency-Modulated Differential Chaos Shift Keying

The objective of frequency-modulated differential chaos shift keying (FMDCSK)is to produce a wideband chaotic signal with constant. The FM-DCSK was proposed by Kolumbanet. al. In this scheme, a chaotic frequency modulated signal generator is needed. The chaotic signal to be input of an FM modulator. A block diagram of a FM-DCSK generator is shown in Figure 2.17. The output of this

Figure 2.17 Chaos frequency-modulated signal generator presented by Volodymyr Lynnyk [4].

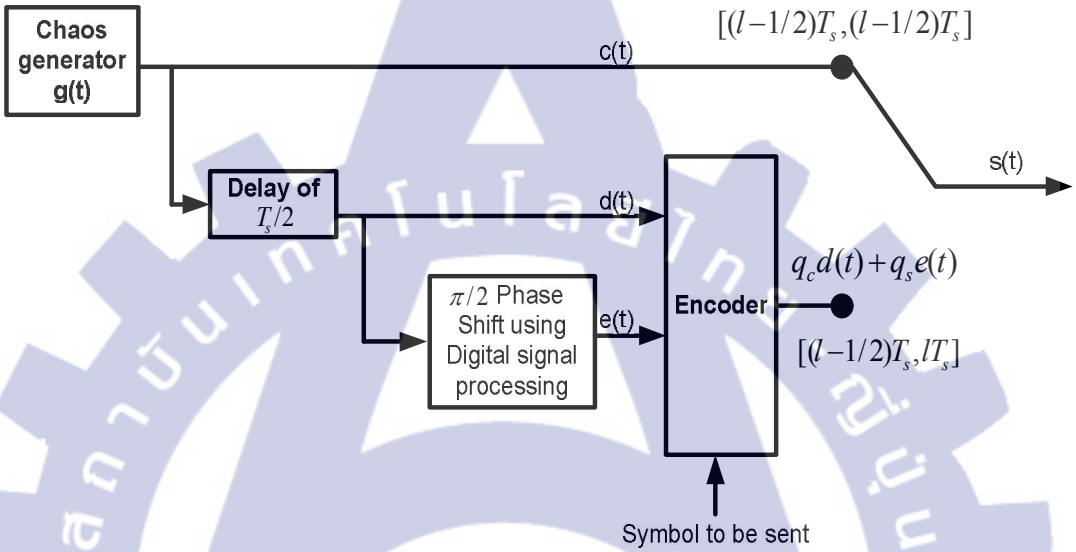

Figure 2.18 Block diagram of the Quadrature chaos shift keying scheme Modulator presented by Volodymyr Lynnyk [4].

FM modulator is chaotic, band limited, and its power spectral density is uniform. The operation of the demodulator is the same as in DCSK, the only difference being that not the chaotic, but the FM modulated signal is the input to the DCSK modulator

2.1.2Quadrature Chaos Shift Keying

In authors proposed a multilevel version of the differential chaos shift keying (DCSK), the so-called Quadrature chaos shift keying (QCSK) communication scheme with double data and higher spectral efficiency. In QCSK a two-bit symbol is encoded as a linear combination of two orthogonal waveforms, sine and cosine. Figure 2.18 and Figure 2.19shows a block diagram of the modulator and demodulator of the

QCSK communication system, respectively. In this diagram, each transmitted symbol consists of two bits of the information. Here, the bit duration is Tb and the symbol duration is *Ts = 2Tb*. The modulation scheme can be described as follows. Let c(t) be a chaotic reference signal defined for *t∈ [0, Ts/2]*. This reference signal has a zero mean value. Next, for producing of d(t) we use the *Ts/2*-delayed version of reference signal c(t). Further, we construct the complementary signal e(t) by shifting the phase of all frequency components in d(t) by *π/2,* which is accomplished by standard digital signal processing(DSP) techniques. In the QCSK modulation scheme, c(t) is sent during the first half symbol period, i.e., *[0, Ts/2]* while the information-bearing signals(t) is sent during the second half symbol period, i.e., *[Ts/2, Ts).*Here, s(t) is a linear combination of two orthogonal waveforms d(t) ands(t).

$$s(t) = q_c d(t) + q_s s(t) \tag{2.30}$$

where q_c and q_s are two bits of information to be sent within the symbol period T_s. At the demodulator, d(t) and e(t) are the first estimated from the noise version of the reference signal $\hat{c}(t)$ Suppose the estimated d(t)and e(t) are $\hat{d}(t)$and $\hat{e}(t)$ respectively. Then, demodulation can be done by correlating the signal received in the second half symbol period, i.e., *[Ts/2, T2),* with $\hat{d}(t)$ and $\hat{e}(t)$. Based on the correlation results a decision on the symbol s_i (two bits of information) received is taken by decision circuit according to estimated value $q_c + iq_s$. The QCSK scheme has the advantage over DCSK of double data rate for a given bandwidth with the same bit error rate performance.

2.2 Literature review

2.2.1 Chaotic and Dynamical Systems

Table 2.1 Show literature review of chaos jerk function, which are initially reviewed as Chaos theory. Six particularly related chaos theory for secure communication have previously been proposed by Ken Kiers and Dory Schmidt(2003), Vinod Patidar and K KSud(2005), GuoboXie and et al.(2008),

LjubišaM. Kocić and Sonja Gegovska-Zajkova (2009) and Buncha Munmuangsae and et al. (2011)

2.2.1.1 Precision measurements of a simple chaotic circuit

Ken Kiers and Dory Schmidt [5], describe a simple nonlinear electrical circuit that can be used to study chaotic phenomena. The circuit employs simple electronic elements such as diodes, resistors, and operational amplifiers, and is easy to construct. A novel feature of the circuit is its use of an almost ideal nonlinear element, which is straightforward to model theoretically and leads to excellent agreement between experiment and theory. The circuit in Fig. 2.19 contains three successive

Table 2.1 Summary of existing chaos jerk functions.

Authors	Year	Title
Ken Kiers and Dory Schmidt	2003	Precision measurements of a simple chaotic circuit
Vinod Patidar and K KSud	2005	Bifurcation and chaos in simple jerk dynamic
uoboXie and et al.	2008	Generation of multidirectional multi-scroll attractors under the third-order Jerk system
Ljubiša M. Kocić and Sonja Gegovska-Zajkova	2009	On a Jerk dynamical systems
Buncha Munmuangsae and et al	2011	Generalization of the simplest autonomous chaotic system

inverting integrators with outputs at the nodes labeled V_2, V_1, and x,as well as a summing amplifier with its output at V_3. If we use Kirchhoff's rules at nodes a-d

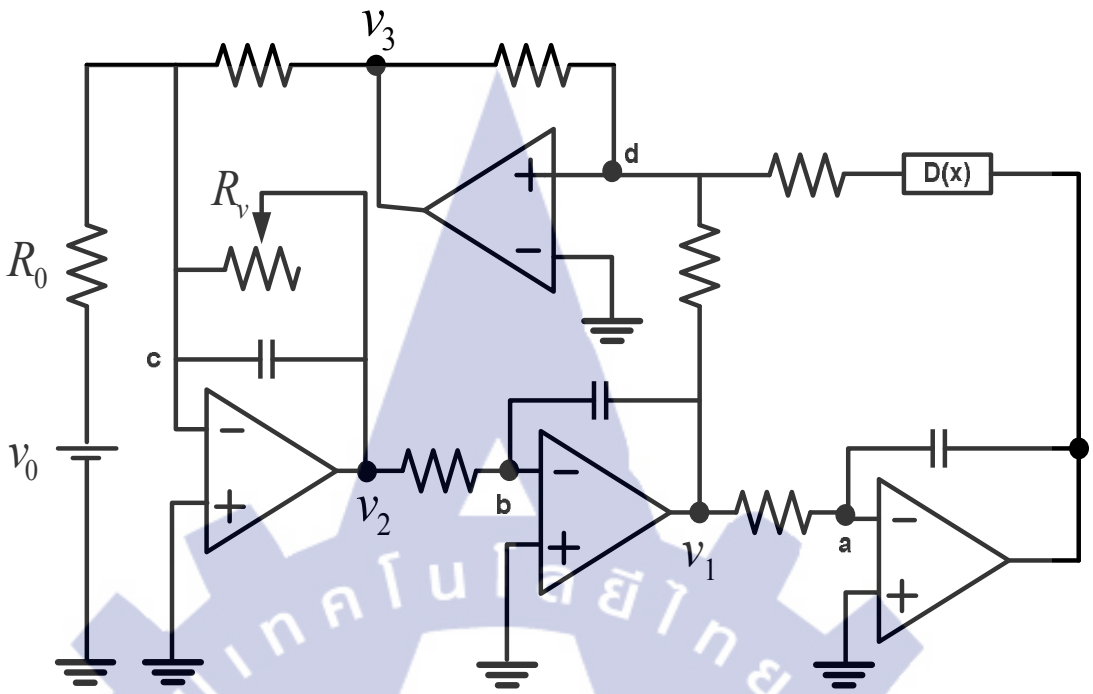

Figure 2.19 Schematic diagram of the circuit presented by Ken Kiers and Dory Schmidt [5].

$$V_1 = -RC\frac{dx}{dt} = -\dot{x}, \qquad V_2 = RC\frac{dV_1}{dt} = \ddot{x}, \qquad RC\frac{dV_2}{dt} = -(\frac{R}{R_v})V_2 - (\frac{R}{R_0})V_0 - V_3,$$

$$V_3 = -V_1 - D(x)$$

where the dots denote derivatives with respect to the dimensionless variable $\tilde{t} = t/(RC)$.

$$\dddot{x} = -(\frac{R}{R_v})\ddot{x} - \dot{x} + D(x) - (\frac{R}{R_0})V_0 \qquad (2.31)$$

We have derived the recursive proportional feedback algorithm and shown that it can be used to control chaotic oscillations in the Kiers, Schmidt, and Sprott electronic circuit. Control is achieved with small perturbations and the mean oscillation maximum during

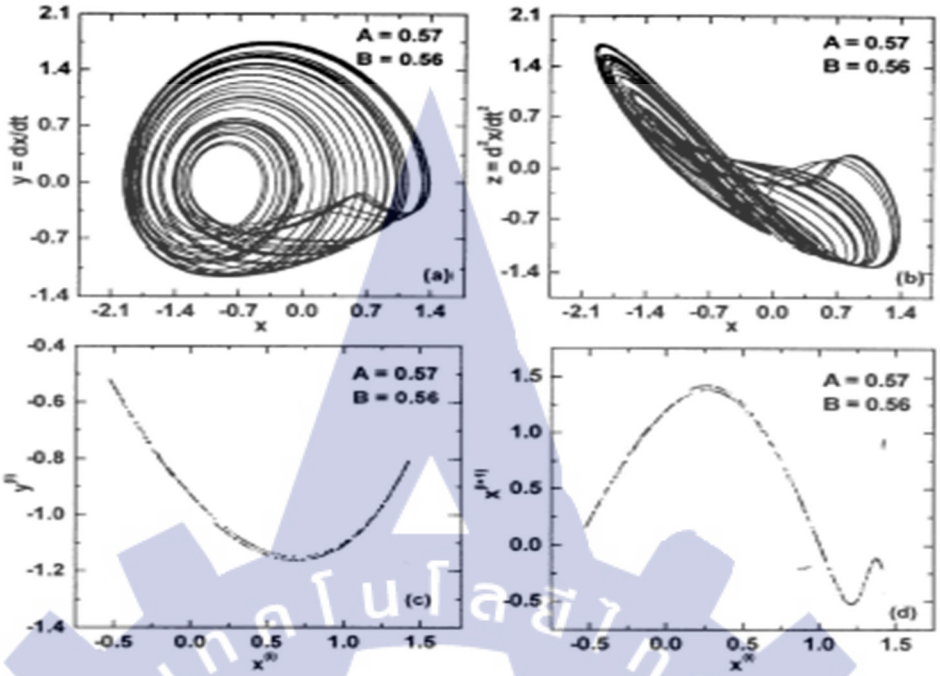

Figure 2.20 Strange attractor of the jerk dynamical system having quadratic on-linearity for A = 0:57 and B = 0:56. Two different projections of the strange attractor are shown in (a) and (b). The Poincare surface of the section defined by y = 0, z < 0 and corresponding to the one-dimensional Poincare map (c) and (d) presented by VinodPatidar and K KSud [6].

Control is well within the uncertainty of the target fixed point. The values of the coefficients used in the recursive proportional feedback algorithm were calculated from experimentally measured values of the output voltage of the circuit during pre-control measurements. Recursive proportional feedback is suitable for highly dissipative systems, of which the KSS circuit is an example. Simple proportional feedback is also suitable for some highly dissipative systems, but cannot be used for the KSS circuit because the movement of the system's chaotic attractor through phase space depends on both the current and previous perturbations.

2.2.1.2 Bifurcation and chaos in simple jerk dynamic

Vinod Patidar and K KSud [6], In recent years, it is observed that the third-order explicit autonomous differential equation, named as jerk equation,

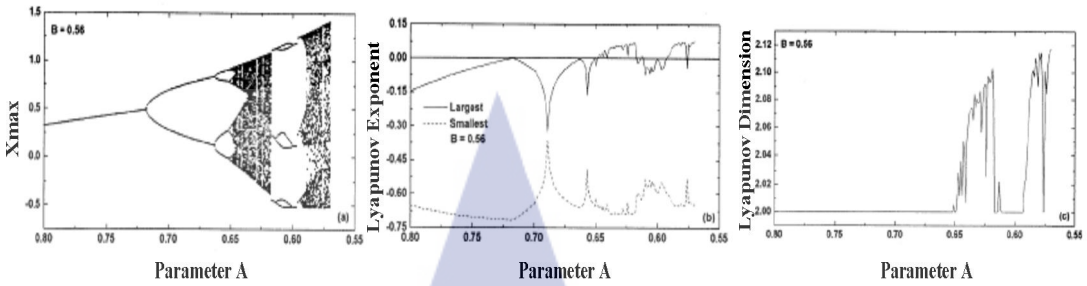

Figure 2.21 Behavior of the jerk dynamical system having quadratic non-linearity for a fixed value of parameter B = 0:56. (a) The bifurcation diagram showing period doubling route to chaos, (b) the two Lyapunov exponents and (c) the Lyapunov dimension presented by VinodPatidar and K KSud [6].

represents an interesting sub-class of dynamical systems that can exhibit many major features of the regular and chaotic motion. In this paper, we investigate the global dynamics of a special family of jerk systems$\dddot{x} = -A\ddot{x} + B\dot{x} + G(x)$.Where$G(x)$is a non-linear function, which is known to exhibit chaotic behavior at some parameter values. We particularly identify the regions of extensive Lyapunov spectra calculation in complete parameter space. We also investigate the effect of weakening as well as strengthening of the non-linearity in the G(x) function on the global dynamics of these jerk dynamical systems.Form two fixed points (±1; 0; 0)

$$\dddot{x} + A\ddot{x} + \dot{x} = B(x^2 - 1) \tag{2.32}$$

As a result, we reach to an important conclusion for these jerk dynamical systems that a certain amount of non-linearity is sufficient for exhibiting chaotic behavior but increasing the non-linearity does not lead to larger regions of parameter space exhibiting chaos.

2.2.1.3 Generation of multidirectional multi-scroll attractors under the third-order Jerk system

GuoboXie and et al. [7], In this paper, An approach for generating multi directional grid chaotic attractors from a third-order Jerk system is proposed via constructing a series of staircase functions, including two-directional and three-

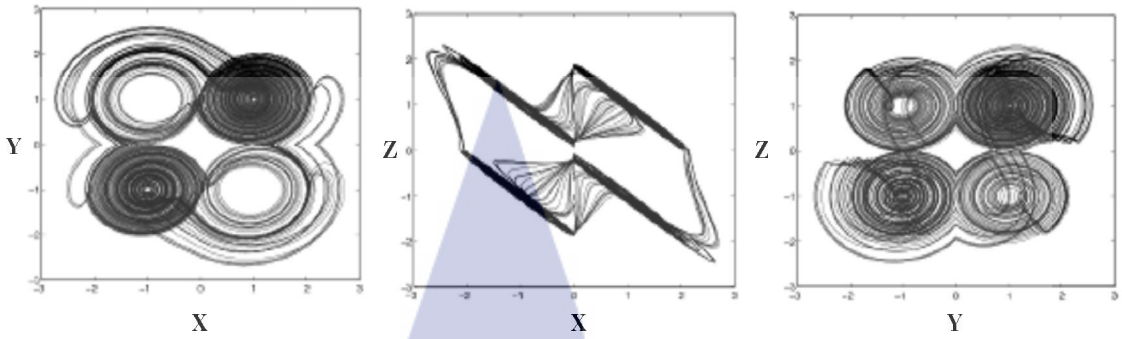

Figure 2.22 2×2×2 grid-scroll chaotic attractors presented by GuoboXie and et al. [7].

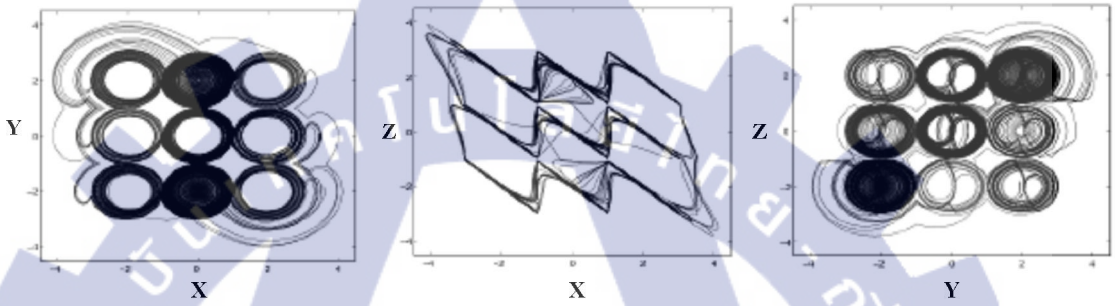

Figure 2.23 3×3×3 grid-scroll chaotic attractors presented by GuoboXie and et al. [7].

directional multi-scroll chaotic attractors. Its dynamical behaviors are investigated by means of theoretical analysis as well as numerical simulation. In order to extend the scrolls to the z -direction, another nonlinear function f 3(z) is introduced to the second and the third equations of, leading to

$$\begin{aligned} \dot{x} &= y - F(x) \\ \dot{y} &= z - F(y) \\ \dot{z} &= a(-x - y - z + F_1(x) + F_2(y) + F_3(z)) \end{aligned} \tag{2.33}$$

where $\xi > 0$, system parameters M and N and L are integers. So we can generate M×N×L scrolls from (2.31) and (2.32)as shown in Figs. 2.22In this papers, a new technique for generating × m× l scroll attractors under a third-order Jerk system has been proposed, analyzed, simulated. One nonlinear piecewise function is used in this

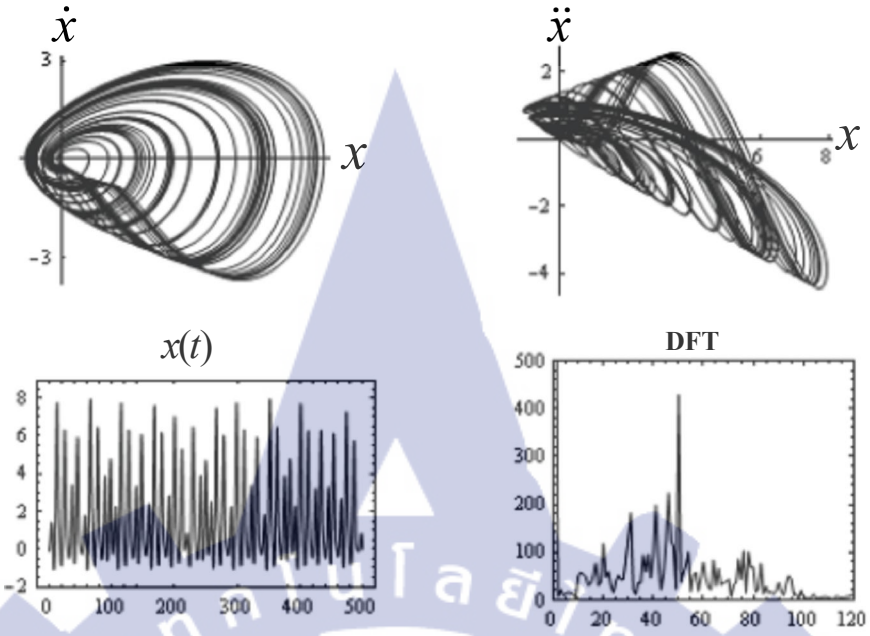

Figure 2.24 The x(t) diagram and the DFT confirms chaotic element with A= 1.3; k = 1; λ_1= 0.0338091presented by Ljubiša M. Kocić and Sonja Gegovska-Zajkova[7].

Jerk system. By setting the constants M, N and L in this function, different numbers of $n \times m \times l$ -scroll attractors can be created as designed for Jerk system

Where a ε [0.47, 0.96] , $F_1(x)$ and $F_2(y)$ and $F_3(z)$ are the staircase function series which are described as follows:

$$F_1(x) = \begin{cases} \xi[\mathrm{sgn}(x) + \sum_{m=1}^{M} \mathrm{sgn}(x - 2\xi m) + \sum_{m=1}^{M} \mathrm{sgn}(x + 2\xi m)] \\ \xi[\sum_{m=1}^{M} \mathrm{sgn}(x - \xi(2m-1)) + \sum_{m=1}^{M} \mathrm{sgn}(x + \xi(2m-1))] \end{cases}$$

$$F_2(y) = \begin{cases} \xi[\mathrm{sgn}(y) + \sum_{n=1}^{N} \mathrm{sgn}(y - 2\xi n) + \sum_{n=1}^{N} \mathrm{sgn}(y + 2\xi n)] \\ \xi[\sum_{n=1}^{N} \mathrm{sgn}(y - \xi(2n-1)) + \sum_{n=1}^{N} \mathrm{sgn}(y + \xi(2n-1))] \end{cases} \quad (2.34)$$

$$F_3(z) = \begin{cases} \xi[\mathrm{sgn}(z) + \sum_{l=1}^{L} \mathrm{sgn}(z - 2\xi l) + \sum_{l=1}^{L} \mathrm{sgn}(z + 2\xi l)] \\ \xi[\sum_{l=1}^{L} \mathrm{sgn}(z - \xi(2l-1)) + \sum_{l=1}^{L} \mathrm{sgn}(z + \xi(2l-1))] \end{cases}$$

2.2.1.4 On Jerk dynamical systems

Ljubiša M. Kocić and Sonja Gegovska-Zajkova[8], chaotic systems of J.C. Sprott emanated from electric circuits turn to be attractive examples of week chaos the only form of chaos that eventually might be acceptable in sensible applications like automatic control or robotics. Here, two modifications of a 3D dynamic flow, known as jerk dynamical system of J.C. Sprott are considered. The left-semi quadratic system$\dddot{x} = -A\ddot{x} + g_k(\dot{x}) - x$. The system preserves chaotic regimeof the original Sprott setting $\dddot{x} = -A\ddot{x} + \dot{x}^2 - x$ for lesser values of A and bigger slopevalues k. The choice A = 1.3 and k = 1 produces recognizable phase diagrams, given in two projections in Fig. 2.24. The x(t) diagram and the DFT confirms chaotic element, and the Lyapunov coefficient is λ1 = 0.0338091.One of the simplest dynamic flows that still exhibits chaotic behavior is Sprott's jerky system, given by equations$\dddot{x} = -A\ddot{x} + \dot{x}^2 - x$, where ψ (ξ) = ξ^2. This system "works" on the "edge" of chaos, which is evident from its small first Lyapunov exponent (λ_1 = 0.0551). Tracing for simpler function ϕ that yet supplies chaotic dynamics, Sprott and Linz tried with ψ (ξ) = |ξ|, the continuous function that represents a kind of piecewise linear approximation of quadratic function. In this case, no chaos has been detected. The present note deals with the "hybrid" case embodied in two semi-quadratic functions, the left- and the right one, see Fig.2.24 for the graphs. Surprisingly, the left semi-quadratic function $g_k(\xi)$ produces chaos for some values of the larger part's variable slope k, and the corresponding value of A, while the symmetric, right semi-quadratic function $h_k(\xi)$ leads only to a non-chaotic dynamics.

2.2.1.5 Generalization of the simplest autonomous chaotic system

Buncha Munmuangsae and et al. [9], an extensive numerical search of jerk systems of the form $\dddot{x} + \ddot{x} + \dot{x} = f(x)$ revealed many cases with chaotic solutions in addition to the one with $f(\dot{x}) = \pm x^2$that has long been known. Particularly simple is the piecewise-linear case with$f(x) = \alpha(1 - x) for x \geq 1$ and zero otherwise, which produces chaos even in the limit of $\propto \rightarrow \infty$ the dynamics in this limit can be calculated exactly, leading to a two-dimensional map. Such nonlinearity suggests an elegant electronic circuit implementation using a single diode.

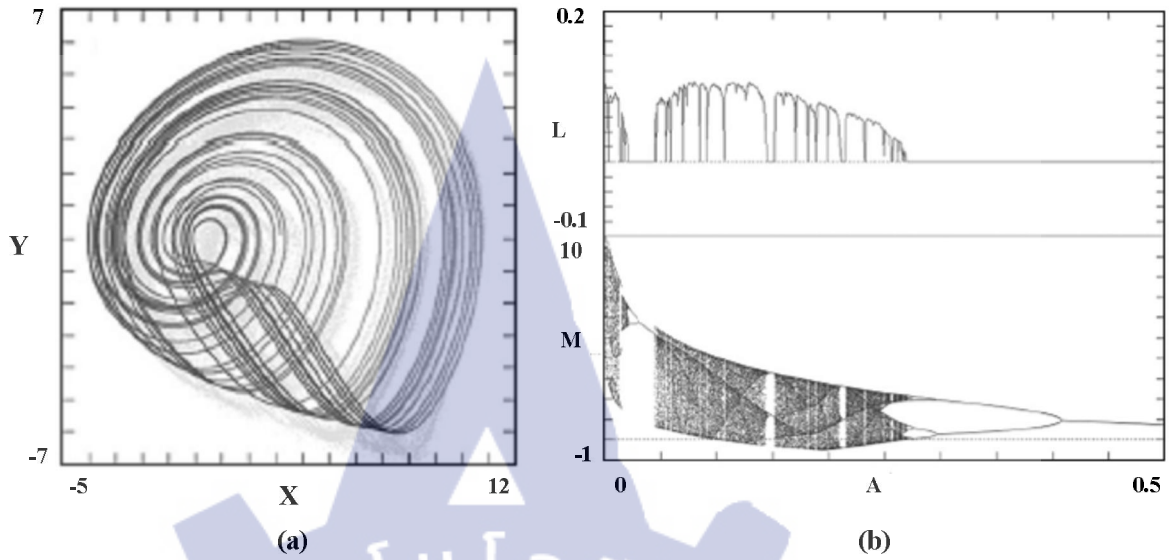

Figure 2.25(a) Attractor form equation and (b) The largest Lyapunov exponent and bifurcation diagram of equation for $f(\dot{x}) = -A\exp(x)$ with 0 < A <0.5 presented by Buncha Munmuangsae and et al. [9]

This raises the question of whether there are other simple chaotic systems of the form $\dddot{x} + \ddot{x} + x = f(\dot{x})$ and $f(\dot{x}) = -A\exp(\dot{x})$ with A = 0.1, is particularly interesting. It has the curious feature of having chaotic solutions in the limit of A→0 as is evident from its largest Lyapunov exponent and bifurcation diagram (the local maxima of x) shown in Figure 2.25, which shows a period-doubling route to chaos. The attractor grows in size as A→0 since a larger $\dot{x}$ is requiredto achieve the same nonlinearity as A decreases The equilibrium point for this case has Eigenvalue = .1.5193, 0.2596 ± 0.7686i, which satisfies the Shilnikov condition since the absolute value of the real Eigenvalue is greater than the absolute value of the real part of the complex Eigenvalue, providing a proof of chaos. For this value of A, the largest Lyapunov exponent is near its maximum with a Lyapunov exponent spectrum of (0.1016, 0, .1.1016) and a Kaplan–Yorke dimension of DKY = 2.0922.In conclusion, several simple chaotic systems of the form$\dddot{x} + \ddot{x} + x = f(\dot{x})$have been studied. They have similar maximum valuesof their largest Lyapunov exponents and corresponding Kaplan.Yorke dimensions. Furthermore, all cases have $F'(x) > -1$with spiralsaddles of index 2. Particularly simple is the piecewise-linear casewith $f(\dot{x}) = \alpha(1 - \dot{x})$for

Table 2.2 Show summarize application chaotic system for communication

Author	Year	Title
Shihua Chen and et al.	2003	Adaptive synchronization of uncertain Rössler hyper chaotic system based on parameter identification
Pehlivan and Y. Uyaroglu	2007	Simplified chaotic diffusion less Lorentz attractor and its application to secure communication systems
GaoBingkun and et al.	2009	The application research of Hyper chaos encryption in security communications
Said SADOUDI and Mohamed Salah Azzaz	2009	Hardware Implementation of the Rössler Chaotic System for Securing Chaotic Communication
Ihsan Pehlivan and et al.	2009	Design and simulations of the Arneodo attractor's chaotic oscillator and signal masking circuit
Ihsan Pehlivan and et al.	2010	Phase synchronization in mutually coupled chaotic Josephson Junctions: Effect of asymmetry and incommensurate frequencies

$\dot{x} \geq 1$and zero otherwise, which produces chaos even in the limit of $\alpha \to \infty$ where the trajectory encountersa
reflecting boundary at$\dot{x} = 1$ .This system can be calculated exactly, leading to a two-dimensional map identical to the one

2.2.2 Synchronization in secure communication system

Table 1.2 Show application chaotic systems for communication, which is initially reviewed as purpose chaotic system for communication. Nine mainly linked chaos application chaotic system for communication have previously been proposed by Shihua Chen and et al.(2003), Pehlivan and Y. Uyaroglu(2007)**,** Dandan Zhao and

et al.(2008), GaoBingkun and et al.(2009), Said SADOUDI and Mohamed Salah Azzaz(2009), Ihsan Pehlivan and et al. (2010), Jiejing Liu and Yanli Zhang(2011) and Jing Pan and Qun Ding(2011)

2.2.2.1 Adaptive synchronization of uncertain Rössler hyper chaotic system based on parameter identification

Shihua Chen and et al. [10], In this letter, an approach of adaptive synchronization and parameters identification of uncertain Rössler hyper chaotic system is proposed. The suggested tool proves to be globally and asymptotically stable by means of Lyapunov method. With this new and effective method, parameters identification and synchronization of Rössler hyper chaotic with all the system parameters unknown, can be achieved simultaneously. Theoretical proof and numerical simulation demonstrate the effectiveness and feasibility of the proposed technique. Rössler hyper chaotic system was provided by Rössler in describing dynamics of some hypothetical chemical reaction and is a first example of hyper chaotic system with two positive Lyapunov exponents. The nonlinear differential equations that describe Rössler hyper chaotic system are

$$\begin{cases} \dot{x} = -y - z \\ \dot{y} = x + ay + w \\ \dot{z} = b + xz \\ \dot{w} = -cz + dz \end{cases} \tag{2.35}$$

According to the drive system and the controlled response system, we get the error dynamical system

$$\begin{aligned} \dot{e}_1 &= -e_1 - e_2 - e_3 \\ \dot{e}_2 &= e_1 - e_2 + e_4 + (\hat{a} - a) y_m \\ \dot{e}_3 &= e_1 - e_3 + \hat{c} e_4 + \hat{b} - b \\ \dot{e}_4 &= -e_2 - \hat{c} e_3 - e_4 - (\hat{c} - c) z_m + (\hat{d} - d) \omega_m \end{aligned} \tag{2.36}$$

Figure 2.26 Graphs of synchronization errors varying with time. $e_1(t) = x_s(t) - x_m(t)$, $e_2(t) = y_s(t) - y_m(t)$, $e_3(t) = z_s(t) - z_m(t)$ and $e_4(t) = w_s(t) - w_m(t)$ presented by Shihua Chen and et al. [10].

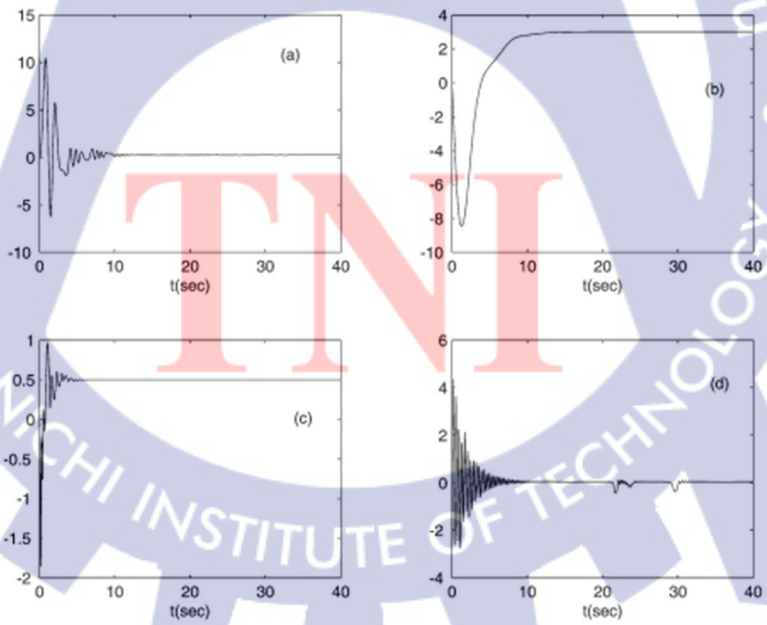

Figure 2.27 Graphs of parameters identification results presented by Shihua Chen and et al. [10].

In order to verify the effectiveness of the proposed method, let the master signals are from Rössler hyper chaotic system with system parameters a =0.25, b = 3, c = 0.5, d = 0.05 and initial condition (−20, 0, 0, 15). Suppose initial condition of the controlled Rössler hyper chaotic system is(5.0, 7.0, 9.0, and 11.0) and the unknown parameters have zero initial conditions. Numerical simulation shows that parameters identification and adaptive synchronization are achieved successfully. Figure. 2.26 display the results. In this Letter, we introduce an adaptive synchronization and parameters identification method for Rössler hyper chaotic system with all the system parameters unknown. With this method one can achieve synchronization and parameters identification simultaneously. Lyapunov direct method is used to prove the stability of the method. Numerical experiment shows the effectiveness of the proposed method.

2.2.2.2 Simplified chaotic diffusion less Lorentz attractor and its application to secure communication systems

Pehlivan and Y. Uyaroglu [11], this show Diffusion less Lorentz equations a simplified one-parameter version of the well-known Lorentz model. Also, it was attained in the limit of high Rayleigh and Prandtl numbers, physically corresponding to diffusion less convection. A simplified, one-parameter version of the Lorentz model called diffusion less Lorentz is proposed, which is suitable for chaotic synchronization and masking communication circuits using Matlab/Simulink and Spice programmers. It is also suitable for a real electronic experimental circuit. This situation is the most interesting case of the two and it is limited to the corresponding parameter regime equation 2.34 reduce to

$$\begin{aligned} \dot{x} &= -y - x \\ \dot{y} &= -xz \\ \dot{z} &= xy + R \end{aligned} \tag{2.37}$$

which has a hyper chaotic attractor when a = 0.25, b = 3, c = 0.5, d = 0.05. For convenience, we denoted the master Rössler hyper chaotic system

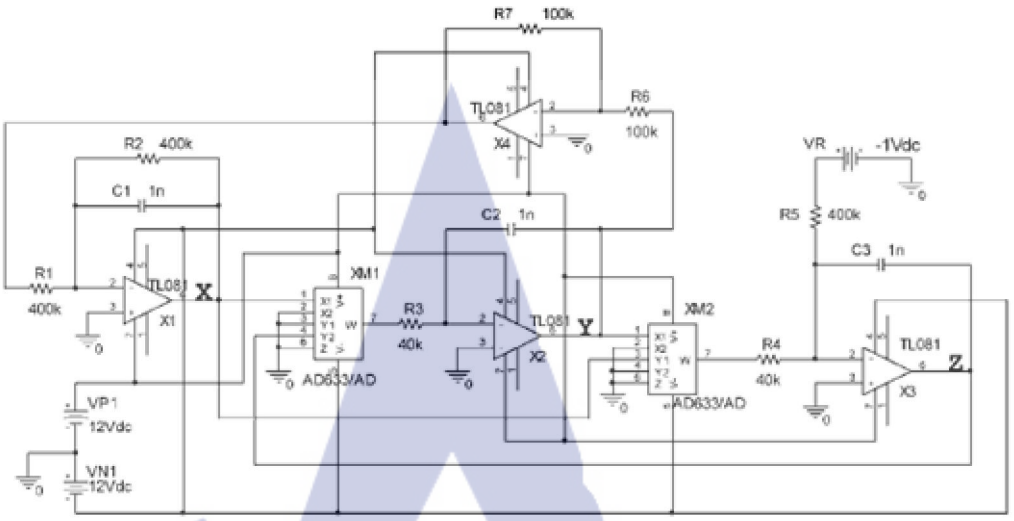

Figure 2.28 Spice circuit presented by Pehlivan and Y. Uyaroglu [11].

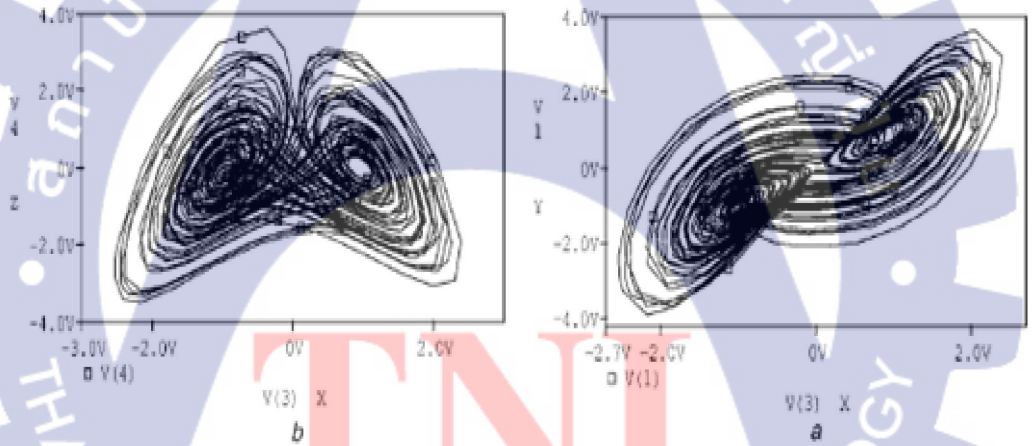

Figure 2.29 Spice simulation results (a) x, y phase portrait (b) x, z phase portrait presented by Pehlivan and Y. Uyaroglu [11].

The single-parameter equations 2.37are referred to in the remainder of this study as the DLE. System 2.37wererederived (with R = 1) during a search for chaotic low-order systems of the form F(x) with F(x) algebraically as simple as possible. The Lyapunov exponents of the DLE are 0.115, 0, and 21.115, namely, only one positive LE ispresent.Fig.2.8 shows the circuit schematic for implementing the DLE Equation 2.27. We use TL081 op-amp, the analog devices AD633JN multipliers, appropriate

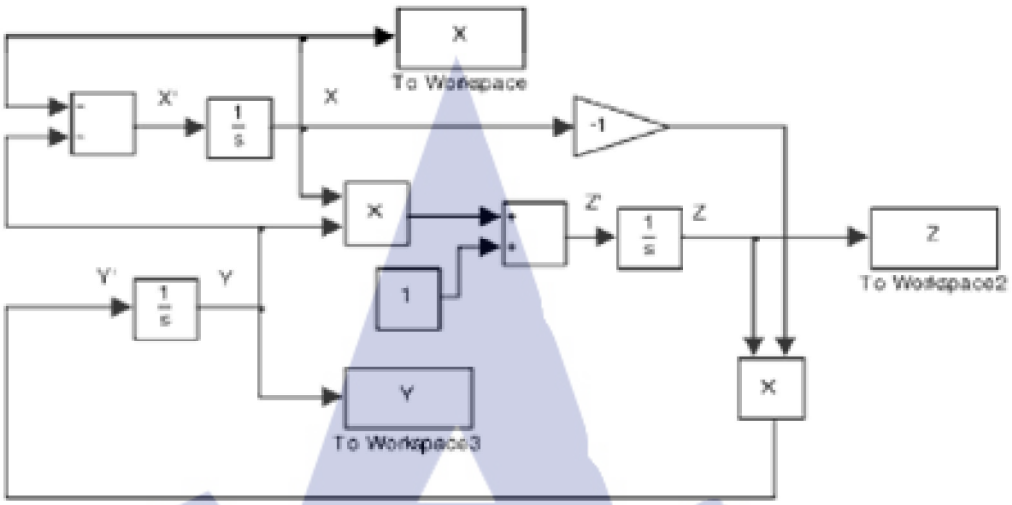

Figure 2.30 Matlab–Simulink models presented by Pehlivan and Y. Uyaroglu [11].

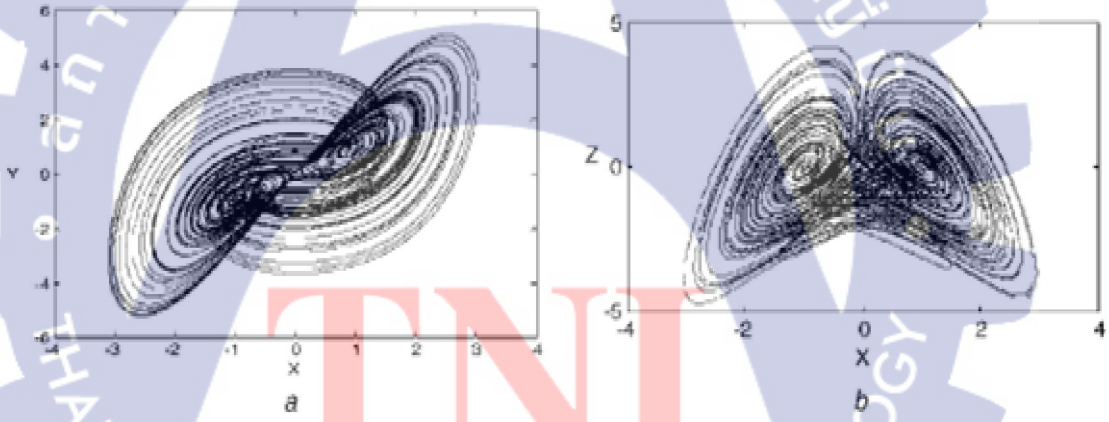

Figure 2.31 Result phase portraits presented by Pehlivan and Y. Uyaroglu [11].

valued resistors and capacitors for Spice simulations. The circuit is supplied +12 V power supplies. Acceptable inputs to theAD633 multiplier IC are 210 to t10 V. The ResistorsR1.R7 are all shown with nominal values in Figure 2.28 also show Spice simulation and results of this circuit.

Areal experimental electronic circuit is implemented for parameter R = 1 and for the initial conditions $x_0 = 1, y_0 = 21$ and $z_0 = 0.01$, and the oscilloscope

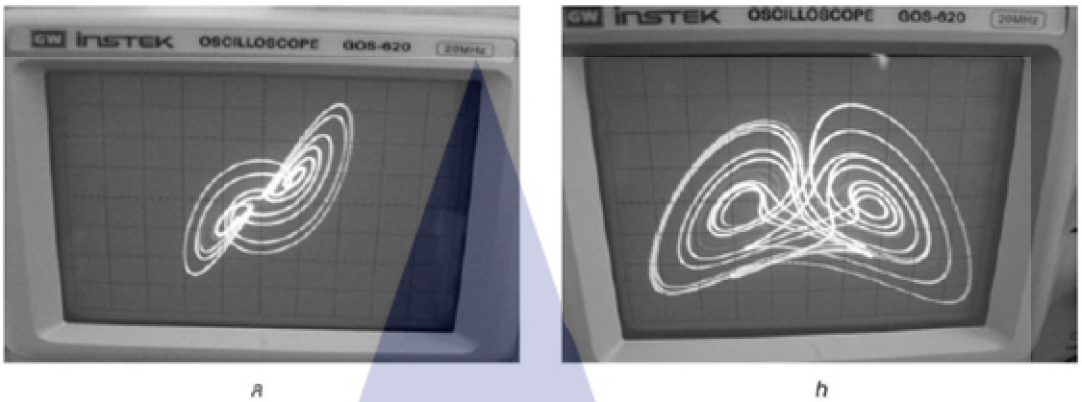

Figure 2.32 Oscilloscope outputs of the electronic circuit (a) x, y phase portrait(b) x, z phase portrait presented by Pehlivan and Y. Uyaroglu [11].

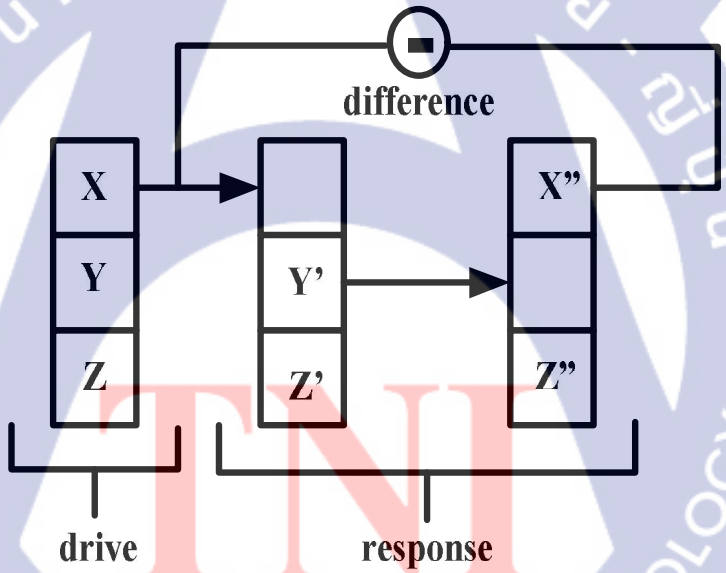

Figure 2.33 Block diagram chaotic synchronize presented by Pehlivan and Y. Uyaroglu [11].

outputs are attained as shown in Figure 2.29. Conclusions from Matlab-Simulink, Spice simulations and also real electronic circuit results of DLE are identical.

Figure 2.34 Simulink modeling presented by Pehlivan and Y. Uyaroglu [11].

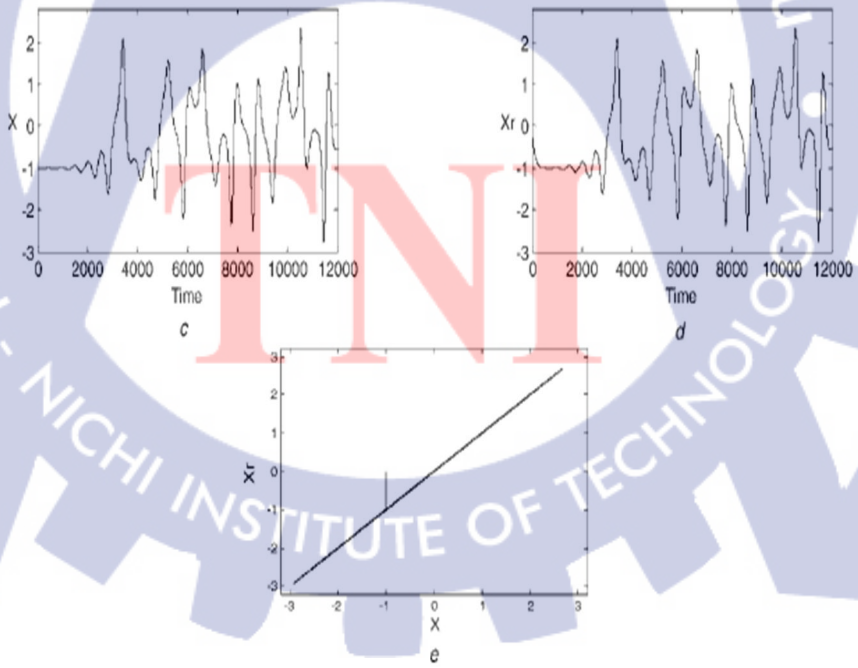

Figure 2.35 Simulation output presented by Pehlivan and Y. Uyaroglu [11].

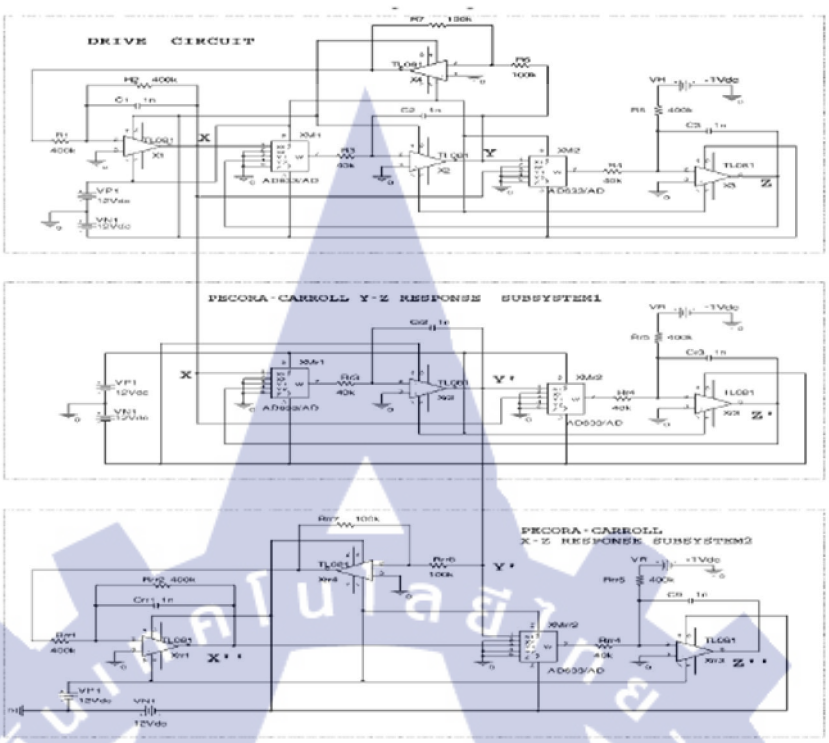

Figure 2.36 Spice circuit presented by Pehlivan and Y. Uyaroglu [11].

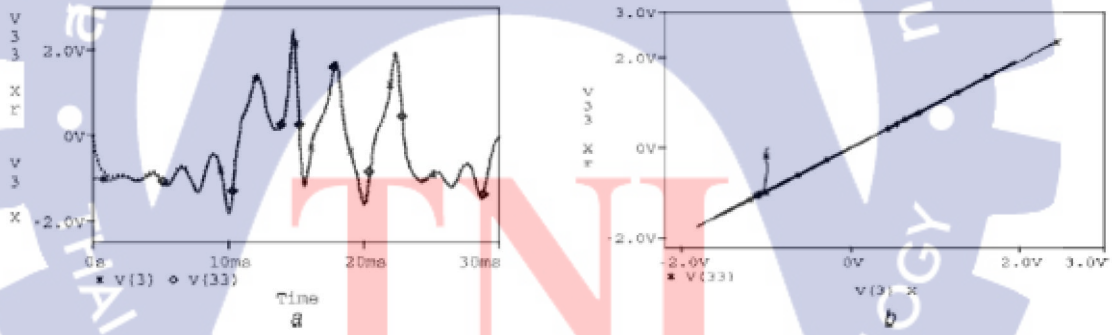

Figure 2.37 simulation outputs (a) Drive system x signal and response system x_r signal against time. (b) Synchronization between x and x_r presented by Pehlivan and Y. Uyaroglu [11].

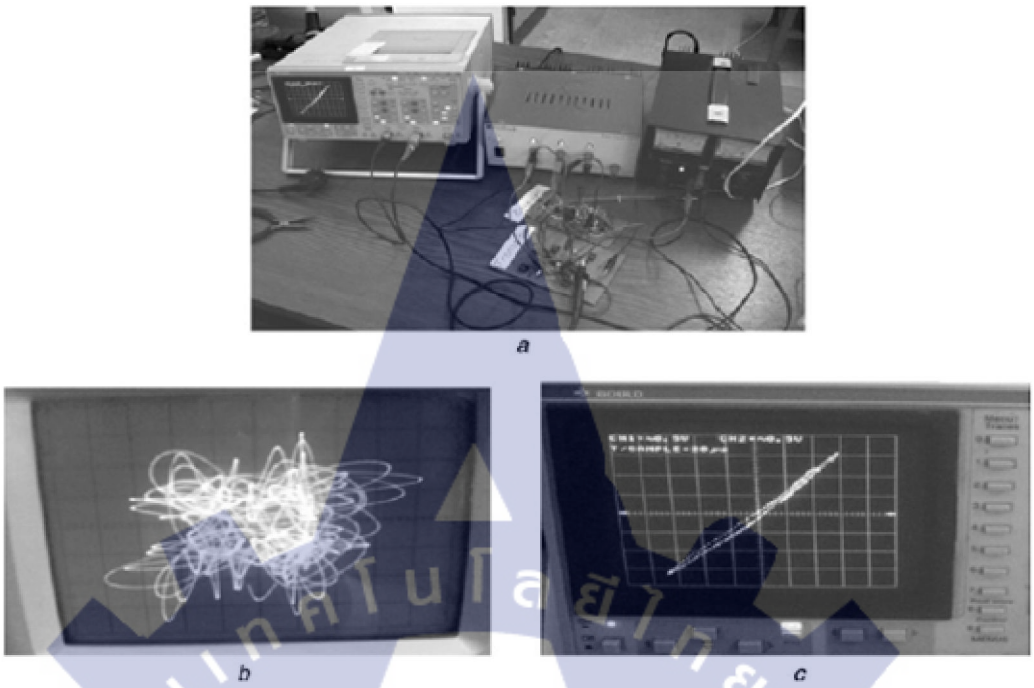

Figure 2.38 Real electronic circuit results of DLE (a) Real electronic circuit realization of the DLE's Pecora–Carroll synchronization (b) Unsynchronized output before synchronization (c) 45° line after synchronization presented by Pehlivan and Y. Uyaroglu [11].

Synchronization between chaotic systems has received considerable attention and led to communication applications. There are two major methods for coupling and synchronizing identical chaotic systems, the cascading method and the one-way coupling method. With these methods, a message signal sent by a transmitter system can be reproduced at a receiver under the influence of a single chaotic signal through synchronization. This paper presents the study of numerical simulation of chaos synchronization for chaotic DLE. The Pecora–Carroll synchronization method is used and drive and response subsystems were constructed. Fig. 2.33 shows the block diagram of a cascaded synchronization system, illustrating simulation modeling and outputs of Pecora–Carroll synchronization of DLE. Synchronization of chaotic motions among coupled dynamical systems, indispensable in communications is an important generalization from synchronization of the linear system. The idea of the

methods is to reproduce all the signals at the receiver under the influence of a single chaotic signal from the driver. Therefore chaos synchronization can potentially be applied in communications and signal processing. However, to build a secure communications system, some other important factors need to be considered.

This paper focuses on the identical synchronization of DLEs and its applications in signal masking and secure communications. The Pecora–Carroll identical cascading synchronization method is used. The behavior of the response system depends on the behavior of the drive system, but is not invertible. We have demonstrated in simulations and also proved in real electronic circuits that chaos can be synchronized and applied to secure communications. We suggest that this phenomenon of chaos synchronicity may serve as the basis for little-known DLEs to achieve secure communication. Chaos synchronization and chaos masking were realized using Matlab–Simulink, Spice programs and also real electronic experimental applications. Related figures in Figs. 2.34-2.37 for synchronization and Figures. 2.34, 2.35 and 2.36 for masking communication show that Matlab–Simulink, Spice outputs and also real electronic experimental application results prove the same conclusions.

2.2.2.3 The application research of hyper chaos encryption in security communications

GaoBingkun, Li Wenchao and Hu Yue [12], Against the nature of Hyper chaos dynamic system, a modified hyper-chaotic sequence encryption algorithm was given. This method used the dynamic system of TNC Hyper chaos. And proved to have the effective ability of exhaustive attack and anti-nonlinear reorganization; Used Sub-NY Quist sampling interval to increase the key space, this method has the ability of anti-nonlinear reorganization attack; realized the algorithm's encryption and decryption by using MATLAB simulation platform and got some satisfactory results which make out that the arithmetic is faster and easier implementation by software, had a large key space and so on.

In hyper chaos equation of 4-dimensional, such as Chen circuit equation, MCK circuit equation, Rössler equation, TNC (Tamasevicius Namajunas Cenyss) circuit equation and so on, we select to use TNC circuit. It can deal with a number of system variables then produce a sequence cryptogram. Sequence

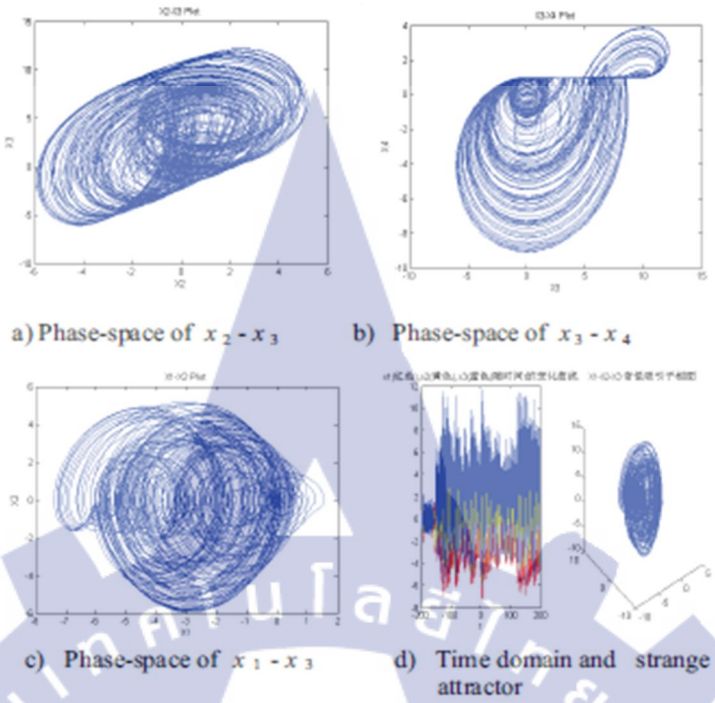

Figure 2.39 Attractors of TNC Hyper chaos circuit presented by GaoBingkun, Li Wenchao and Hu Yue[12].

cryptogram designs flexible and has a large design space. It can enhance security, provide possibilities of a solution to improve the limited effect which result in short cycles, provide a guarantee for improving anti-exhaustive attacks. It can provide a large key space. TNC circuit equation has a large number of system variables and parameters which can be used as the seed key for the sequence cryptosystem. The algorithm not only has a large key space but also can improve the security. When parameter of hyper chaos equation satisfied the certain conditions, the system emerges in the ultra-chaotic state; it represents complex, disorder and randomness. Fig.2.38 is the simulation graph of hyper chaos attractor diagram, it shows TNC hyper chaos system has not only more extensive parameters than others but also has more complex phase diagram, its path presents much better non- periodicity which makes attackers more difficult to analysis, moreover, it simulates quickly .Therefore we select 4-dimensional TNC hyper chaos system to produce encryption sequences, the equation described as follows:

$$\begin{aligned}\dot{x}_1 &= x_2 \\ \dot{x}_2 &= -x_1 + a_1 x_2 - x_3 \\ \dot{x}_3 &= -3x_4 + a_2 x_2 \\ \dot{x}_4 &= a_4 (x_4 - 1) h(x_4 - 1) + a_3 x_3\end{aligned} \tag{2.38}$$

when x4-1<0, h(x4-1) =0, otherwise, h(x4-1) =1. Assume the system parameters as a1=0.7, a2=3.0, a3=3.0, a4=-30, the initial state as x(0)=[0.5, 0.5, 0.5, 0.5], temporality, the system in the state of hyper chaos. Simulation of TNC hyper chaos strange attractor shows as Fig. 2.39.

In this paper, a modified hyper-chaotic sequence encryption algorithm and encryption/decryption model is given. We use hyper chaos sequence as encryption keys which produced by TNC hyper chaotic system. We use the method of statistical characteristics to apply the hyper chaos encryption technology to the communications in WLAN. And successfully obtain the data of encryption/decryption by the means of Matlab simulation platform. The results show that: The sequences which produced by TNC hyper chaos encryption systems have the ability of anti-attack and provide a large number of key spaces; Sub-Nyquist sampling interval can resist the attacks of reconstructed linear and expand key space; The new method of generated Hyper chaotic sequences will be beneficial to improve resist choice attack; Longer length of equivalent key make the encrypt system stronger to comfort the attacks; The design of the parameters are not only meet the requirements of encryption in WLAN security but also get more improvement. Although there are many advantages to use hyper chaos in security communications, there still many theoretical and practical application problem need to be study and discuss.

2.2.2.4 Hardware Implementation of the Rössler Chaotic System for Securing Chaotic Communication

Said Sadoudi and Mohamed Salah Azzaz [13], In this paper, a real-time implementation of the Rössler chaotic system in a Field Programmable Gate Array(FPGA) is presented. At first, we use directly the VHDL language for the hardware description of the system, contrary to some previous works where the Xilinx system generator of MATLAB-Simulink used to generate the VHDL code. Then,

after a step of optimization, to reduce the resources of the circuit target Virtex-II xcv1000-4fg456, we implement the chaotic system on FPGA. The real-time chaotic signals obtained at the output of the FPGA are then compared with those obtained by MATLAB and Models simulation, in order to validate our results. However, the goal of this work is to introduce this chaotic system in an eventual secure digital chaotic communication system. O. E. Rössler introduced his equations system in1976. Therefore, a great interest is given for this kind of chaotic system. This system has only single non-linear term (zx) contrary to the Lorenz system and is given as follow:

$$\begin{cases} \dfrac{dx}{dt} = -(y + X) \\ \dfrac{dy}{dt} = x + ay \\ \dfrac{dz}{dt} = b + z(x - c) \end{cases} \tag{2.39}$$

The original classical Rössler chaotic system has such parameters a = b = 0.2, c = 5.7. The corresponding chaotic signals and strange attractor in the phase plan (x-z) and (x-y) are represented in figure 2.40 and 2.41 and 2.42 respectively.

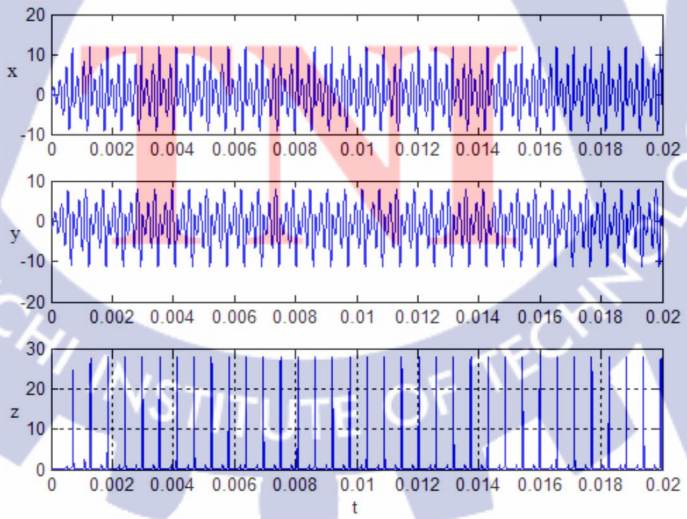

Figure 2.40 Chaotic signals of Rössler generator presented by Said Sadoudi and Mohamed Salah Azzaz [13].

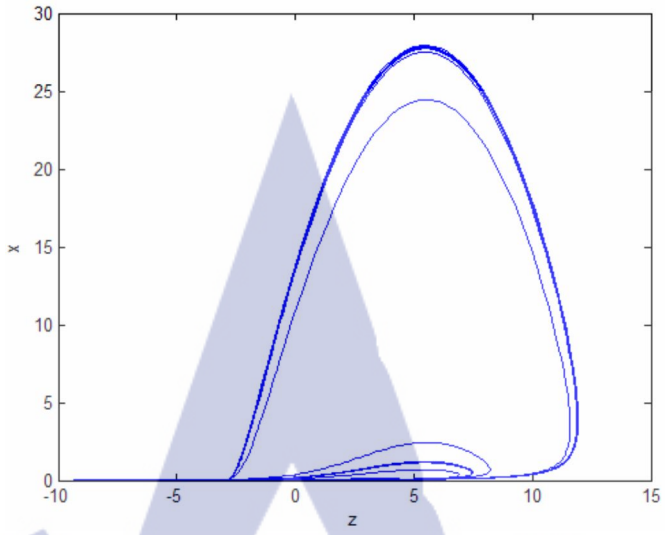

Figure 2.41 Rössler strange attractor (phase plan x-z)presented by Said Sadoudi and Mohamed Salah Azzaz [13].

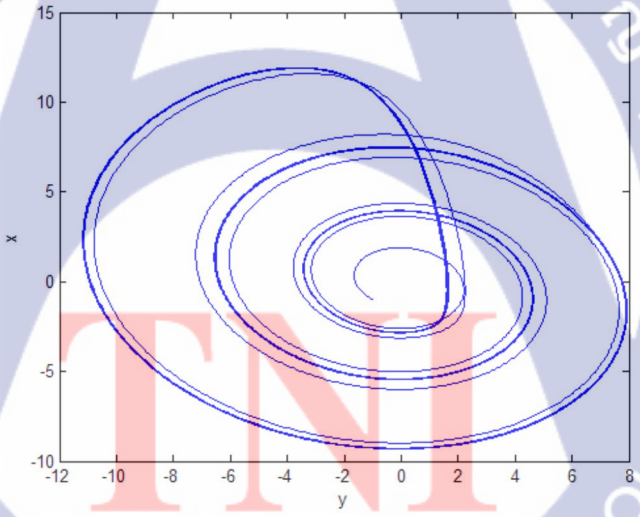

Figure 2.42 Rössler strange attractor (phase plan x-y) presented by Said Sadoudi and Mohamed Salah Azzaz[13].

From the scheme, we note that we have two principal blocks. The Automat block and the Rössler block. The first one represents the head of the system. In fact, it directs the totality of the tasks of the system. It orders the Rössler block to solve the system with the RK-4 method. Once the chaotic signals (x, y and z 32 bits) are obtained, it

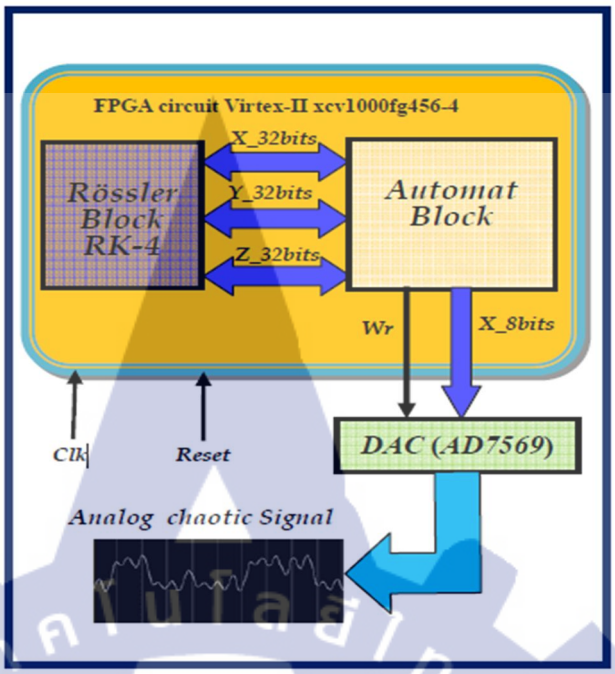

Figure 2.43 Scheme of the digital implementation of Rössler chaotic system on FPGA presented by Said Sadoudi and Mohamed Salah Azzaz [13]

truncate each one of them and then given on 8 bits, because of the DAC (AD7569) available in our laboratory works on 8 bits. Just after, the truncated chaotic signals are sending to the DAC and the process is repeating in time. Therefore, the real-time chaotic signals obtained at the output of the DAC can be visualized on an oscilloscope to confirm the exactitude of the results

A new and simple method for real-time implementation in the FPGA circuit, of continuous chaotic generator systems, is developed. The developed method consists of using only and directly the VHDL language to obtain exploitable real-time chaotic signals at the output of the FPGA circuit. Contrary to some methods existing in the literature, which uses initially the Xilinx System generator tools of MATLAB/SIMULINK to generate the VHDL code, and then pass to the implementation step. The real-time Rössler chaotic signals

Obtained are almost identical to those of the simulations under Matlab and Models. However, with this implementation we have realized good performances in term of debit and cost. In fact, after optimization we have obtained an improvement out of

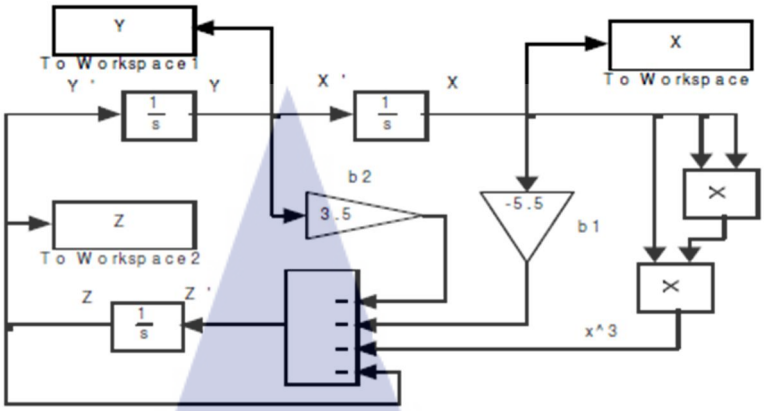

Figure 2.44 Matlab-Simulink Model of the Arneodo Attractor, Ihsan Pehlivan and M. Ali Yalcinve Selçuk Coskun [14].

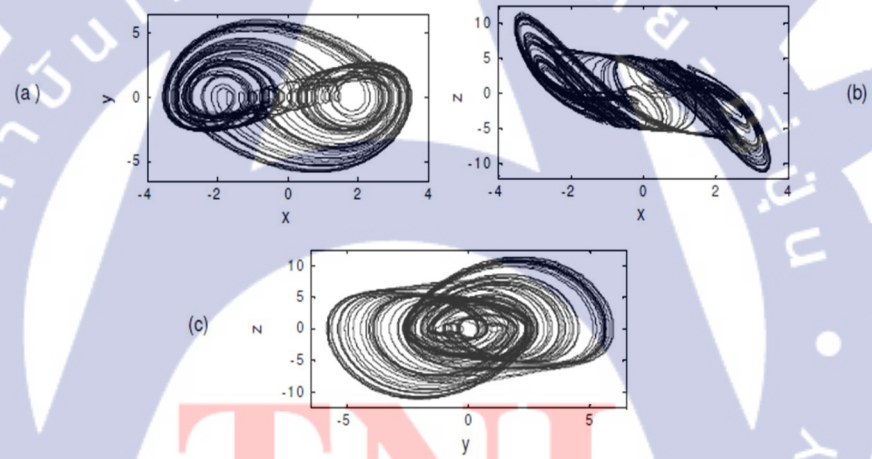

Figure 2.45 Phase portraits ((a) x-y, (b) x-z , (c) y-z) of the Arneodo Attractor when 1 2 3 4 b = - 5.5, b = 3.5, b = 1 and b = -1 , $x_0 = 0.5$, $y_0 = -1$ $z_0 = 0.5$ presented by Ihsan Pehlivan and M. Ali Yalcinve Selçuk Coskun [14].

100% of debits. In addition, our method is optimal and can be used for the implementation of all the others Rössler like chaotic systems such as Lorenz, Chua, Lü, Che etc. Therefore, this work will permit to use in choice the different continuous chaotic systems in a possible secure digital chaotic communication system.

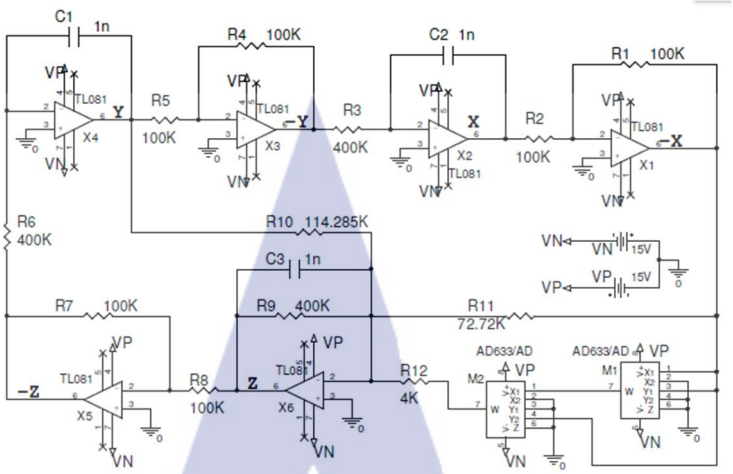

Figure 2.46 Designed Circuit Schematic of the Arneodo Attractor presented by Ihsan Pehlivan and M. Ali Yalcinve Selçuk Coskun [14].

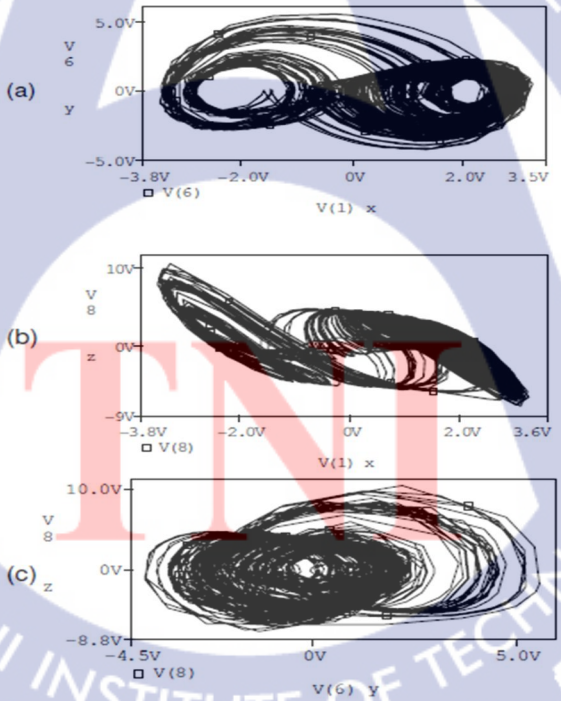

Figure 2.47 PSpice simulation results of the Arneodo Attractor, (a) x, y phase portrait (b) x, z, (c) y, z phase portraits presented by Ihsan Pehlivan and M. Ali Yalcinve Selçuk Coskun [14].

2.2.2.5Design and simulations of the Aroneodo attractor's chaotic oscillator and signal masking circuit

Ihsan Pehlivan, Yılmaz Uyarogluand M. Ali Yalcinve Selçuk Coskun[14], In this paper, synchronizing two coupled ratchet Josephson junctions subjected to a quasiperiodic field is achieved. In the limit of weak perturbation of irrational frequencies equal to the square root of the transcendental number π and for small damping parameters, phase locking occurs as the coupling between both junctions is increased. It turns out that the transition from non-synchronous to synchronous chaotic state does not involve attractors appearing and disappearing. The undertaken symmetry analysis of the system demonstrates the suppression of the massive phase fluctuations as the coupling rises, allowing chaos synchronization between both junctions to take place. The calculations also reveal the persistence of the synchronous state for high coupling strengths, taking into consideration the symmetry particularity of the external drive and potential

Following nonlinear autonomous ordinary differential equations are the Arneodo chaotic system.

$$\begin{aligned} \dot{x} &= y \\ \dot{y} &= z \\ \dot{z} &= -b_1 \cdot x - b_2 \cdot y - b_3 \cdot x^3 \end{aligned} \tag{2.40}$$

The Lyapunov exponents of the Arneodo Attractor are 0.232, 0, and -1.232. Namely, only one positive LE is present. The Figure 2.44 and Figure 2.45 Show the Simulink modeling and the simulation results of the Arneodo Attractor respectively. Figure 2.46 shows the circuit schematic for implementing the Arneodo Attractor. We use TL081 op-amps, the Analog Devices AD633JN multipliers, appropriate valued resistors and capacitors for Spice simulations. The circuit is supplied ±15 V power supplies. Acceptable inputs to theAD633 multiplier IC are –10 to +10 V. The resistors R1-R12 are all shown with nominal values in Figure 3 – Figure4 also shows Spice simulation results of this circuit. Electronic circuit Spice simulations of this circuit are implemented for b = - 5.5, b = 3.5, b = 1, b = -1parameters and initial conditions x_0 = 0.5, y_0 = - 1, z_0 = 0.5. Matlab-Simulink and Spice simulation results of Arneodo \

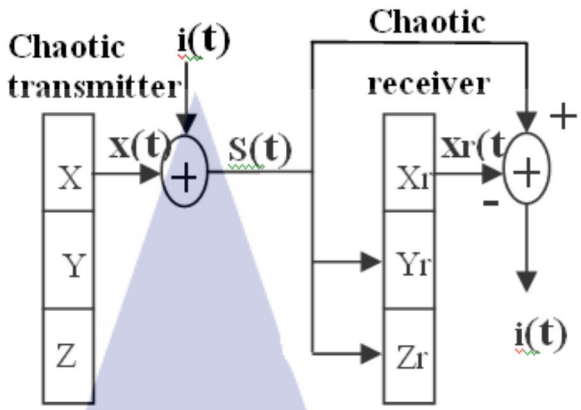

Figure 2.48 Principle scheme of a general secure communication system with masking technique presented by Ihsan Pehlivan and M. Ali Yalcinve Selçuk Coskun [14].

Attractor. Figure 2.47 give the same conclusions. Due to the fact that output signal can recover input signal, it indicates that it is possible to implement secure communication for a chaotic system. Figure 2.48 shows the principle scheme of a general secure communication system that employs the masking technique. Figure 2.48 shows Matlab Simulink modeling of chaotic masking communication circuit of the Arneodo Attractor.

The presence of the chaotic signal between the transmitter and receiver has proposed the use of chaos in secure communication systems. The design of these systems depends on the self-synchronization property of the Arneodo Attractor. Transmitter and receiver systems are identical except for their initial values, in which the transmitter system are 0.5, -1, 0.5 and the receiver system are 0.5, 1, and 0.5 as shown in Figure 2.49. It is necessary to make sure the parameters of transmitter and receiver are identical for implementing the chaotic masking communication. In this masking scheme, a low-level message signal is added to the synchronizing driving chaotic signal in order to regenerate a clean driving signal at the receiver. Thus, the message has been perfectly recovered by using the signal masking approach through cascading synchronization in the Arneodo Attractor. Computer simulation results have shown that the performance of Arneodo Attractor in chaotic masking and message recovery.

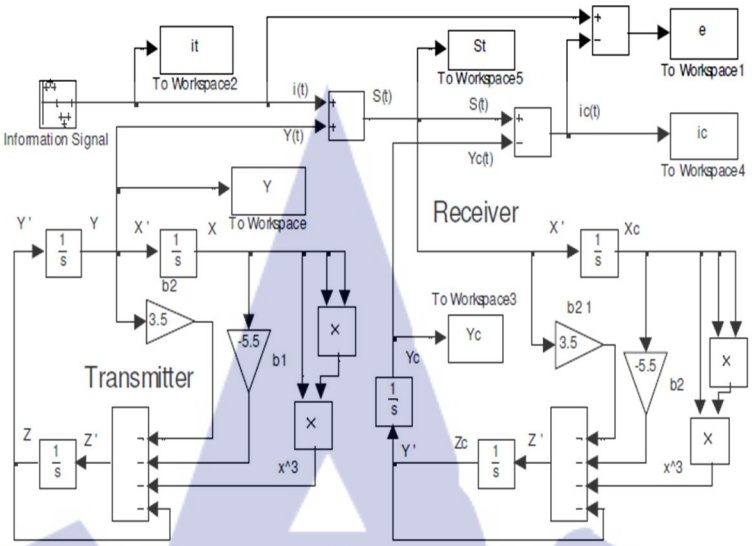

Figure 2.49 Simulink modeling of chaotic masking communication circuit of the Arneodo Attractor presented by Ihsan Pehlivan and M. Ali Yalcinve Selçuk Coskun [14].

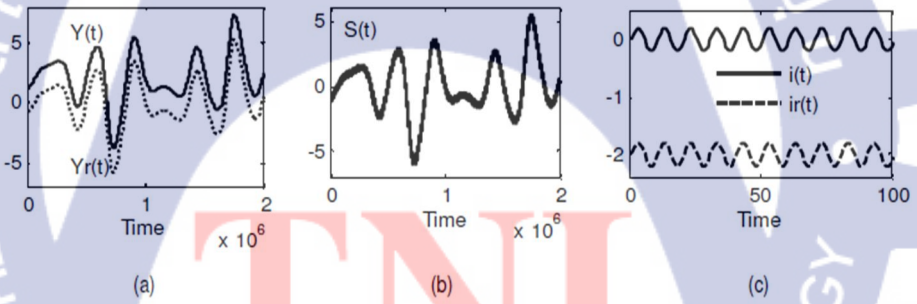

Figure 2.50 Simulink outputs of Masking Communication Scheme of Arneodo Attractor (a) Drive (y) and response (yr) system chaotic signals vs. Time, (b) Transmitted signal S(t) = y(t) + i(t), c) Information i(t) and retrieved ir(t) signals(sinus signal) has 0.2V amplitude and frequency 10 KHz presented by Ihsan Pehlivan and M. Ali Yalcinve Selçuk Coskun [14].

One disadvantage of using one-way coupling method is that compared to this cascading method, it takes longer to synchronize the coupled systems, especially when the coupling parameter is small. This may cause problems in practical

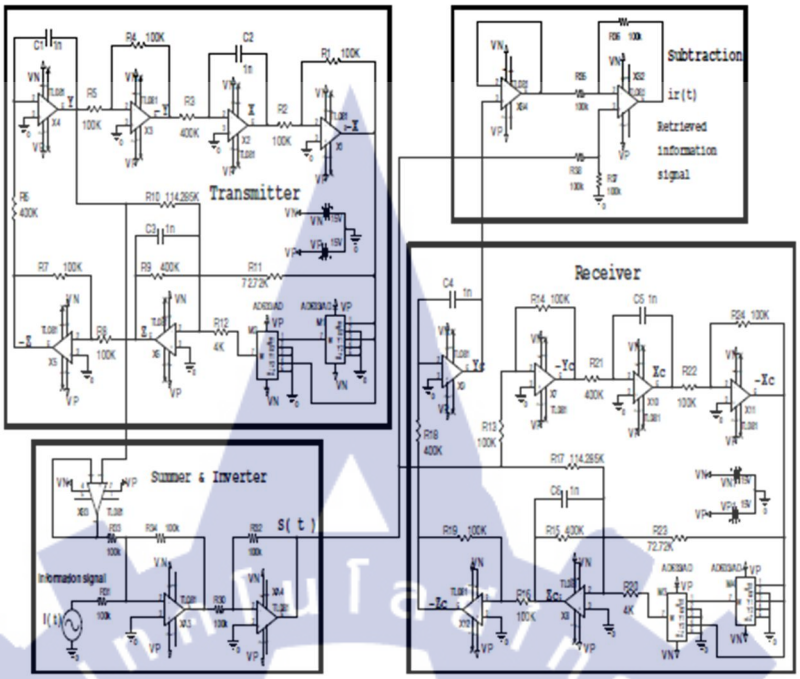

Figure 2.51 Arneodo Attractor Chaotic Masking Communication Circuit presented by Ihsan Pehlivan and M. Ali Yalcinve Selçuk Coskun [14].

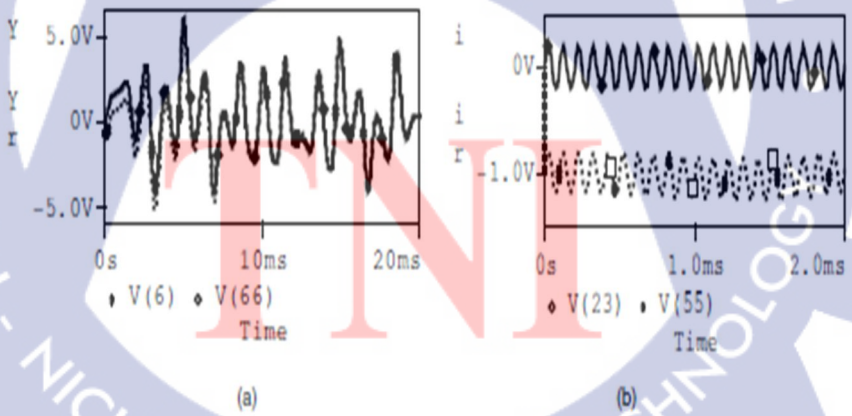

Figure 2.52 Spice outputs of Arneodo Attractor Masking Communication Circuit (a) Drive system y signal and response system y_r signal vs. time (b) Information and retrieved signal (0.2 V, 10 KHz)presented by Ihsan Pehlivan and M. Ali Yalcinve Selçuk Coskun[14].

applications such as secure communications since information may be delayed or lost during the first period of matching time.

Transmitter and receiver circuits are identical except for their initial values, in which the transmitter circuit are 0.5, -1, 0.01 and the receiver circuit are 0.5, 0, 0.5 as shown in The transmitted signal is a sinus wave of amplitude 0.2volts and of 10 KHz frequency. The sinus wave signal is added to the generated chaotic x signal, and the S(t)= y +i(t) is feed into the receiver. The chaotic y signal is regenerated allowing a single subtraction to retrieve the transmitted signal, *[y+i(t)]-y r = i(t),* If *y = yr.* This is a result of synchronization as in Figure 2.50.(a). Figure 2.50 (c) shows the information signal-sinus wave and the retrieved signal output of scope. Figure 2.51 shows the circuit schematic for implementing the Arneodo Attractor's Chaotic Masking Communication. Figure 2.51 shows Spice simulation results of this Chaotic Masking Circuit. The transmitted signal is as minus wave of amplitude 0.2V and frequency 10 KHz. Figure 2.51. Simulink and Spice simulations Figure 2.49, 2.50 of chaotic masking circuit give the same conclusions.

This paper focuses on the Arneodo Attractor's chaotic oscillator circuits and their applications in signal masking communications. Arneodo Attractor's chaotic oscillator circuits were designed and simulated. Chaotic signal masking circuits were realized using Matlab-Simulink and Spice program. Related figures in Figure 2.50 - 2.52 point out that Matlab-Simulink and Spice outputs prove the same conclusions. We have demonstrated in simulations that chaos can be synchronized and applied to secure communications. We suggest that this phenomenon of chaos synchronism may serve as the basis for little known Arneodo Attractor to achieve secure communication. Simulation results are used to visualize and illustrate the effectiveness of Arneodo chaotic system in signal masking. All simulations results performed on Arneodo chaotic system are verified the applicable of secure communication.

2.2.2.6 Phase synchronization in mutually coupled chaotic Josephson junctions: effect of symmetry and incommensurate frequencies

Sameer Al-Khawaja(2010), The nonlinear chaotic autonomous Arneodo system is algebraically simple but can generate complex chaotic attractors. In this

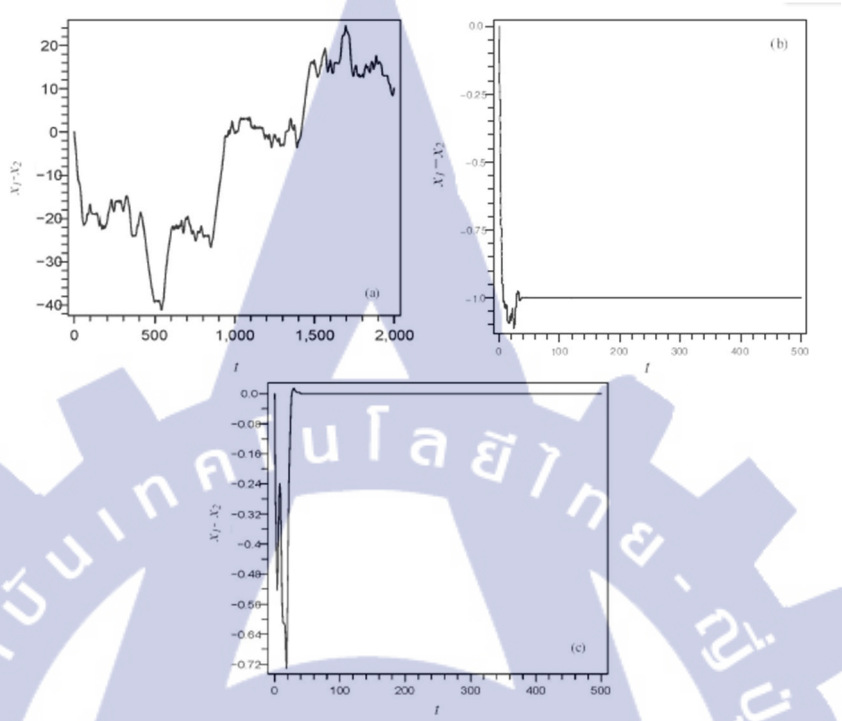

Figure 2.53 (a) The phase difference dynamics of the decoupled ratchets ($\varepsilon = 0$), $\alpha_1 = \alpha_2 = 0{:}01$, $a_1 = a_2 = 0{:}08092$, $a_3 = a_4 = 0{:}08092$, $n = \omega_1/\omega_2 = \sqrt{\pi}$, $m = \omega_3/\omega_4 = \sqrt{\pi}$. (b) The phase difference dynamics for $\varepsilon = 0{:}32$, the phase is bounded andsettled at a negative direction before the fulfillment of synchronization. (c) Complete phase synchronization at $\varepsilon = 0{:}66$ after nearly 40 s transient time and for the same parameters as in (a) and (b) presented by Sameer Al-Khawaja [15],

paper, Arneodo Attractor's chaotic oscillator circuits were designed and simulated. Also Arneodo Attractor is addressed suitable for chaotic masking communication circuits using Matlab/Simulink and Orcad-PSpice programs. We have demonstrated in simulations that chaos can be synchronized and applied to signal masking communications. We suggest that this phenomenon of chaos synchronism may serve as the basis for little known Arneodo attractor to achieve signal masking communication applications. Simulation results are used to visualize and illustrate the

effectiveness of Arneodo chaotic system in signal masking. All simulations results performed on Arneodo chaotic system are verified the applicable of secure communication. The phase θ of an under damped Josephson junction can be described by the following nonlinear differential equation

$$\omega_p^{-2}\frac{d^2\theta}{dt^2}+\omega_c^{-1}\frac{d\theta}{dt}+\frac{dU(\theta)}{d\theta}=F(t) \tag{2.41}$$

Where ω_p, ω_c are the plasma and characteristic frequency respectively, and linked to the junction parameters, such as the critical current, shunt resistance and capacitance. The third term on the left in Equation (2.41) represents the derivative of the potential U(θ) ascribed to the Josephson tunneling fluxions, which is considered asymmetric of the ratchet type. F(t) is the external time-dependent excitation that is normally taken in the form of current. After having performed a proper normalization Equation (2.41) could be assimilated, in the absence of any noise components, to the inertial equation of a particle moving in one dimension under the influence of a quasiperiodic external driving in a ratchet potential, such that

$$\ddot{x}+\alpha\dot{x}+\frac{dU(x)}{dx}=a_1\cos(\omega_1 t)+a_2\cos(\omega_2 t) \tag{2.42}$$

Since we can set $\omega_1/\omega_2 = n$, for which n can be rational or irrational depending on $\omega_{1;2}$values, we can reformulate Eq. (2) as a three-dimensional system in (x; y; z),so that it yields

$$\begin{aligned}\dot{x}&=y\\ \dot{y}&=a_1\cos nz+a_2\cos z-\alpha y-\frac{dU(x)}{dx}\\ \dot{z}&=\omega_2\end{aligned} \tag{2.43}$$

Synchronization between two coupled ratchets Josephson junction's under the influence of a quasi-periodically varying field have been examined. The system has been modeled using the coupled rotators equations in the weak perturbation and low

damping limit, for which irrational relation between the frequencies has been considered. For zero coupling, the dynamics were highly uncorrelated with initially non-identical and non-diffused attractors, becoming identical but diffused as the coupling ε reached 0.66. The latter transition from non-synchronized to synchronous chaotic state is not associated with attractors appearing and abolishing as our results show. The synchronization state also permanently and markedly retains for higher than0.66 coupling strength. The analysis of the symmetry properties related to the external excitation and ratchet potential of tunneling flux quanta has further demonstrated that the symmetry of the system is broken. The corresponding enormous phase fluctuations prevailing for the case of decoupled junctions can be quenched as the coupling is gradually raised in the system, allowing phase–phase locking to take effect and synchronization is thereby achieved. We put emphasis on exploring chaos synchronization in solution Josephson junctions, for which spatial contributions may be influential on the transport characteristics. Controlling chaos in such systems is of mounting interest especially for the implementation of directed transport in inertial solution

Chapter 3
Research Methodology

This thesis is based on the chaotic theory and dynamical system and applications on secure communication. The research methodology includes the study of theories, observation, comparison, analysis and experimentation. The research for secure communication based on the jerk function can be performed through the equation model by Jerk chaotic application. The simulation approach concerns with generalization and the formulation of chaos theory until the circuit implementation.

3.1 Overall Research Process mainly study in 5 directions consist as follows

3.1.1 Study Chaos theory and dynamical systems.

3.1.2 Study the chaotic circuits and synchronizations in secure communication systems

3.1.3 Design low cost-effective chaotic circuit

3.1.4 Simulation and create of chaos attractor and chaos circuit

3.1.5 Design and implement the chaos-masking secure communication system

3.2 Utilizing Data

To generalize the form of the chaotic oscillator, the simulated data in the parametric excitation include;

3.2.1 I_s: reverse saturation currents of diode

3.2.2 V_D: voltage drop across the diode

3.2.3 n: non-ideality factor of diode

3.2.4 V_T: thermal voltage at room temperature

3.2.5 R_a: R adjust value variable a

3.2.6 R_b: R adjust value variable b

3.2.7 x, y, z : variable x, y, z

3.2.8 a, b: variable a, b, c

3.3 Research Tools

In the thesis, the entire of simulation results were perform through MATLAB® version R2008a.

3.4 Data Analysis Methods

3.5.1 Numerical analysis of chaotic theory such as Eigen-value and Jacobian matrix which specify the characteristic of the chaotic behavior in phase space diagram.

3.5.2 The mathematic simulation function were analyzed though MATLAB version R2008 program as an indicating tools for detect the chaotic behavior such as positive Lyapunov (LE^{+}) indicate the systems is in chaotic state where $D_{KY}>2$ and complex in bifurcation diagram can be also obtain in chaotic state.

3.5 Research Procedures

3.6.1 Analyze the chaotic model through the dynamic system by using time-scaling method, Eigen value, Eigen-Vector, Jacobian-Matrix and Stability analysis.

3.6.2 Use the numerical result from 3.6.1 to analyzed by chaotic indicators such as attractor, time-domain, Poincare' section, Bifurcation, Lyapunov diagram and Kaplan-York dimension.

3.6.3 Optimize the system parameters in 3.2. And the research will also enhance the model of chaotic Jerk function by generalize the form of the jerk oscillator equation.

3.6.4 Implement the 3.3 circuit and demonstrate the chaotic circuit application in the constructed Circuit.

3.6 Conclusions

Secure communication based on chaotic oscillator using parameters optimization and measurement can be performed in this thesis as chaotic-masking method to enhance the accuracy of the system and also implementation of circuit. The method proposed in this thesis has been utilized advance knowledge of chaotic theory

and dynamic systems such as mathematical analysis corresponding its simulations complicate data analysis and also the extremely small jerk oscillator circuits.

Chapter 4

Experiment and Result

This chapter deals with three chaotic systems for application to secure communications. Dynamical properties are described base including equilibrium, eigenvalues, Poincare, frequency spectrum, bifurcation, chaotic attractor and chaotic synchronization. This chapter focuses on design of chaotic oscillator and signal masking circuit using Matlab-Simulink for simulation and implement chaotic circuit for secure communication.

4.1 Rössler Attractor using Diode Equation

In 1963, Edward Lorenz [21] encountered sensitively dependent initial conditions of an atmospheric convection model while performing numerical simulations leading to the discovery of the Lorenz system with seven-terms in three-dimensional ordinary differential equations and two quadratic nonlinearities. In 1976, Rössler [24] proposed a chaotic system with seven terms and a single quadratic nonlinearity, which is algebraically simpler than Lorenz system. In addition, a single folded-band attractor of Rössler system is topologically simpler than a two-scroll Lorenz attractor. Such Lorenz and Rössler systems have consequently led to considerable research interests in searching for new chaotic systems with fewer terms in ODEs [5-10] or more complex attractor topology.

Several chaotic systems with fewer than seven terms and two quadratic nonlinearities continuously been reported as variants in Lorenz system family. Complex three-scroll and four-scroll attractors based on Lorenz system have also been suggested through the use of three or more quadratic nonlinearities. On the other hand, simple chaotic systems with a single nonlinearity similar to Rössler system are rarely found. In fact, Rössler himself had proposed another system with six terms and a single quadratic nonlinearity in 1979 [30-35]. In 1994, Sprott [15-19] found fourteen cases with six terms and a single quadratic nonlinearity through an intensive numerical computer search. Recently, many simple systems have been proposed in simple Jerk equations with single quadratic or non-quadratic nonlinearities. Despite

the fact that these simple Jerk chaotic systems with a single nonlinearity potentially resemble the single folded-band Rössler attractor , the Kapelan-York dimension (D_{KY}) as a measure of complexity is somewhat lower than the original Rössler attractor that possesses the greatest value of D_{KY} =2.1587. This leads to a question of whether the original Rössler system in dynamic forms can be simplified into fewer terms with simple nonlinearity, or modified for more complex attractor. No simplifications of Rössler system has never been found so far.

4.1.1 Dynamical Properties

Based on the Rössler system proposed in 1979, the first and the second equations, i.e. $\dot{x} = -y - z$ and $\dot{y} = x + ay$, initiate a normal band of the attractor through an outward spiral motion into the x-y phase plane. Nonlinear interactions between x and z variables in the third equation, i.e. $\dot{z} = b + z(x - c)$, form an additional folded band to the overall attractor. It is noticeable that the folded band in Rössler attractor rises and returns exponentially in z-dimension especially for positive values of x variable under the flows. This aspect implies that the third equation may be modified through the use of an exponential nonlinearity. Therefore, a new chaotic system is therefore presented in three-dimensional autonomous ODEs expressed in a general form as

$$\begin{aligned} \dot{x} &= -y - z \\ \dot{y} &= x + ay \\ \dot{z} &= -z + bF(x) \end{aligned} \tag{4.1}$$

where $(x, y, z) \in \Re^3$ are dynamical variables, $(a, b) \in \Re^+$ are system parameters, and F(x) is a nonlinear function required for chaos. Two particularly simple cases of the nonlinear function F(x) are presented using exponential functions. In other words,

$$F_1(x) = e^x \tag{4.2}$$

4.1.2 Numerical analysis

The existence of attractor can be described by the divergence of flows as $\nabla \cdot V = \partial\dot{x}/\partial x + \partial\dot{y}/\partial x + \partial\dot{z}/\partial x$. For a dissipative chaotic system, $p<0$ and therefore a is limited into the region $0 < a < 1$. The exponential rate of contraction is $dV/dt = e^{(a-1)}$ and hence a volume element V_0 is contracted in time t by the flows into a volume element V_0e^{-t}. Each volume containing the system trajectories shrinks to zero as time *t* approaches $+\infty$. All system orbits will be confined to a specific limit set of zero volume, and the asymptotic motion converges onto an attractor. It can be concluded that the existence of attractors is constant and independent to the nonlinear term *bF(x)*.

4.1.2.1 Bifurcations, Lyapunov Exponents, and Kaplan-Yorke Dimension

Numerical simulations have been performed in MATLAB using the initial condition of (x0, y0, z0) = (1, 0, 1). In fact, the initial condition is not crucial, and can be selected from any point that lies in the basin of attractor. In order to find the control parameter *a* that offers the maximum values of chaoticity and complexity, Figure 4.1 shows the bifurcation diagram of the peak of z (z max) versus the parameter *b*. It is seen in Figure 4.1 that the system exhibits a period-doubling route to chaos. In addition, Figure 4.2 shows the plots of the positive LE versus the parameter b. The chaoticity is a measure of the greatest LE, which is the average rate of growth of the distance between two nearby initial conditions that grows exponentially in time when averaged along the trajectory, leading to long-term unpredictability property. The Lyapunov exponents can be employed for the estimation of the rate of entropy production and the fractal dimension commonly known as Kaplan-Yorke dimension D_{KY}, i.e.

$$D_{KY} = j + \frac{1}{|LE_{j+1}|}\sum_{i=1}^{j} LE_i = k + \frac{LE_1 + LE_2}{|LE_3|} \tag{4.3}$$

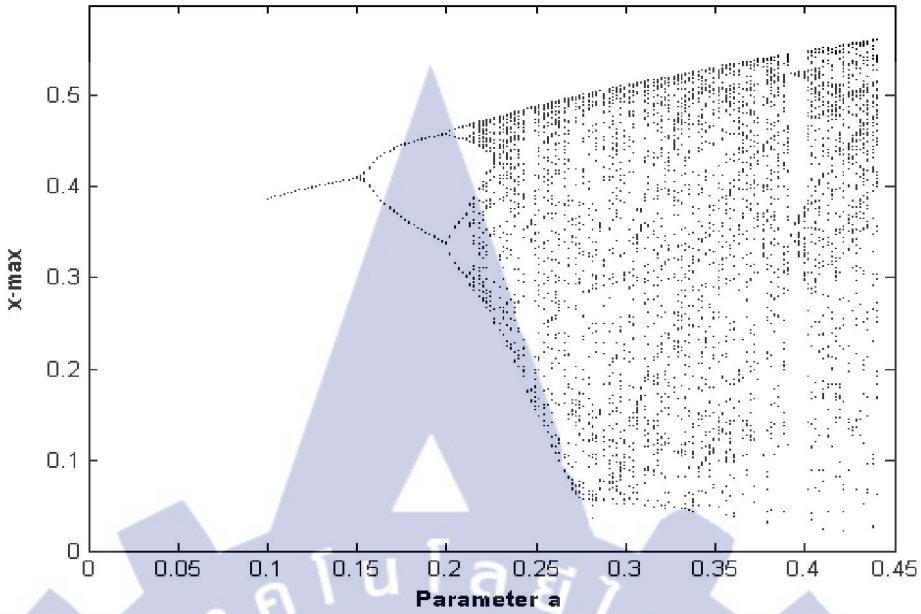

Figure 4.1 Bifurcation diagram fixed b=0.0007.

Where k is a non-integer constant, and typically equals to 2 for three-dimensional chaotic systems.

4.1.2.2 Numerical Equilibria and Eigenvalue

The Jacobian of the system is

$$\begin{aligned} 0 &= -y - z \\ 0 &= x + ay \\ 0 &= -z + be^{x} \end{aligned} \tag{4.4}$$

where x, y and z are the state variables and a, bare positive real constants. The system displays a typical chaotic attractor when a = 0.2 and b=0.00045. The new system has equilibrium points (0, 0, 0)

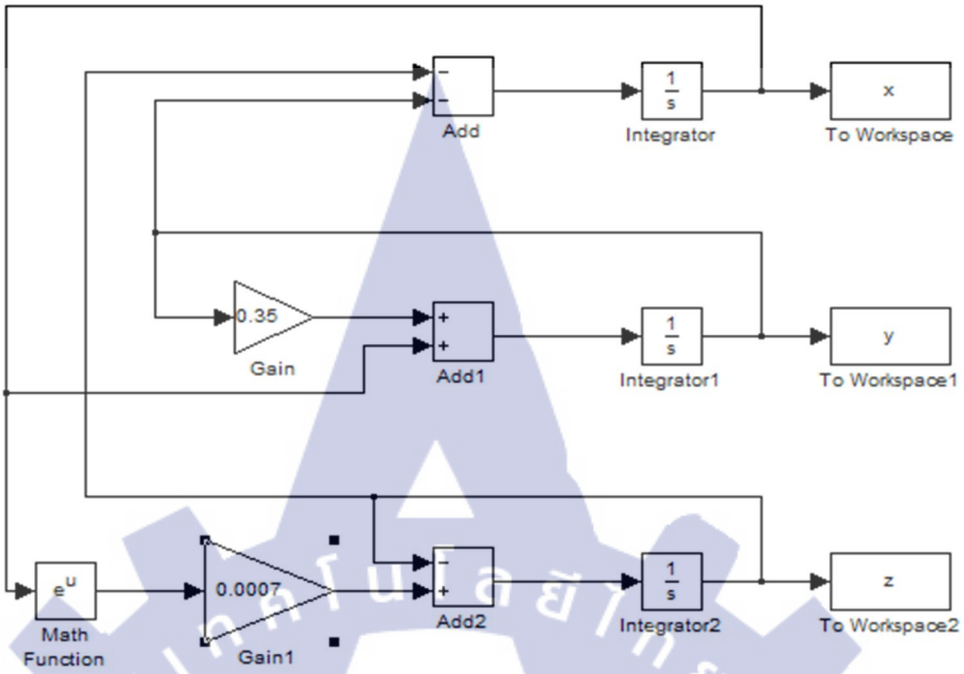

Figure 4.2 Chaotic scheme Rössler attractor using Matlab Simulink.

$$J = \begin{bmatrix} 0 & -1 & -1 \\ 1 & a & 0 \\ bF' & 0 & -1 \end{bmatrix} \tag{4.5}$$

Applying the equilibrium point P into this Jacobian matrix and analyzing $|I\lambda - J| = 0$ reveal a resulting characteristic polynomial as follows:

$$\lambda^3 + (1-a)\lambda^2 + (bF' - a + 1)\lambda + (abF' - 1) = 0 \tag{4.6}$$

According to the Routh–Hurwitz stability criterion, the system (1) is unstable when $F' < (1 + (1-a)^2)/(b-2ab)$. Note that dynamic behaviors depend on two parameters aandb, and can be characterized completely by the plot of parameter space without redundancy. For all particular values of a and b in the subsequent numerical analyses, the resulting eigenvalue λ_1 is a positive real number and λ_2 and λ_3 are a pair of

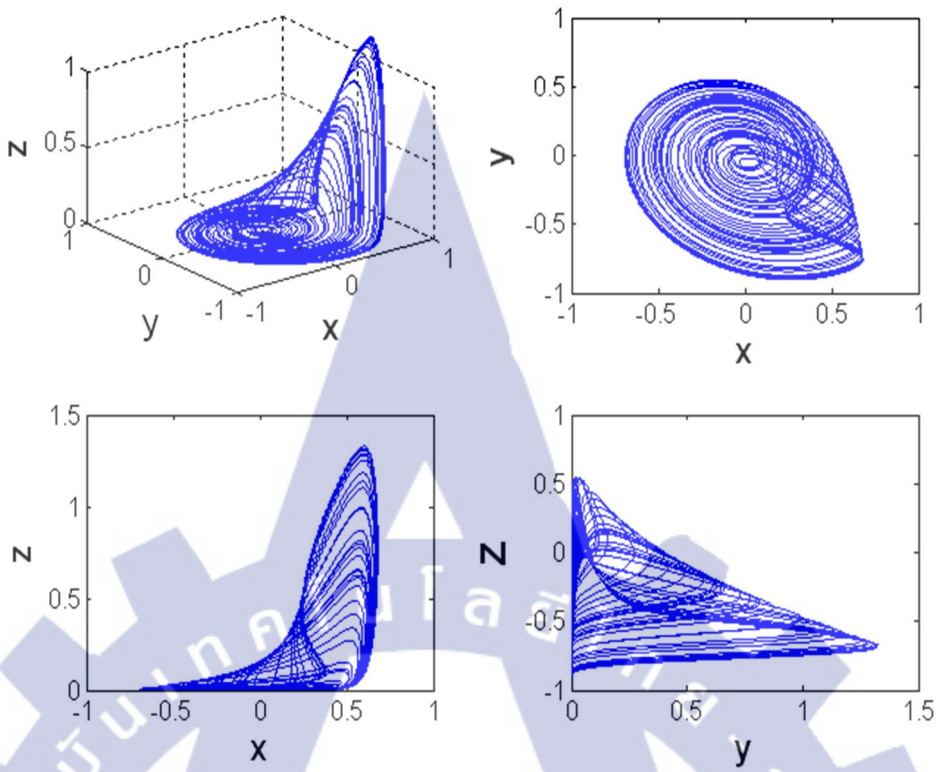

Figure 4.3 Simulation Phase portraits with $F_1(x) = e^x$ at a =0.30 and b=0.0007, LEs = (0.0638, 0, -0.8641), D_{KY} =2.0738.

complex conjugate with positive real parts, indicating that the equilibrium points are all saddle focus points

4.1.3 Secure Communication Systems based Rössler

There are number of possible methods that have been developed for synchronization in chaotic communications. In the masking method, synchronization is achieved by simply if the conditional Lyapunov exponents for the systems are negative for the given operating parameters Thus, one could simply recover the message signal from the received chaotic signal through by means of a subtraction at the receiver. This synchronization is robust against small perturbations of the carrier signal. In the chaotic modulation method the message signal becomes part of the dynamics, which is more robust because of the greater symmetry between chaotic oscillator and response. In the chaos masking technique the message information is

encoded onto the attractor by means of modulating a parameter of the chaotic oscillator, typically in a binary manner. In all these three schemes synchronization is an obvious way of recovering the original information. Fig.4.1 shows the principle scheme of a general secure communication system with masking technique the transmitter can be used as a single drive system for a dual-channel transmitter independent of its response subsystem at the receiver.

4.1.3.1 Transmitter

At the transmitter, A Modified Rössler attractor described in equation 4.1 can be used as a single drive system for a dual-channel transmitter independentof its response subsystem at the receiver as follows: A Modified Rössler System using Diode Equation and its Application toSecure Communications $\dot{x} = -y - z$, $\dot{y} = x + 0.2y$ and $\dot{z} = 0.0045e^{x} - z$. As show in Figure 4.1, the dual channel transmitter consists of two parallel. Transmitter signal. The first transmitter signal is $s_1(t) = x_t(t) + i_1(t)$,where $x_t(t)$ is a chaotic signal and $i_1(t)$ represent the first original input which is transmit. The second transmitter signal is a $s_2(t) = z_t(t) + i_2(t)$, where $Z_t(t)$ is a chaotic masking signal and $i_2(t)$ represent the second original message which is transmitter.

4.1.3.2 Receiver

At the receiver, A Modified Rössler attractor described in (a) can be used as single response subsystem for dual-channel receiver as follow: $\dot{x}_r = -y_r - z_r$, $\dot{y}_r = s_1(t) + 0.2y_r$ and $\dot{z}_r = 0.0045e^{s_1(t)} - z_r$ As show in fig. 4.1, the dual channel consist of two parallel received signals $s_1(t)$and $s_2(t)$, each of which regenerates a clean masking signal $z_r(t)$ and $x_r(t)$, respectively

4.1.4 Simulation and Experimental Results

This section, present simulation bifurcation diagram simulation chaotic attractor, application for secure communication using MATLAB-SIMULINK, implements real chaotic circuit and implement real circuit for application secure communication.

4.1.4.1 Simulation Results

4.1.4.1.1 Dynamical properties

It can also be considered from Figure 4.2 that the value of a.is relatively small when b is fixed at 0.2. Shows the bifurcation diagram of the local maxima of x versus the parameter a. The corresponding attractors in the x-y phase plane over a range of a are displayed in Figure. 4.3 where chaotic regions apparently arise after a period-doubling cascade. With reference to Figures4.3 and 4.4, the normal folded-band attractor appears when $0.36<a<0.48$ and the screw-type attractor with the third band appears when $0.47<a<0.55$. For a = 0.52, the attractor yields the largest Lyapunov exponent L= (0.1868, 0,-0.3719) and consequently the complexity D_{KY}= where $D_{KY} = 2 + (L_1+L_2)/L_3$ and $L=(L_1, L_2, L_3)$ is a set of Lyapunov exponents. For the particular cases of parameters considered above, summarizes the Equilibria, eigenvalues and types of equilibrium points of the system (4.1) with.$F_1(x) = e^x$. It can be that one equilibrium point is located very closely to the origin and involved in the flows while another is in some distance from the origin excluded from the flows. In addition, the two equilibrium points are all saddle focus nodes since the eigenvalue λ_1 is a positive real number and λ_2 and $\lambda_3$are a pair of complex conjugate with positive real parts. In conclusion, the system (4.1) with $F_1(x) = e^x$ not only contributes an addition to simple chaotic system with six terms in ODEs and a single simple exponential nonlinearity, but also offers a high complexity in terms of D_{KY}.

4.1.4.1.2 Application for chaotic communication

Due to the fact that output signal can recover input signal, it indicates that it is possible to implement secure communication for a chaotic system. Fig. 4.1 shows the principle scheme of a general secure communication system that employs the masking technique. Figure 4.4 shows Simulink modeling of chaotic masking communication circuit of the Rössler Attractor. The presence of the chaotic signal between the transmitter and receiver has proposed the use of chaos in secure communication systems. The design of these systems depends on the self-synchronization property of the Rössler Attractor. Transmitter and receiver systems are identical except for their initial values, in which the transmitter system is 1, 0, 1

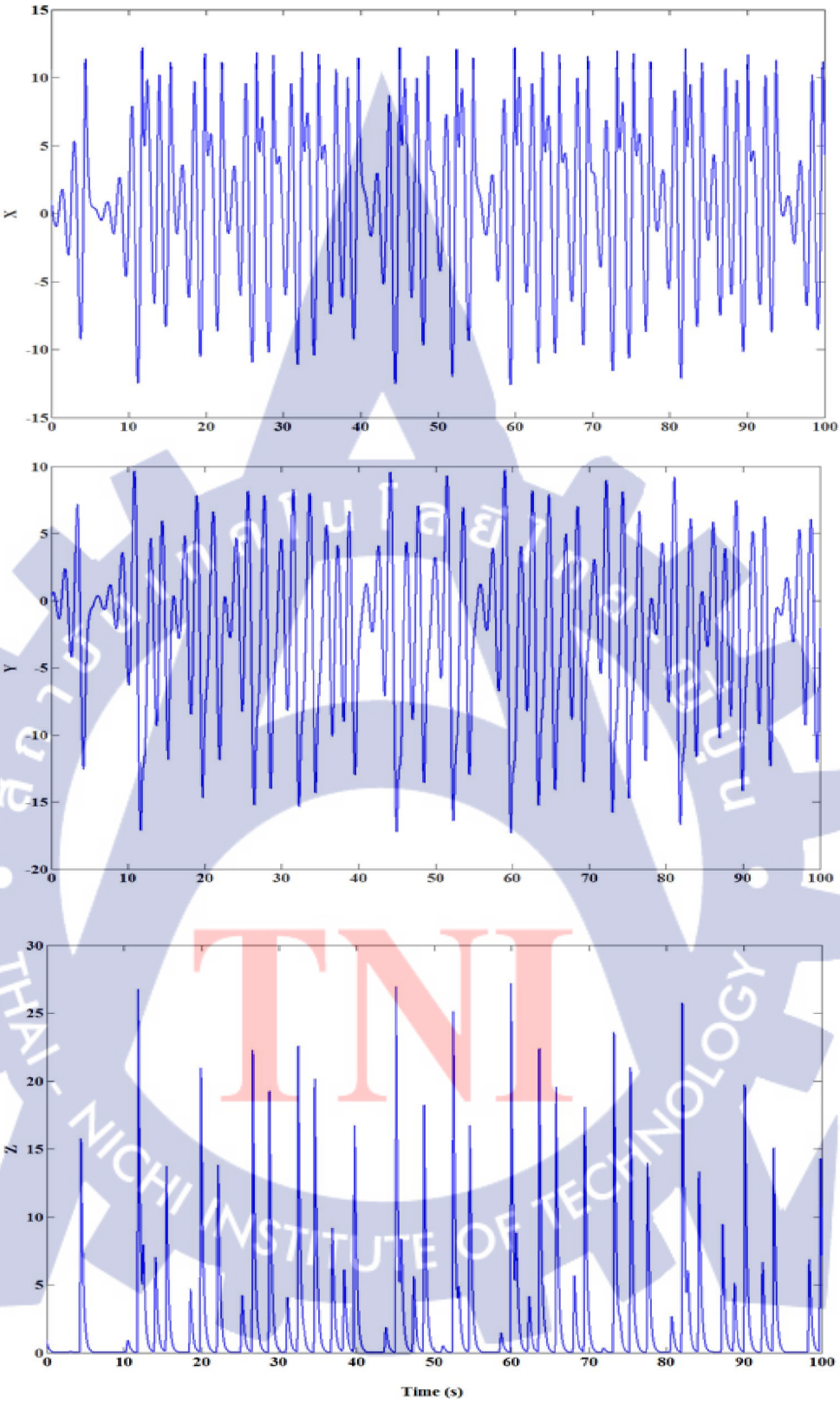

Figure 4.4 Simulation Time domain of x, y and z.

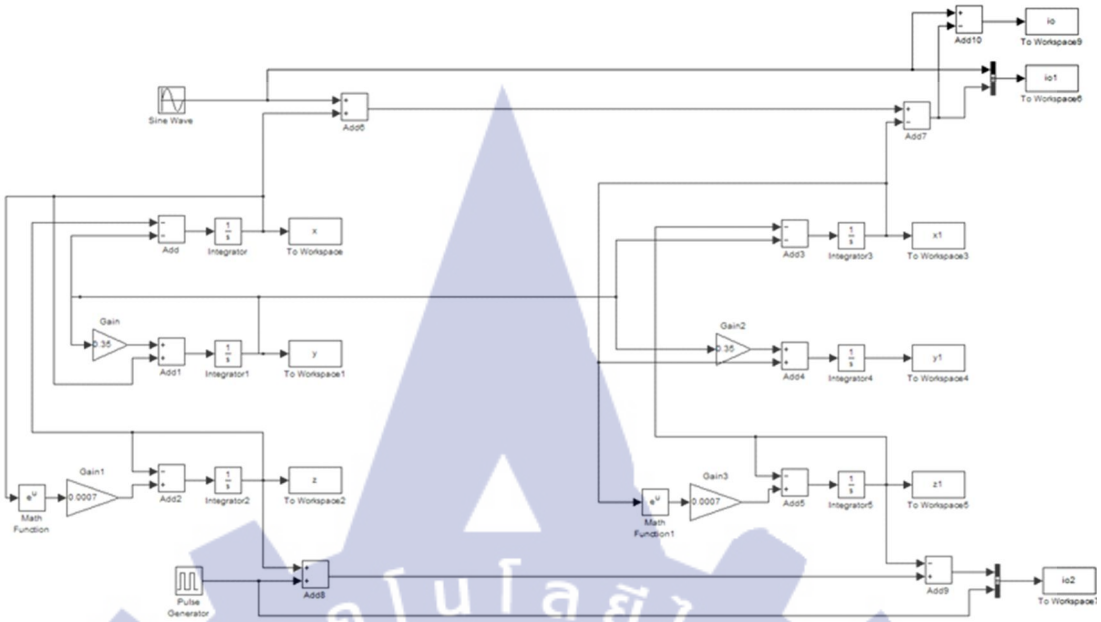

Figure 4.5 Matlab-Simulink models of chaotic communications.

and the receiver systems are 3, 0, and 3 as shown in Figure 4.5. It is necessary to make sure the parameters of transmitter and receiver are identical for implementing the chaotic masking communication. In this masking scheme, message signal is added to the synchronizing driving chaotic signal in order to regenerate a clean driving signal at the receiver. Thus, the message has been perfectly recovered by using the signal masking approach through cascading synchronization in the make sure the parameters of transmitter and receivers are identical for implementing the chaotic masking communication. In this masking scheme, a message signal is added to the synchronizing driving chaotic signal in order to regenerate a clean driving signal at the receiver. Thus, the message has been perfectly recovered by using the signal masking approach through cascading synchronization in the Rössler Attractor. Computer simulation results have shown that the performance of Rössler Attractor in chaotic masking and message recovery. One disadvantage of using one-way coupling method is that compared to this cascading method, it takes longer to synchronize the coupled systems, especially when the coupling parameter is small. This may cause problems in practical applications such as secure communications since information may be delayed or lost during the first period of matching time Rössler Attractor.

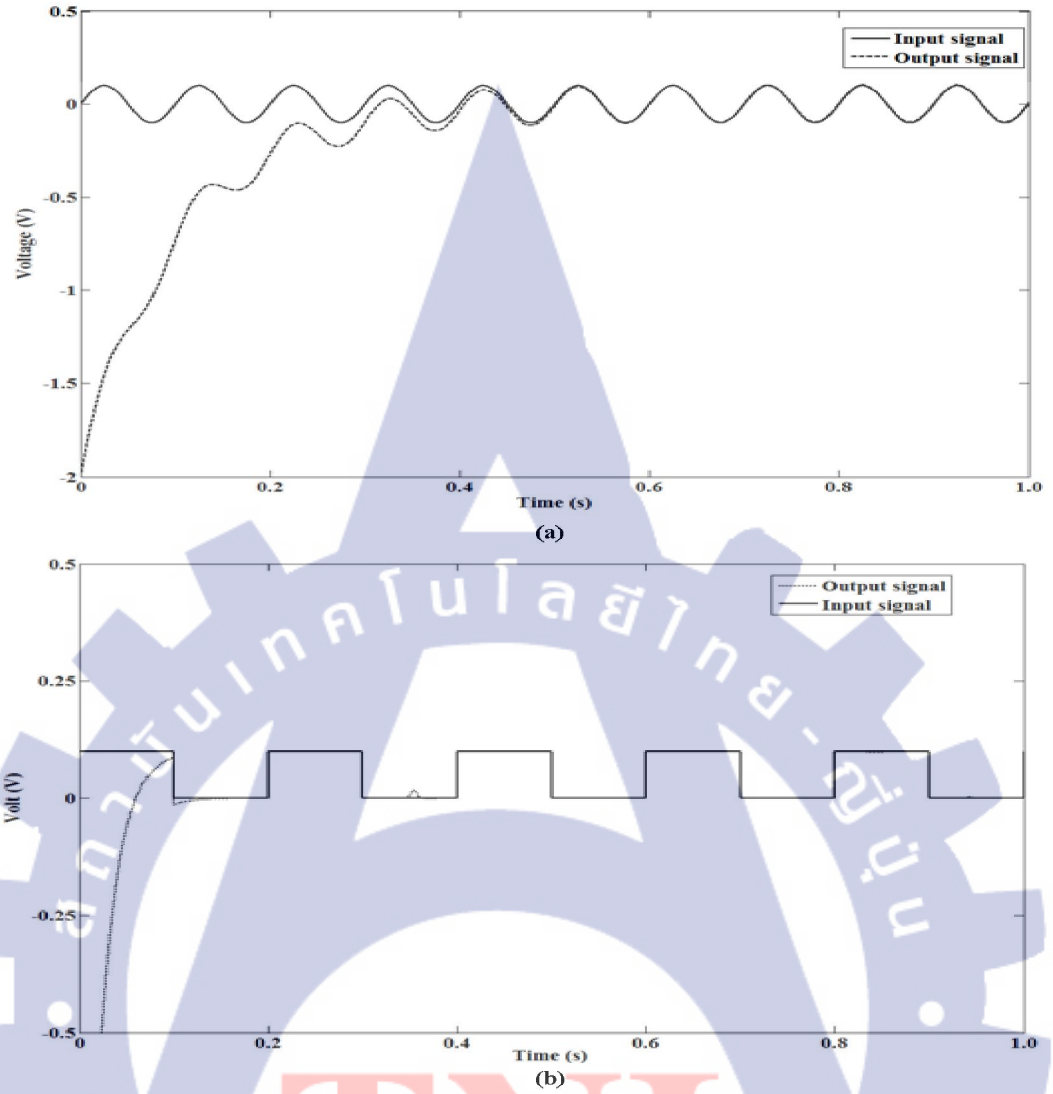

Figure 4.6 (a) Synchronization results input and recovered output signal at the receiver digital (b) Synchronization results input and recovered output signal at the receiver analog.

Computer simulation results have shown that the performance of Rössler Attractor in chaotic masking and message recovery. One disadvantage of using one-way coupling method is that compared to this cascading method, it takes longer to synchronize the coupled systems, especially when the coupling parameter is small. This may cause problems in practical applications such as secure communications since information may be delayed or lost during the first period of matching time.

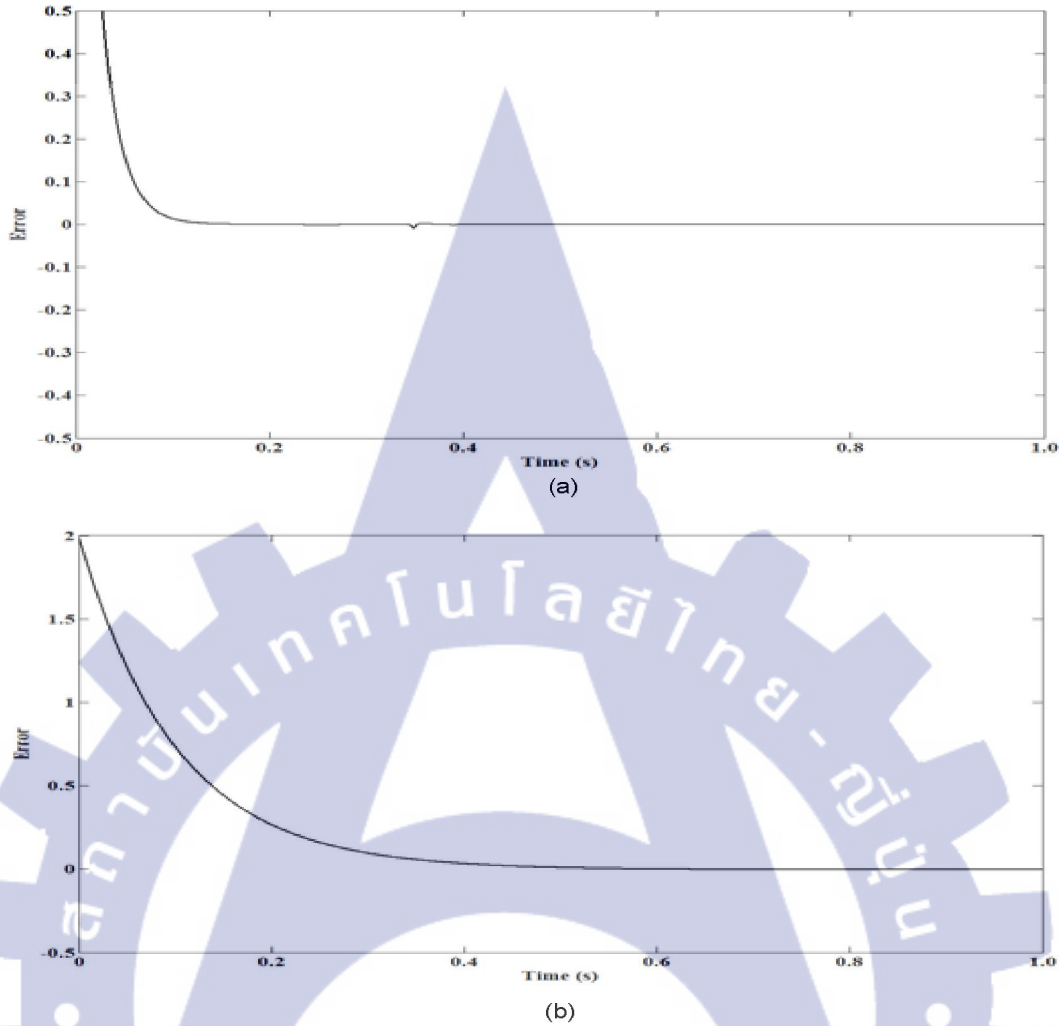

Figure 4.7 (a) Synchronize error of digital signal and (b) Synchronize error of analog signal.

Form equation 4.1, we implement schematic using by Matlab-Simulink show as Figure. 4.3 when a = 0.35 and b=0.0007 and s equilibrium points (0, 0, 0). As show Figure 4.4, chaotic attractor result simulation plot xyz, xy, yz and zx using by Matlab-Simulink.

4.1.4.2 Experimental Results

4.1.4.2.1 Dynamical properties

Fig.4.9 shows the circuit schematic for implementing real electronics circuit form eq. 4.1. We use TL081 op-amps, diode 2N4148, R =10kΩ, C=

1nF and R adjust k_1 = 44 kΩ and k_2 =0.7 kΩ. The circuit is supplied ± 9V. As show Figure 4.8, result experimental chaotic attractor from oscilloscope.

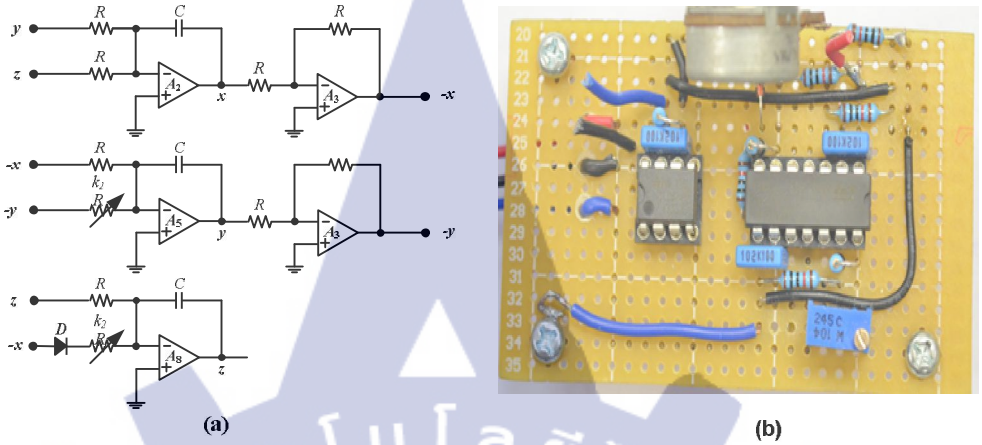

Figure 4.8 Chaotic circuits (a) design chaotic circuit and (b) real chaotic circuit

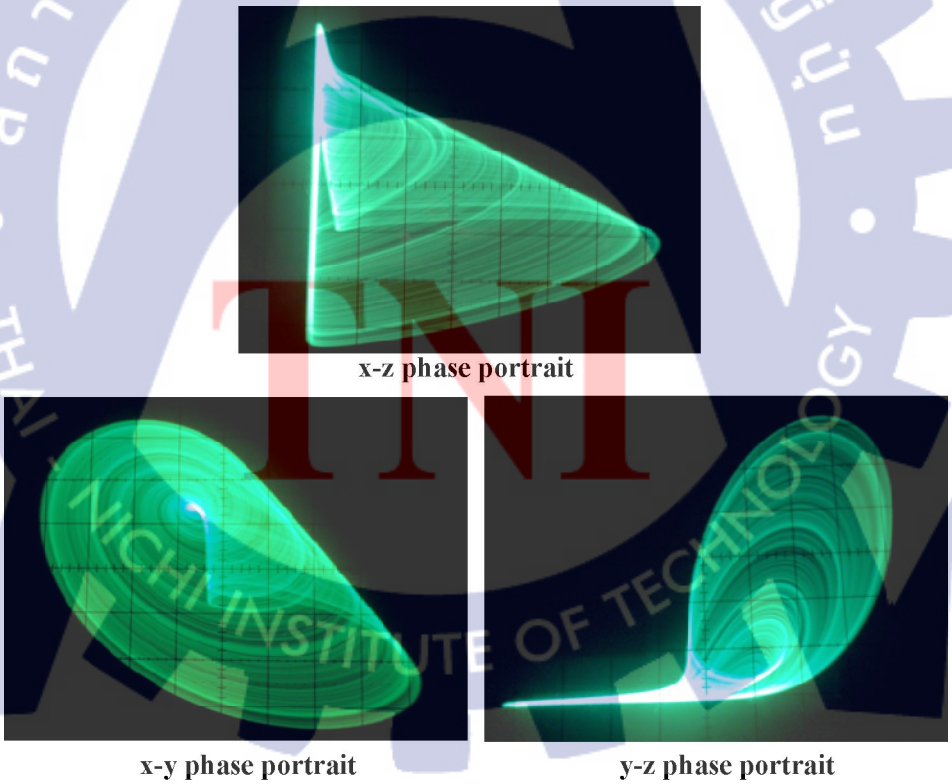

Figure 4.9 Result chaotic attractor of real electronics circuit.

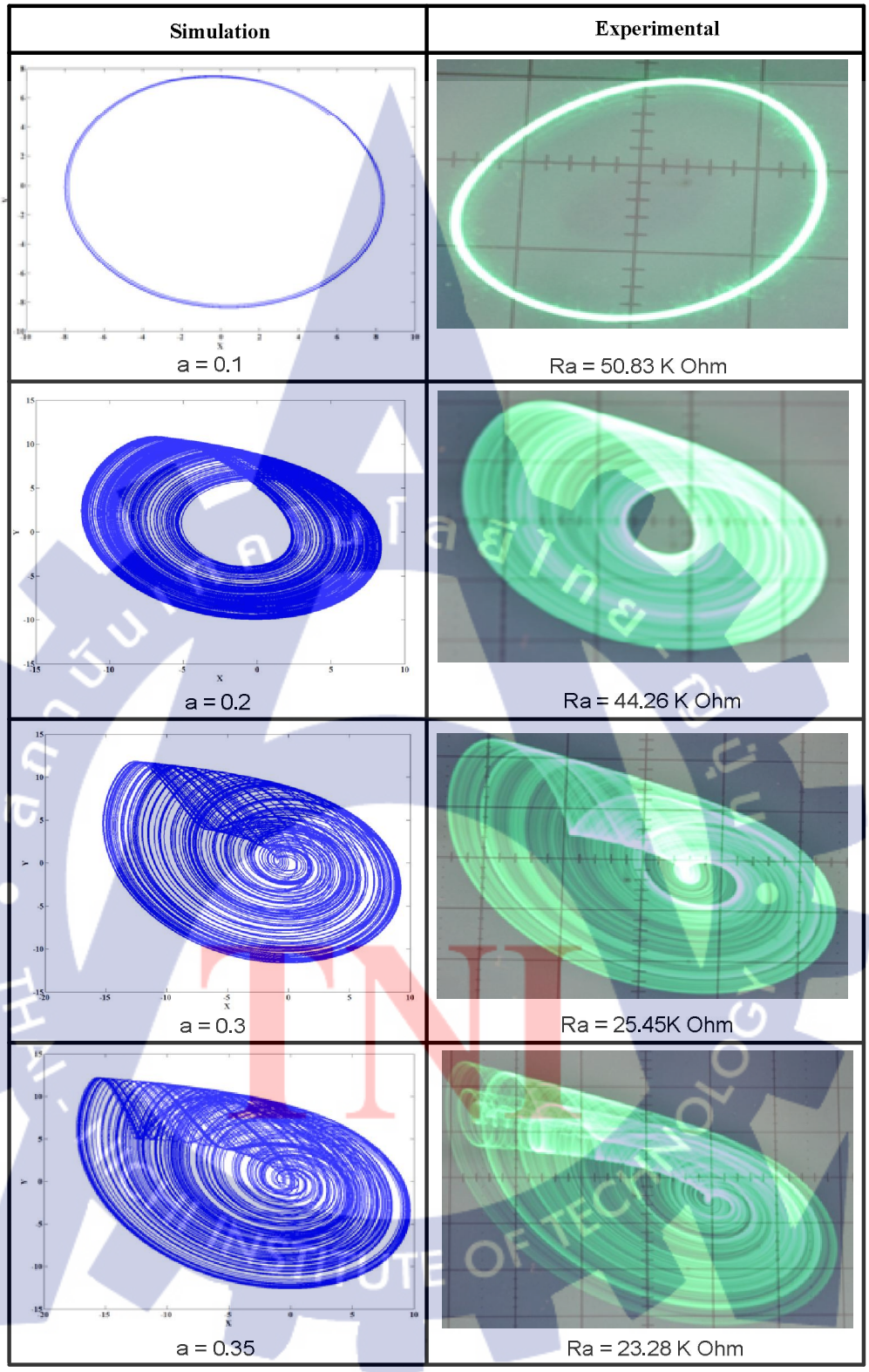

Figure 4.10 Compared between simulation and experiment when b = 0.0007 and Rb = 0.7 kΩ.

4.1.4.2.2 Chaotic communication

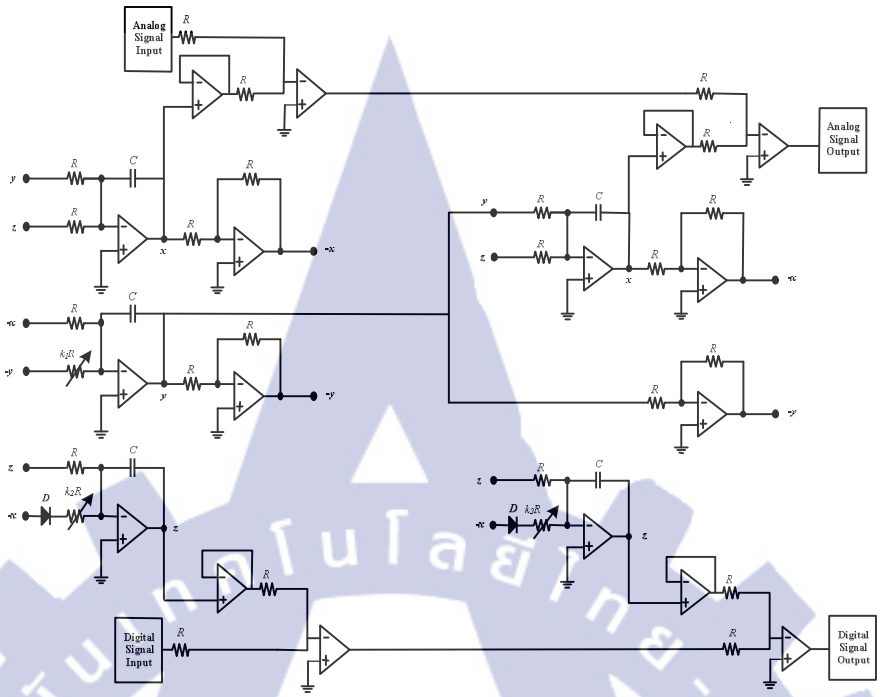

Figure 4.11 Circuit Chaotic Synchronize.

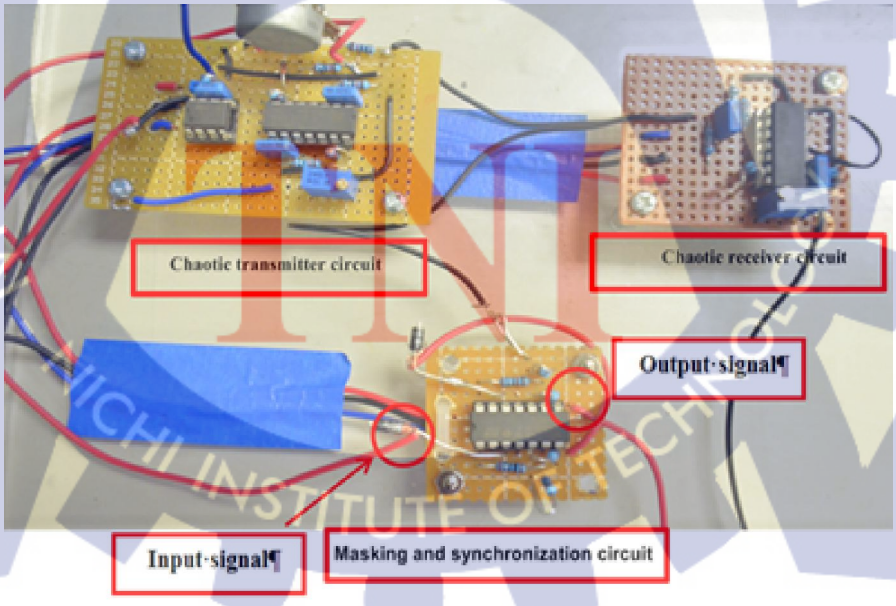

Figure 4.12 Real circuits chaotic synchronize.

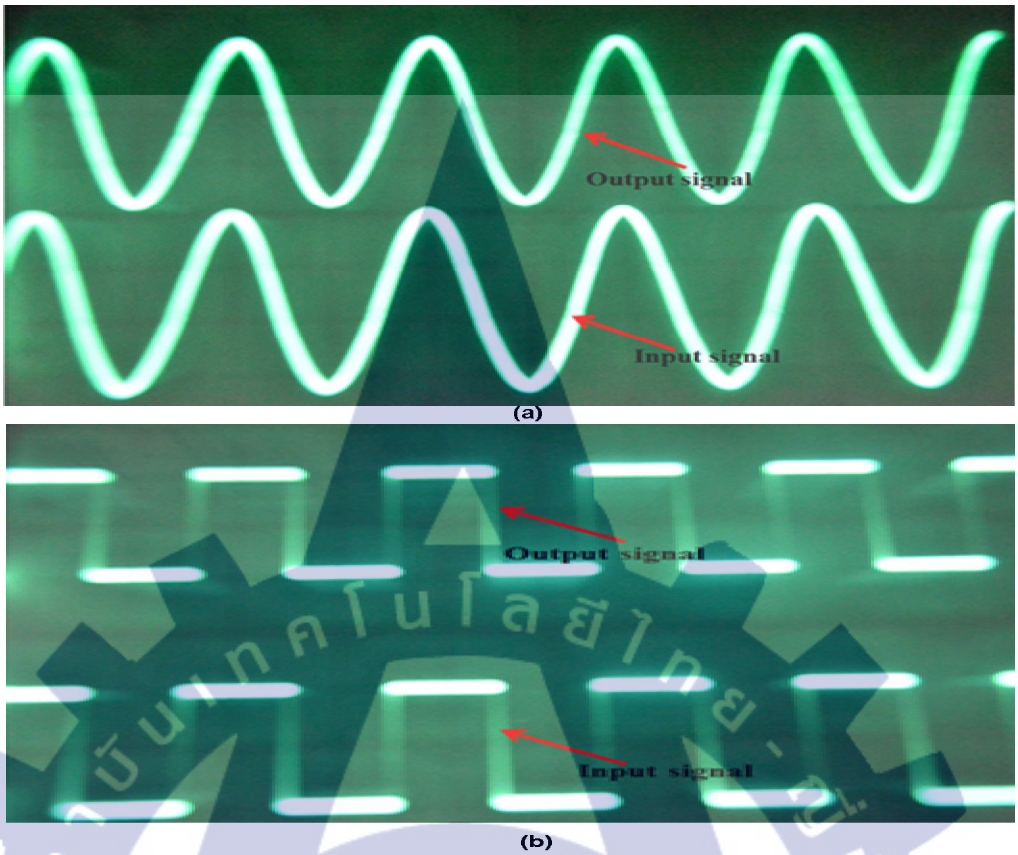

Figure 4.13 Result chaotic synchronize (a) analog signal and (b) digital signal.

This section, we implement real Electronic circuit chaotic direct synchronize for two channel input is digital signal and analog signal input as show in Figures. 4.13 - 4.14 as show, real circuit chaotic synchronize when op-amp TL084 and TL082 R = 1KΩ, C = 1nF, Ra = 25.45 kΩ and Rb = 0.7 kΩ. Diode 2N4148 and fig 4.15 shows as result chaotic synchronization

4.2 Chaotic Jerk Oscillator

This section presents a very simple autonomous RC chaotic jerk oscillator with nine electronic components. The nonlinearity required for chaos is implemented through the use of a well-known diode equation. Basic dynamical properties [35-44] are described including equilibrium, eigenvalue of Jacobian matrix, chaotic attractors, time-domain waveforms, power spectrum, and bifurcations. Potential application of

such a simple autonomous RC chaotic jerk oscillator is presented in message-masking for secure Communications.

The results show that the chaotically masked message is fully synchronized at the receiver through the use of very simple circuit. Consequently, the proposed new paradigm on secure communication schemes offers not only a simple mathematical system, but also very cost-effective circuit and system implementations.

The term 'jerk' comes from the fact that successive time derivatives of displacement are velocity, acceleration, and jerk. Most chaotic jerk oscillators have employed nonlinearity only in the x term of the jerk function. The simplest dissipative chaotic flow has, however, employed a quadratic nonlinearity in the ẋ term of the jerk function. Recently, have shown minimal jerk flow of (4.1) with nonlinearity in the $\dot{x}$ term of the form

$$\dddot{x} + \ddot{x} + x = -\alpha e^{\dot{x}} \tag{4.7}$$

In which chaos occurs for α = 0.27. Such a nonlinear function is of particular interest as it resembles diode characteristics. Sprott [6] has subsequently implemented (1) in the form

$$\dddot{x} + \ddot{x} + x = -10^{-9}\left\{e^{\left(\frac{\dot{x}}{0.026}\right)} - 1\right\} \tag{4.8}$$

The oscillator (4.7), however, requires large counts of 14 electronic components including 4 op-amps. Although the oscillator has been implemented by a minimal chaotic jerk equation of (4.7), the required number of electronic components does not seem to be minimal. It is natural to wonder in the opposite direction whether or not a slightly more complicated chaotic jerk equation may greatly reduce the large counts of electronic components for the chaotic oscillator.

This section presents a very simple autonomous RC chaotic jerk oscillator with nine electronic components. The nonlinearity required for chaos is implemented

through the use of a well-known diode equation. Basic dynamical properties are described including equilibrium, eigenvalue of Jacobian matrix, chaotic attractors, time-domain waveforms, power spectrum, and bifurcations. Potential application of such a simple autonomous RC chaotic jerk oscillator is presented in message-masking for secure Communications

The results show that the chaotically masked message is fully synchronized at the receiver through the use of very simple circuit. Consequently, the proposed new paradigm on secure communication schemes offers not only a simple mathematical system, but also very cost-effective circuit and system implementations.

4.2.1 Circuit Realizations

In an attempt to reduce the number of electronic components, the minimal form (4.7) may be modified with a slightly more complicated jerk function and a simple diode equation expressed as

$$I_D = I_S \left\{ \exp\left(\frac{V_D}{nV_T} \right) - 1 \right\} \tag{4.9}$$

In the following form

$$\dddot{x} = J(\ddot{x}, \dot{x}, x) + I_D R \tag{4.10}$$

where the voltage drop across the diode is $V_D = (\dot{x} + 2x)$, I_S is the reverse saturation current of diode, V_T is the thermal voltage at room temperature, n is the non-ideality factor of diode, R is a parameter and $J(\ddot{x}, \dot{x}, x)$ is a jerk function. Figure 4.11 illustrates an electronic circuit realization of the autonomous RC chaotic jerk oscillator, consisting of an amplifier, three resistors, three capacitors and a single diode. These components implement an integrator and a second-order RC passive filter in a feedback loop with a smaller nonlinear feedback loop containing a diode. Applying nodal analysis,

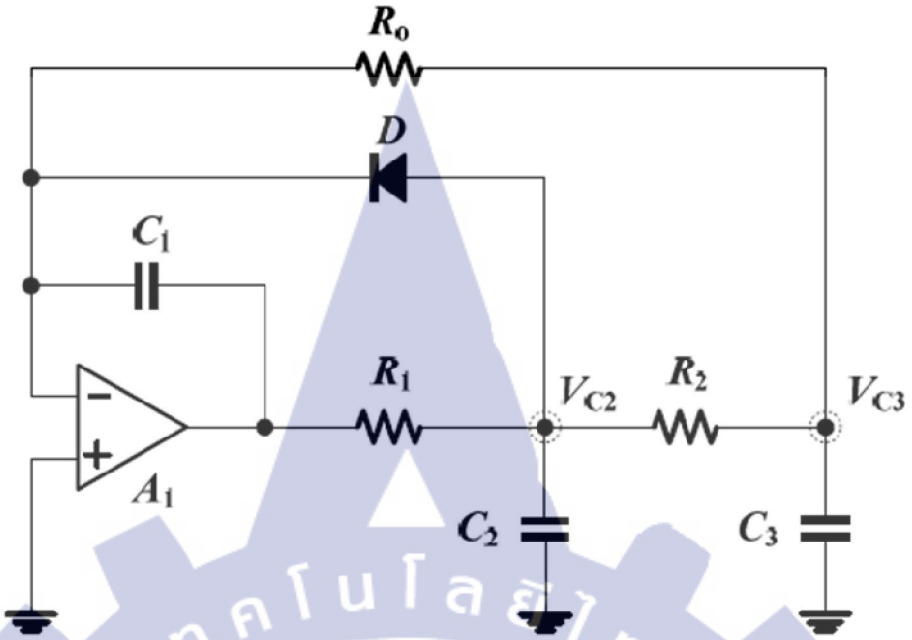

Figure 4.14 RC-Base chaotic oscillator

$$\begin{bmatrix} \dot{V}_{C3} \\ \dot{V}_{C2} \\ \dot{V}_{C1} \end{bmatrix} = \begin{bmatrix} -2/\tau_o & 1/\tau_o & 0 \\ 1/\tau_o & -2/\tau_o & 1/\tau_o \\ -1/\tau_1 & 0 & 0 \end{bmatrix} \begin{bmatrix} V_{C3} \\ V_{C2} \\ V_{C1} \end{bmatrix} + \begin{bmatrix} 0 \\ -I_D/C_2 \\ -I_D/C_1 \end{bmatrix} \tag{4.11}$$

Equation (4.11) can be expressed in terms of a normalized dynamical representation through the use of dimensionless variables and parameters as follows:

$$\begin{bmatrix} \dot{X} \\ \dot{Y} \\ \dot{Z} \end{bmatrix} = \begin{bmatrix} -2 & 1 & 0 \\ 1 & -2 & 1 \\ -1/A & 0 & 0 \end{bmatrix} \begin{bmatrix} X \\ Y \\ Z \end{bmatrix} + \begin{bmatrix} 0 \\ -BI_D \\ -CI_D \end{bmatrix} \tag{4.12}$$

$$\begin{bmatrix} \dot{X} & X & A \\ \dot{Y} & Y & B \\ \dot{Z} & Z & C \end{bmatrix} = \begin{bmatrix} dX/d\tau & V_{C3} & \tau_O/\tau_1 \\ dY/d\tau & V_{C2} & (\tau_O/C_2)/nV_T \\ dZ/d\tau & V_{C1} & (\tau_O/C_1)/nV_T \end{bmatrix} \tag{4.13}$$

where the time constants $\tau_0=C_2R=C_3R$, $\tau_1=C_1R$ and $\tau=t/\tau_0$. It is seen from (4.7) that $X=(\dot{X}+2X)$ and consequently the diode equation I_D can be expressed as $I_D=I_S\{exp[V_{C2}/(nV_T)]-1\} = I_S\{exp[Y]-1\}$, resulting in

$$I_S\{\exp[\dot{X}+2X]-1\}=i_D-I_S \tag{4.14}$$

Where $I_Sexp(Y) = I_Sexp\ (\dot{X}+2X)$. Alternatively, the dynamical representation in (4.14) can also be written in a jerk representation as

$$\dddot{x}=-\ddot{X}(4+Bi_D)-\dot{X}(3+2Bi_D)+AX-CI_D \tag{4.15}$$

It is obvious that a jerk model in (4.14) is described in the form shown in (4.15) as $\dddot{x}=J(\ddot{x},\dot{x},x)+I_DR$. In addition, the proposed circuit shown in Fig.4.11 has been designed with components $R = 1\ k\Omega$, $C_1 = 0.1\ \mu F$, $C_2 = C_3 = 10\ \mu F$, R_O is a potentiometer. The Diode model is 1N4148 where $I_S=14.11x10^{-9}$, n=1.984, and $V_T=25.85x10^{-3}$. The counting number of electronic components is only 8 and is therefore reduced by 43 % compared to that of 14 counts in. In particular, only a single op-amp is necessary for circuit implementation.

4.2.2 Dynamical Property Analysis and Numerical Simulations

Dynamic properties were mathematically analyzed using nonlinear theorems and numerically investigated using MATLAB. The initial condition was set at (0.1, 0, 0), which lies in the basic of attractor. The chaotic behaviors were simulated using the Fourth-order Runge-Kutta method with time step size of $5x10^{-6}$. The system is invariance under the transform (x, y, z) to (-x, -y, z), i.e. is symmetric around the z-axis and remains confined to the positive half-space with respect to the z state variable. The divergence of flow of the dynamic system is described as

$$\nabla.V=\frac{\partial\dot{x}}{\partial x}+\frac{\partial\dot{y}}{\partial y}+\frac{\partial\dot{z}}{\partial z}=-\frac{4}{\tau_O}=-4\times10^3 \tag{4.16}$$

Therefore, the chaotic system is a dissipative system with an exponential rate of contraction as

$$\frac{dV}{dt} = \exp(-\frac{4}{\tau_O}) = \exp(-4\times10^3) \tag{4.17}$$

In other words, a volume element V_0 becomes smaller by the flow in time t into a volume element $V_0\exp(-t)$. Each volume containing the trajectories shrinks to zero as $t\to\infty$ at an exponential rate of $-4x10^3$. System orbits are ultimately confined into a specific limit set of zero volume, and the system asymptotic motion settles onto an attractor of the system. In order to investigate the linear stability, the system (4.5) was linearized, and a single fixed point was found at (0, 0, 0). The Jacobian matrix of partial derivatives is defined as

$$J = \begin{bmatrix} -2/\tau_o & 1/\tau_o & 0 \\ 1/\tau_o & -(2/\tau_o)-\beta_{C_2} & 1/\tau_o \\ -1/\tau_1 & -\beta_{C_1} & 0 \end{bmatrix} \tag{4.18}$$

where the parameters $\beta_{C1} = \{I_S\exp(V_{C2}/nV_T)\}/nV_TC_1$ and $\beta_{C2} = \{I_S\exp(V_{C2}/nV_T)\}/nV_TC_2$. The resulting eigenvalue of the Jacobian matrix in (4.18) evaluated at the fixed point are consequently equal to $\lambda_1 = -6.1531$, $\lambda_2 = 1.0765 + 3.8852i$ and $\lambda_3 = 1.0765 - 3.8852i$ It is evident from (4.19) that the fixed point is a saddle focus node as the eigenvalue λ_1 *i*s negative real value and $\lambda_{2,3}$ are a pair of complex conjugate eigenvalue with positive real parts

4.2.3 Secure Communication Systems based on chaotic masking

There are number of possible methods that have been developed for synchronization in chaotic communications. In the masking method, synchronization is achieved by simply if the conditional Lyapunov exponents for the systems are negative for the given operating parameters. Thus, one could simply recover the message signal from the received chaotic signal through by means of a subtraction at

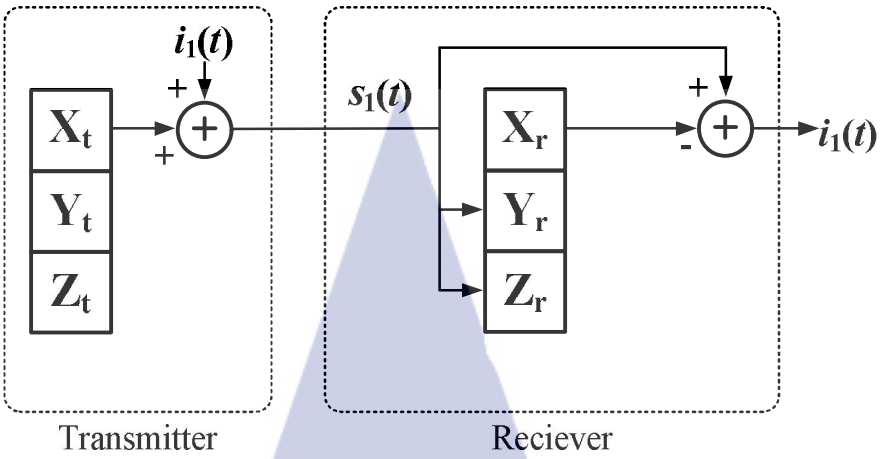

Figure 4.15 Block diagram secure communication

the receiver. This synchronization is robust against small perturbations of the carrier signal. In the chaotic modulation method the message signal becomes part of the dynamics, which is more robust because of the greater symmetry between chaotic oscillator and response. In the chaos shift keying [38-48] technique the message information is encoded onto the attractor by means of modulating a parameter of the chaotic oscillator, typically in a binary manner. In all these three schemes synchronization is an obvious way of recovering the original information. Figure 4.17shows the principle scheme of a general secure communication system with masking technique the transmitter can be used as a single drive system for a dual-channel transmitter independent of its response subsystem at the receiver.

4.2.4 Simulation and Experimental Results

4.1.4.1 Simulation Results

It is obvious that the proposed chaotic system circuit truly possesses chaotic behaviors with a single folded-band topology orbiting around the fixed point at (0, 0, 0). Figure 4.16 shows the bifurcation diagram of the peak of $V_{C3}(X)$ versus the parameter R_O, exhibiting a route to chaos. It is seen that the bifurcating parameter R_O can be tuned for chaos in wide region of 0.8 kΩ to 3 kΩ. Figure. 4.17 as show, schematic by using MATLAB-Simulation**,** when R_0 = 0.0045 and initial condition (0.1, 0, 0)

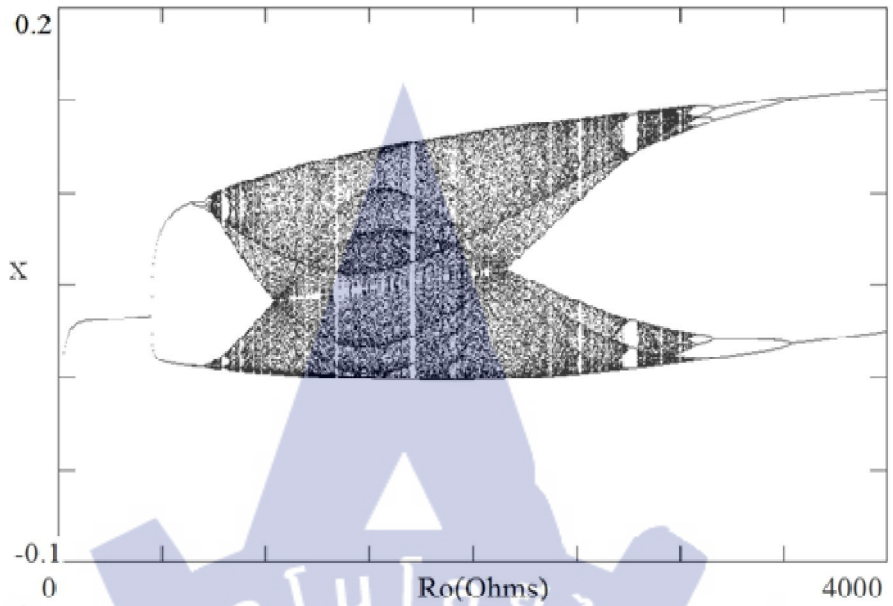

Figure 4.16 Bifurcation diagram of the output V_{C3} (X) versus the bifurcating resistor R_O.

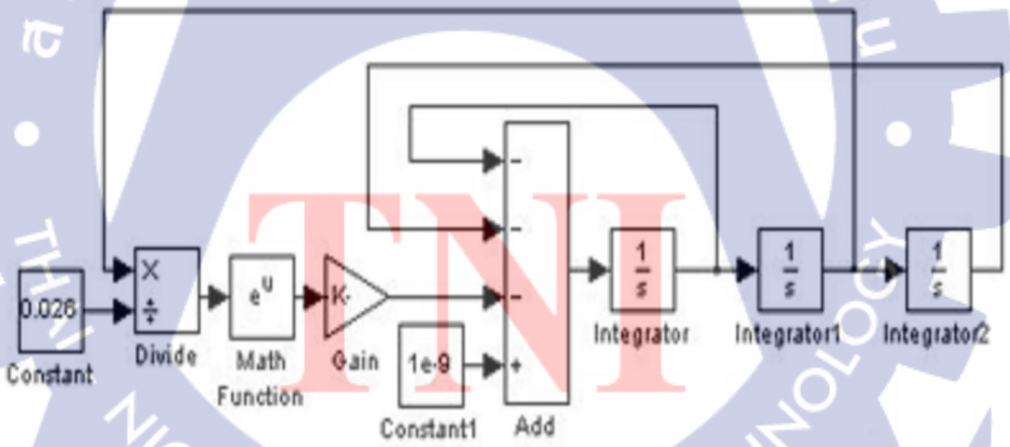

Figure 4.17 schemetic chaotic using MATLAB-Simulation

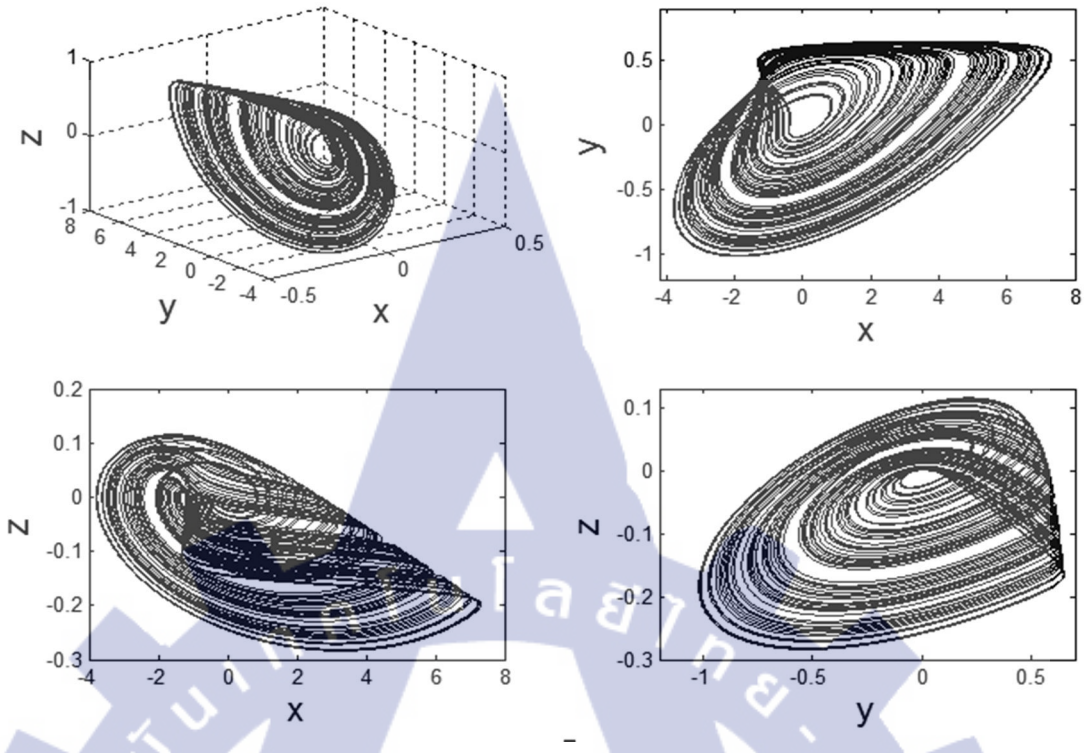

Figure 4.18 Chaotic attractors in three-dimensional view, an x–y plane, an x–z plane, and a y–z plane.

Upon setting R_O to a value of 1.2 kΩ, the chaotic attractors are displayed in Fig. 3 for a three-dimensional view, an x–y phase plane, an x–z phase plane, and a y–z phase plane. The attractor of three-dimensional view remains confined to the positive half-space of the z-axis. Figure 4.16 shows the consistent chaotic attractors in x-y plane obtained from experiment chaotic attractors in x–z plane. Figure 4.17 shows the synchronization results, (a) input and recovered output signal at the receiver, (b) synchronization errors. It is seen from Figure 4.18 that the masked signal can be retrieved shortly with low errors. In addition, other types of signals such as rectangular or common human speech can also be applied to this method autonomous RC chaotic jerk oscillator is presented in message-masking and synchronization for secure digital communications. The results show that the chaotically masked message is fully synchronized at the receiver through the use of very simple circuit. Consequently, the proposed new paradigm on secure communication schemes offers

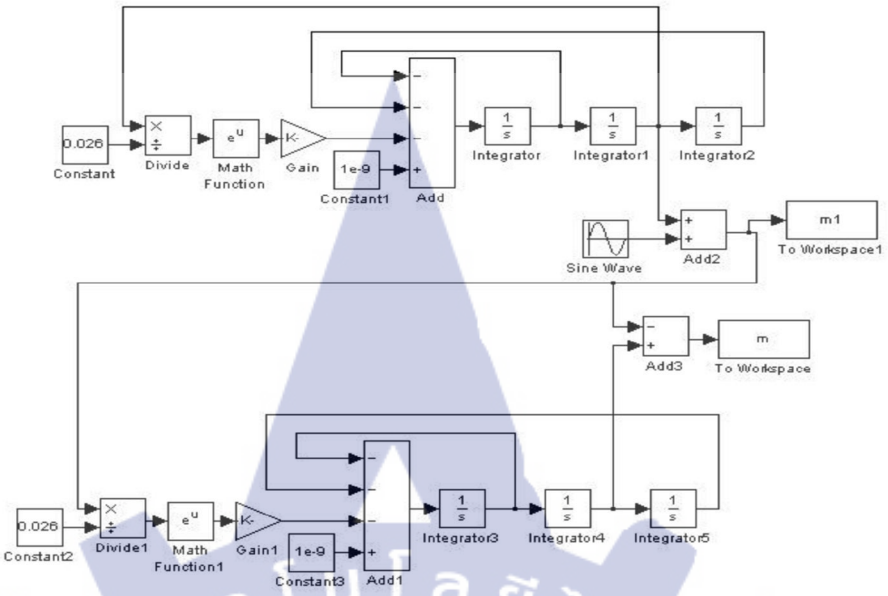

Figure 4.19 Matlab–Simulink models secure communication base on chaotic.

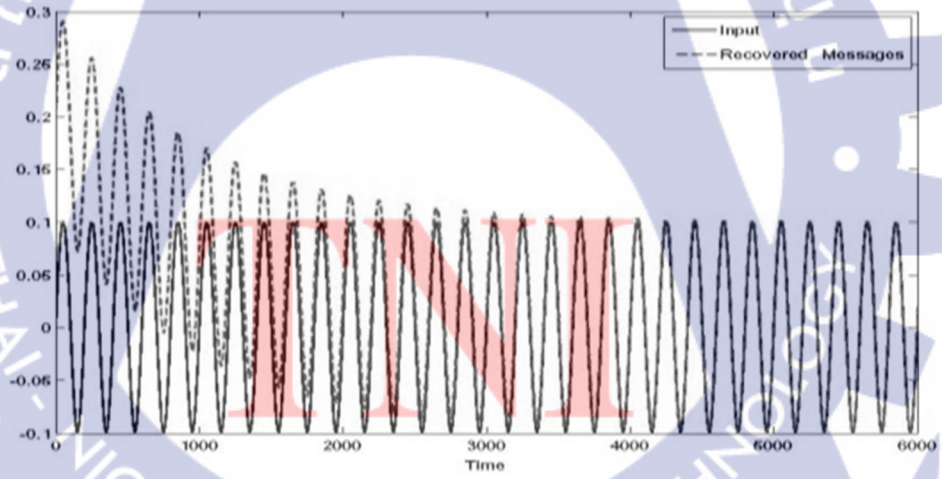

Figure 4.20 Synchronization results input and recovered output signal at the receiver

not only a simple mathematical system, but also very cost-effective circuit and system implementationsFig.4.16 shows the synchronization results input and recovered output signal at the receiver, Figure 4.17 synchronization errors. It is seen from Figure 4.18 that the masked signal can be retrieved shortly with low errors. In addition, other

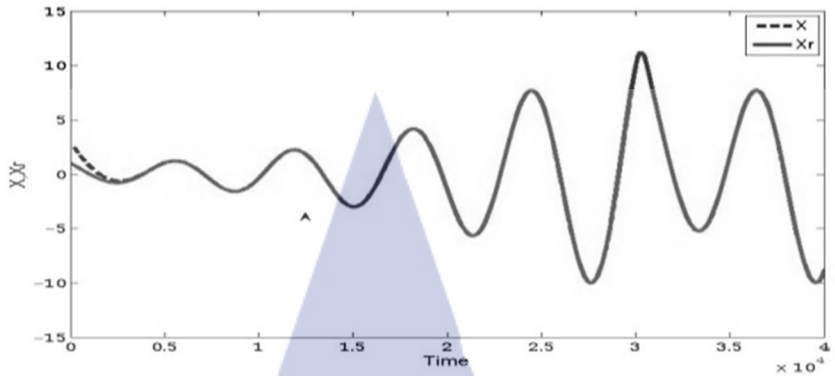

Figure 4.23 Synchronization errors.

4.1.4.2 Experimental Results

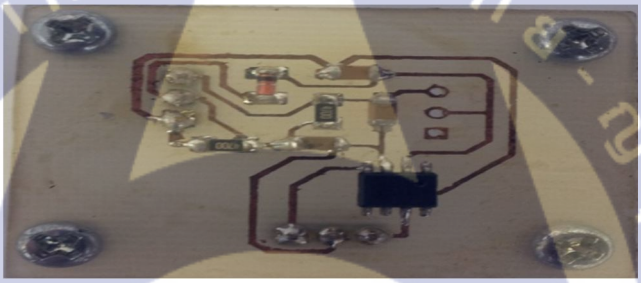

Figure 4.24 real circuit chaotic Jerk oscillators.

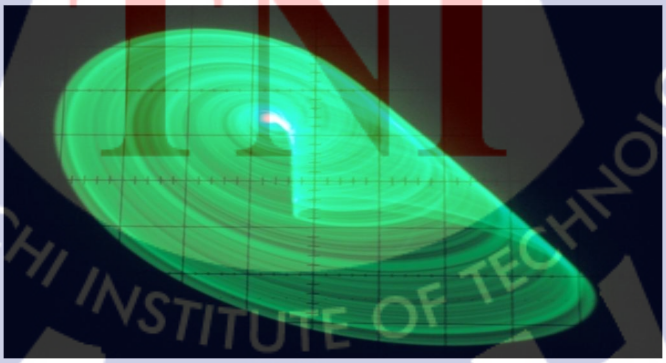

Figure 4.25experiment chaotic attractors inx–z plane.

types of signals such as rectangular or common human speech can also be applied to this method. Electronic circuit experiment was conducted on board using discrete

components. The components value were set at R = 470Ω, C_1 = 0.1 μF, C_2 = C_3 = 10 μF, Diode is 1N4148 and an Op-amp is LM741, R_O is 1.2 kΩ.

4.3 A Back-to-Back Twisted Chaotic Jerk Attractor using Inherent Hyperbolic Sine Function

Chaotic systems have recently been of great interests due to many possible potential applications in various fields of science and technology. Considerable research interests have been made in searching for new chaotic systems with minimal algebraic representations and simple circuit implementations. Chaos behavior can occur everywhere, even in very simple and low-dimensional nonlinear systems. The well-known Poincare'-Bendixon theorem [19-35], requires an autonomous continuous time state space model to be at least three-dimensional in order to have bounded chaotic solutions. On the other hand, for non-autonomous systems, chaos can appear in two-dimensional models. A measure of chaoticity has been based on the Kaplan-Yorke dimension (DKY), whilst a measure of complexity (or strangeness) has been based on the maximum positive Lyapunov Exponent (LE).

There are many examples, such as Lorenz [19], and Rössler [20] systems that have been widely studied. Electronic circuits that consist of two nonlinear elements can be used to verify theoretical predictions. As an example, nonlinear Duffing forced oscillators have been experimentally studied [25]. Another popular example is the nonlinear Chua's circuit, built and experimentally examined [45]. Up to now, various chaotic systems are introduced in [36] Chaos and chaotic systems have many fields of applications. One of the popular practical applications is secure communication. Synchronization of chaotic systems and chaos based secure communications has become an area of active research in recent years [30-40]. Different approaches are proposed and being pursued.

Chaotic signals depend very sensitively on initial conditions have unpredictable features and noise like wideband spread spectrum. So, it can be used in various communication applications because of their features of masking and immunizing information against noise. Chaos-based secure communication systems have been alternative of the standard spread-spectrum systems, since they are able to

spread the spectrum of the information signals and simultaneously encrypt the information signals with chaotic circuitry which is simple and inexpensive. Many researchers have investigated the implications of chaotic signals in communication systems. For example, Kocarev et. al., and Cuomo et al., [30], have used chaotic signals in communication security, and spread spectrum communication.

This section deals with the signal masking application of chaotic signals. Here a chaotic signal is generated with a new autonomous three dimensional chaotic system and this signal is used as a masking signal. Information signal is added to the chaotic signal at transmitter and at receiver the masking signal is regenerated and subtracted from the receiver signal. For synchronization of transmitter and receiver, Pecora – Carroll method of identical synchronization technique is used. In this method, receiver consists of two subsystems and with one state received from transmitter, receiver is able to generate the same masking signal as the signal generated at transmitter.

4.3.1 Dynamical Properties

4.3.1.1 Hyperbolic Sine Function in Anti-Parallel Diodes

With reference to the anti-parallel diodes in Fig.1, the currents I_{D1} and I_{D2}, which respectively flow through the diodes D_1 and D_2, can typically be modeled as

$$I_{D1}(v_D) = I_{S1}(e^{\frac{v_D}{nV_T}} - 1) \tag{4.20}$$

$$I_{D2}(v_D) = -I_{S2}(e^{\frac{-v_D}{nV_T}} - 1) \tag{4.21}$$

where I_{S1} and I_{S2} are reverse bias saturation currents of the diodes D_1 and D_2, respectively. The voltages v_D and V_T are a voltage across the two diodes and the typical thermal voltage, respectively. The parameter n is a diode quality factor. Applying Kirchhoff's current law, the total current I_{DT} flowing back to the Integrator 1 is can be expressed as

$$I_{DT}(v_D) = I_{S1}(e^{\frac{v_D}{nV_T}} - 1) - I_{S2}(e^{\frac{-v_D}{nV_T}} - 1) \tag{4.22}$$

In the case where similar diode models are employed, the reverse bias saturation currents may be equal, i.e. I_S=I_{S1} = I_{S2}, and the current IDT can be arranged as follows;

$$I_{DT}(v_D) = I_S(e^{\frac{v_D}{nV_T}} - e^{\frac{-v_D}{nV_T}}) \tag{4.23}$$

Typically, the values of Is, V_T and n are constant, determining by manufacturers, two new parameters $k_1 = 2I_S$ and $k_2 = 1/nV_T$ are introduced in the analysis for the sake of simplicity. Therefore, Eq. (4.23) can alternatively be expressed as

$$I_{DT}(v_D) = k_1 \frac{(e^{k_2 v_D} - e^{-k_2 v_D})}{2} = k_1 \sinh(k_2 v_D) \tag{4.24}$$

It can be considered from (4.24) that the voltage v_D across the diodes is a voltage difference between v_X and v_Y, i.e. $v_D = v_X - v_Y$. The voltage v_X also equal to and, as will be seen later, v_Y is a virtual ground of the inverting terminal of the operational amplifier. Therefore, the voltage v_D is equal to $\dot{x}$. As a result, the total current I_{DT} flowing through two anti-parallel diodes obeys an inherent hyperbolic sine function with two scaling factors k_1 and k_2 as follows;

$$I_{DT}(\dot{x}) = k_1 \sinh(k_2 \dot{x}) \tag{4.25}$$

4.3.1.2 Chaotic Jerk System using Hyperbolic Sine Function

Based on the three successive integral functions in eq. (4.25), the proposed chaotic jerk function using hyperbolic sine function with two scaling factors k_1 and k_2 derived from two anti-parallel diodes is given by

$$\dddot{x} + a\ddot{x} + x = Rk_1 \sinh(k_2 \dot{x}) \tag{4.26}$$

where a is chaos control parameter and the factor R, which is resistance value, is required to convert from a current signal to a voltage signal. It is apparent in (4.26) that all parameters in the nonlinear hyperbolic sine function are constant, obtaining from practical electronic circuit values, and chaos can be controlled through a single system parameter a. For dynamical property analysis, the dynamical form of (4.27) can be expressed as

$$\begin{aligned} \dot{x} &= y \\ \dot{y} &= z \\ \dot{z} &= -az - x - Rk_1 \sinh(k_2 y) \end{aligned} \tag{4.27}$$

Analyzing (8), the system possesses only single equilibrium point, i.e.

$$P(x_{1E}, x_{2E}, x_{3E}) = P(0,0,0). \tag{4.28}$$

for the equilibrium point found in (4.28), the Jacobian matrix (J) of the linearized system is given by

$$J = \begin{bmatrix} 0 & 1 & 0 \\ 0 & 0 & 1 \\ -1 & -Rk_1 & -a \end{bmatrix} \tag{2.29}$$

where sinh(y) is a sin hyperbolic function of the variable y. Applying the equilibrium point P into this Jacobian matrix and analyzing $|\lambda I - J|=0$ reveal a resulting characteristic polynomial as follows:

$$\lambda^3 - a\lambda^2 + Rk_1\lambda + 1 = 0 \tag{4.30}$$

4.3.2 Numerical analysis

4.3.2.1 Simulations for Maximum Chaoticity and Complexity

Numerical simulations have been performed in MATLAB using the initial condition of (x0, y0, z0) = (0.1, 0, -0.1). Such initial conditions are in fact not

essential, and can be selected from any point that lies in an attractor basin. In particular, the diode model 1N4148 was chosen in this work and the values of component parameters are as follows; I_S = 5.84x10^{-9} A, n=1.94, and V_T =26mV. The small resistor R of 10Ω was realized. Consequently, Eq. (7) can be expressed as

$$\dddot{x} + a\ddot{x} + x = 1.17\times10^{-7}\sinh(19.8\dot{x}) \tag{4.31}$$

it is seen in (4.27) that the single parameter a is a chaos control parameter, and its value can somewhat be determined at the maximum chaoticity and complexity. The chaoticity is a measure of the greatest positive Lyapunov exponents, which is the average rate of growth of the distance between two nearby initial conditions that grows exponentially in time when averaged along the trajectory, leading to long-term unpredictability property. The Lyapunov exponents can be employed for the estimation of the rate of entropy production and the fractal dimension commonly known as Kaplan-Yorke dimension DKY, i.e.

$$D_{KY} = j + \frac{1}{\left|LE_{j+1}\right|}\sum_{i=1}^{j} LE_i = l + \frac{LE_1 + LE_2}{\left|LE_3\right|} \tag{4.32}$$

where k is a non-integer constant, and typically equals to 2 for three-dimensional chaotic systems.

4.3.2.2 Numerical Equilibria and Eigenvalue

The Jacobian of the system is

$$\begin{aligned} \dot{x} &= y \\ \dot{y} &= z \\ \dot{z} &= -az - x - Rk_1\sinh(k_2 y) \end{aligned} \tag{4.33}$$

where x, y and z are the state variables and a, R, k_1, k_2 are positive real constants. The system displays a typical chaotic attractor when a = 0.7, R = 10Ω, k_1=1.17 x 10^{-7}and k_2 =19.8. The new system has equilibrium points (0, 0, 0)

$$J = \begin{bmatrix} 0 & 1 & 0 \\ 0 & 0 & 1 \\ -1 & -10\times10^{-7} & -0.7 \end{bmatrix} \tag{4.34}$$

where sinh (k_2y) is a sin hyperbolic function of the variable y. Applying the equilibrium point P into this Jacobian matrix and analyzing $|\lambda I - J|=0$ reveal a resulting characteristic polynomial as follows:

$$\lambda^3 - 0.7\lambda^2 + 10\times10^{-7}\lambda + 1 = 0 \tag{4.35}$$

the eigenvalue are $\lambda1 = -0.745$, $\lambda2 = 0.162 + 1.147$ i, $\lambda3 = 0.162 - 1.147$ i at the equilibrium point (0, 0, 0). As Eigen values has positive real parts which implies chaos.

4.3.3 Secure Communication Systems based on chaotic masking

There are number of possible methods that have been developed for synchronization in chaotic communications. In the masking method, synchronization is achieved by simply if the conditional Lyapunov exponents for the systems are negative for the given operating parameters Thus, one could simply recover the message signal from the received chaotic signal through by means of a subtraction at the receiver. This synchronization is robust against small perturbations of the carrier signal. In the chaotic modulation method the message signal becomes part of the dynamics, which is more robust because of the greater symmetry between chaotic oscillator and response. In the chaos masking technique the message information is encoded onto the attractor by means of modulating a parameter of the chaotic oscillator, typically in a binary manner. In all these three schemes synchronization is an obvious way of recovering the original information. Fig.4.11 shows the principle scheme of a general secure communication system with masking technique the transmitter can be used as a single drive system for a dual-channel transmitter independent of its response subsystem at the receiver.

4.1.3.1 Transmitter

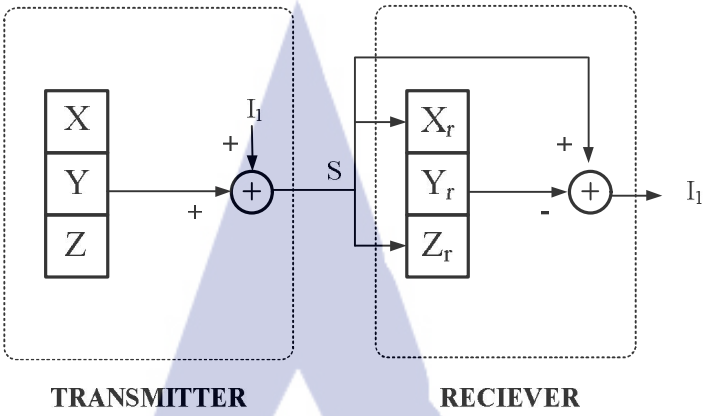

Figure 4.24 Block diagram secure communication.

At the transmitter, A Modified Hyperbolic Sine Function attractor described in equation 4.1 can be used as a single drive system for a dual-channel transmitter independentof its response subsystem at the receiver as follows: A Modified hyperbolic sineSystem using Diode Equation and its Application toSecure Communications $\dot{x} = y$, $\dot{y} = z$ and $\dot{z} = -az - x\text{-sinh}(y)$. As show in fig. 4.26**,** the dual channel transmitter consists of two parallel. Transmitter signal. The first transmitter signal is $s_1(t) = x_t(t) + i_1(t)$,where $x_t(t)$ is a chaotic signal and $i_1(t)$ represent the first original input which is transmit.

4.1.3.2 Receiver

At the receiver, A Modified hyperbolic sine attractor described in () can be used as single response subsystem for dual-channel receiver as follow: $\dot{x}_r = y_r$, $\dot{y}_r = z_r$ and $\dot{z}_r = -az_r - x_r\text{-sinh}(y_r)$ As show in fig. 4.26**,** the single channel consist of received signals $s_1(t)$.

4.3.4 Simulation and Experimental Results

4.3.4.1 Simulation Results

4.3.4.1.1 Dynamical properties

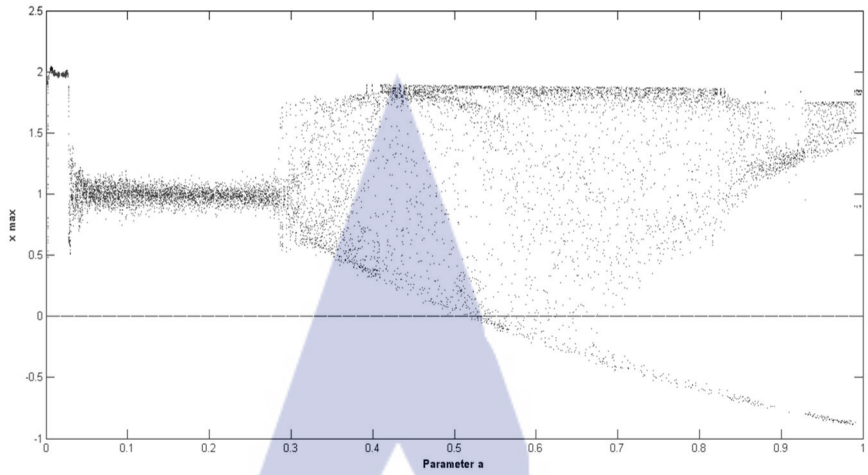

Figure 4.25 bifurcation diagram

It can also be considered from Figure 4.25 that the value of a is relatively small when initial condition x = 0.1, y = 0 and z = -0.1. For the particular cases of parameters considered above, summarizes the Equilibria, eigenvalue and types of equilibrium points of the system (4.27).

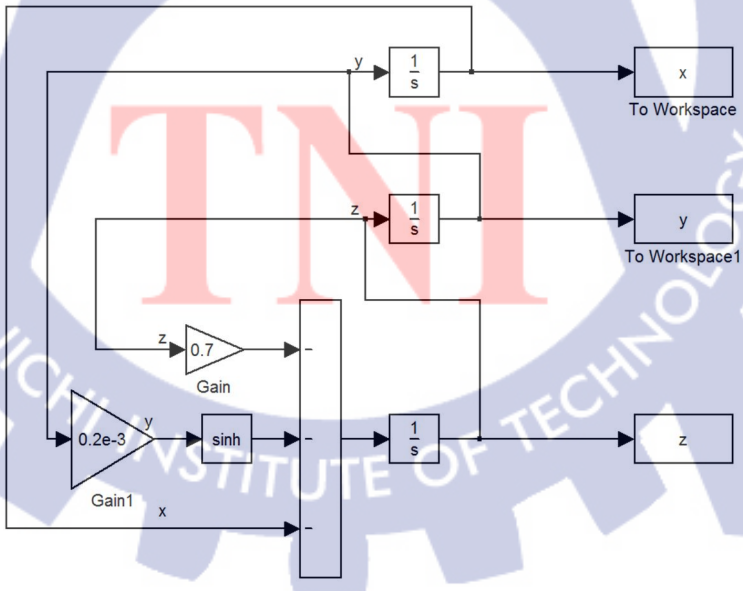

Figure 4.26 Chaotic scheme sine hyperbolic attractor using Matlab Simulink.

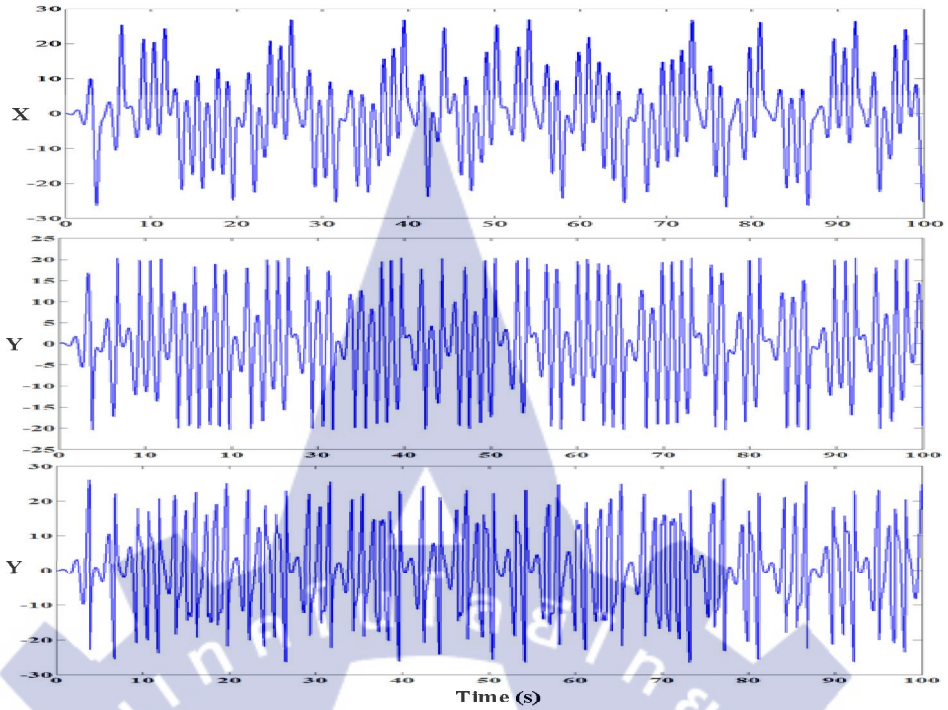

Figure 4.27 Simulation Time domain of x, y and z.

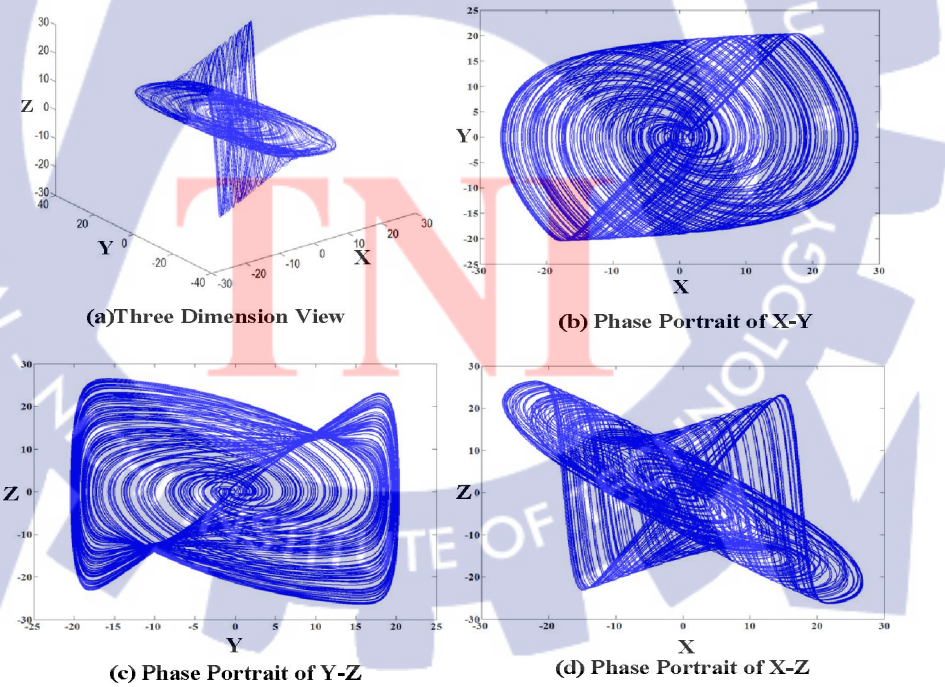

Figure 4.28 Simulation Phase portraits with at a =0.7.

4.3.4.1.2 Application for chaotic communication

Due to the fact that output signal can recover input signal, it indicates that it is possible to implement secure communication for a chaotic system. Figure 4.24 shows the principle scheme of a general secure communication system that employs the masking technique. Figure 4.29 shows Simulink modeling of chaotic masking communication circuit of the Rössler Attractor. The presence of the chaotic signal between the transmitter and receiver has proposed the use of chaos in secure communication systems. The design of these systems depends on the self-synchronization property of sine hyperbolic Attractor. Transmitter and receiver systems are identical except for their initial values, in which the transmitter system is 0.1, 0, -0.1 and the receiver systems are 0.1, -0.143, and -0.2 as shown in Figure 4.30. It is necessary to make sure the parameters of transmitter and receiver are identical for implementing the chaotic masking communication. In this masking scheme, message signal is added to the synchronizing driving chaotic signal in order to regenerate a clean driving signal at the receiver. Thus, the message has been perfectly recovered by using the signal masking approach through cascading synchronization in the make sure the parameters of transmitter and receivers are identical for implementing the chaotic masking communication. In this masking scheme, a message signal is added

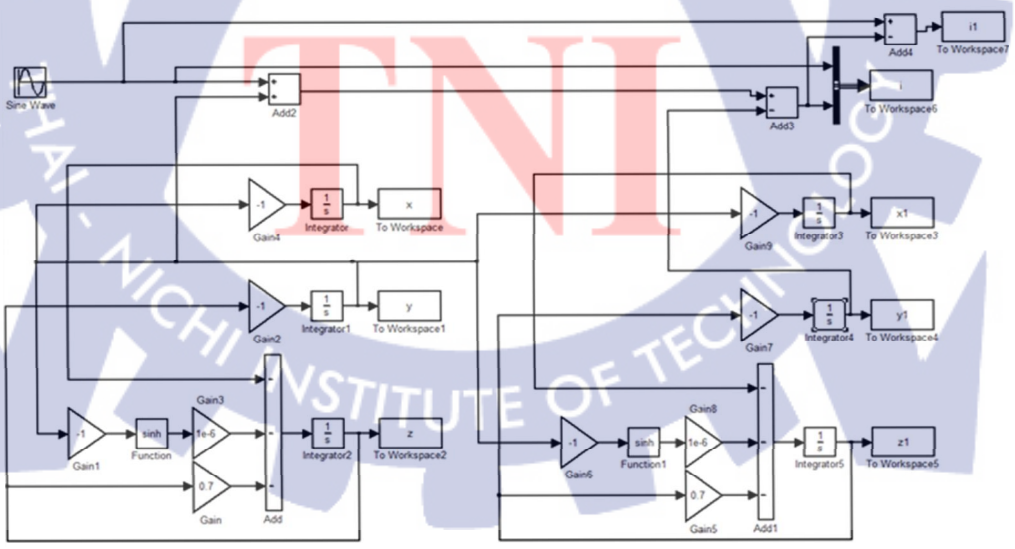

Figure 4.29 shows Simulink modeling of chaotic masking communication.

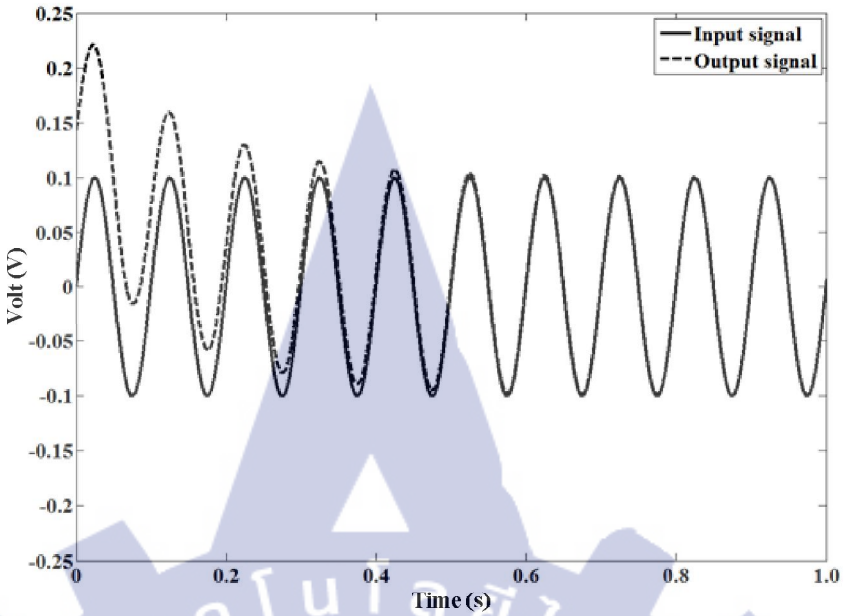

Figure 4.30 Synchronization results input and recovered output signal.

to the synchronizing driving chaotic signal in order to regenerate a clean driving signal at the receiver. Thus, the message has been perfectly recovered by using the signal masking approach through cascading synchronization in the sine hyperbolic Attractor. Computer simulation results have shown that the performance of sine hyperbolic Attractor in chaotic masking and message recovery. One disadvantage of using one-way coupling method is that compared to this cascading method, it takes longer to synchronize the coupled systems, especially when the coupling parameter is small. This may cause problems in practical applications such as secure communications since information may be delayed or lost during the first period of matching time Rössler Attractor. Computer simulation results have shown that the performance of sine hyperbolic Attractor in chaotic masking and message recovery. One disadvantage of using one-way coupling method is that compared to this cascading method, it takes longer to synchronize the coupled systems, especially when the coupling parameter is small. This may cause problems in practical applications such as secure communications since information may be delayed or lost during the first period of matching time.

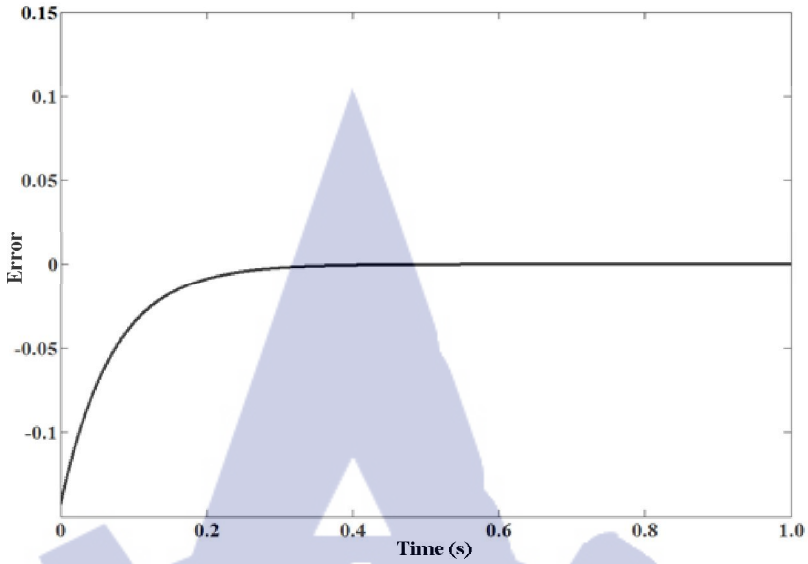

Figure 4.31 Synchronize errors.

4.1.4.3 Experimental Results

4.3.4.2.1 Dynamical properties

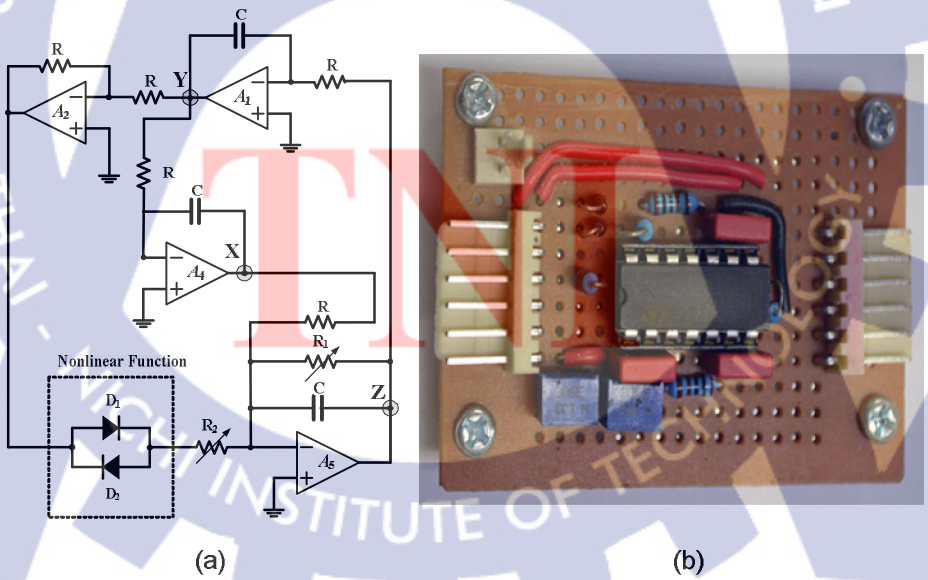

Figure 4.32 Chaotic circuits (a) design chaotic circuit and (b) real chaotic circuit.

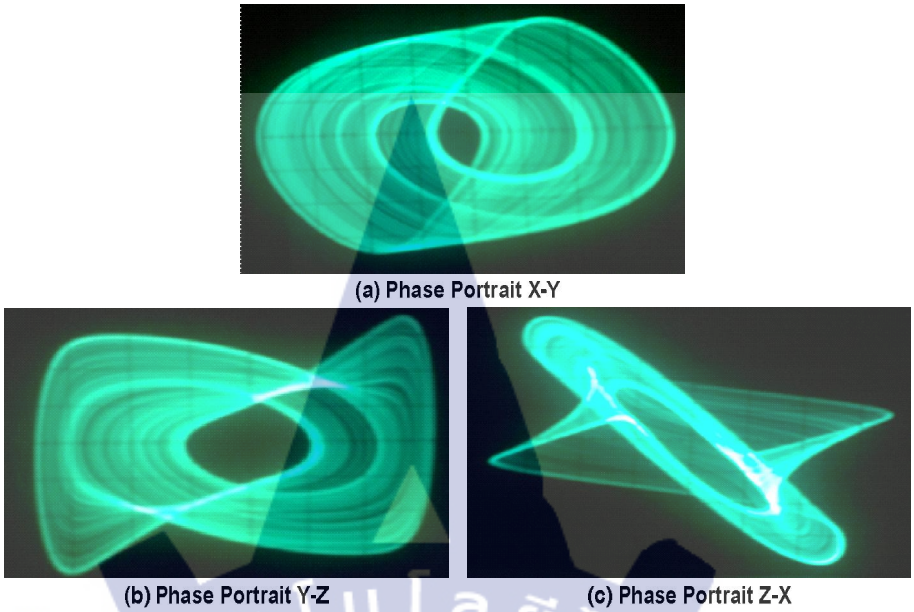

Figure 4.33 Result chaotic attractor of real electronics circuit.

4.4 Application for walky-talky communication

4.4.1 Design circuit

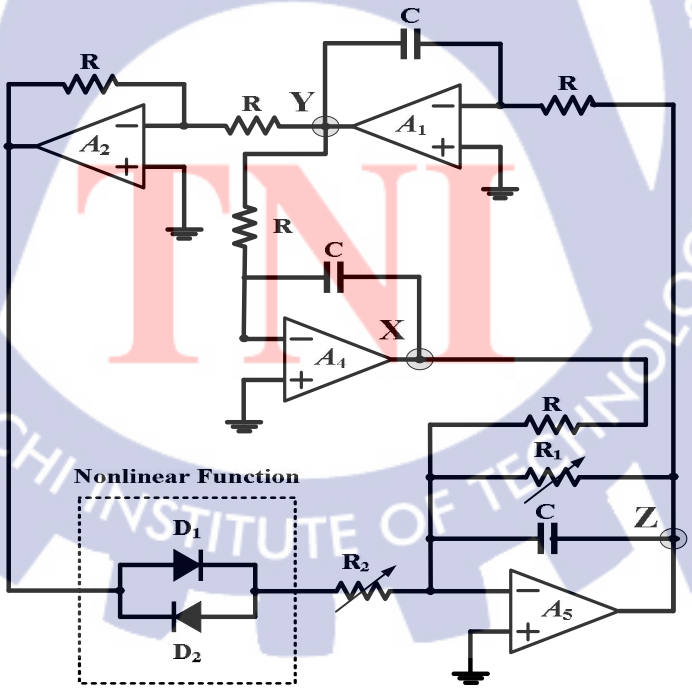

Figure 4.34 Chaotic circuit transmitters.

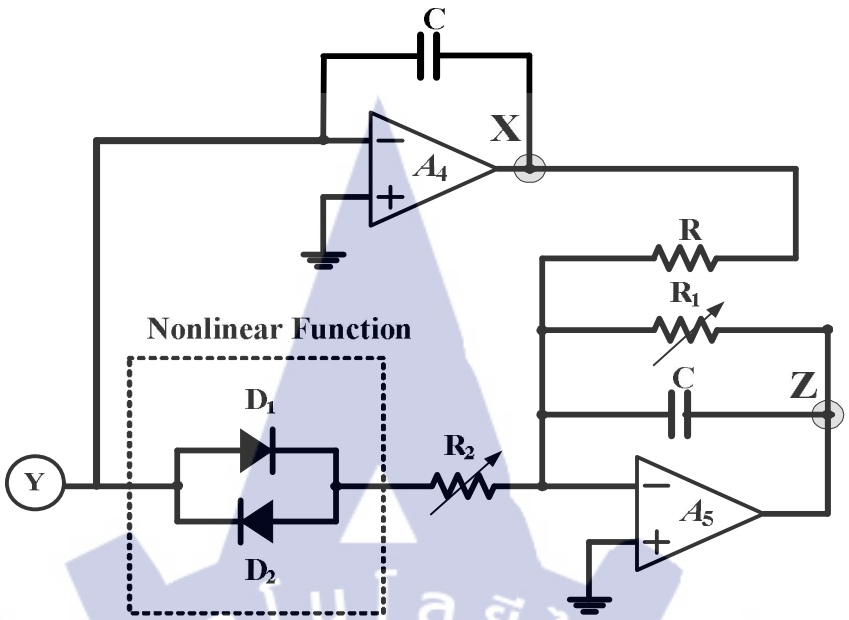

Figure 4.35 Chaotic circuit receivers.

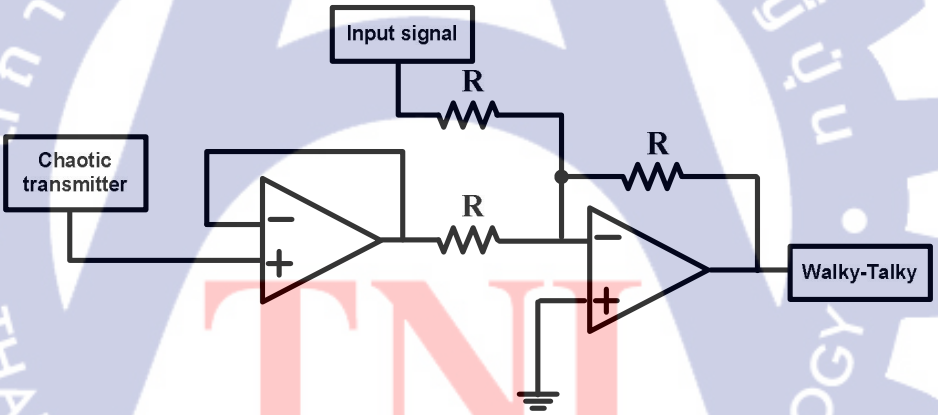

Figure 4.36 Chaotic masking circuit.

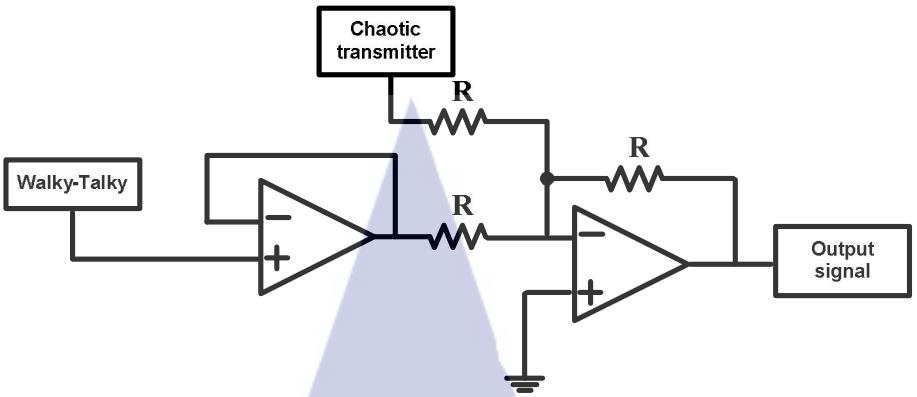

Figure 4.37 Chaotic synchronizes circuit.

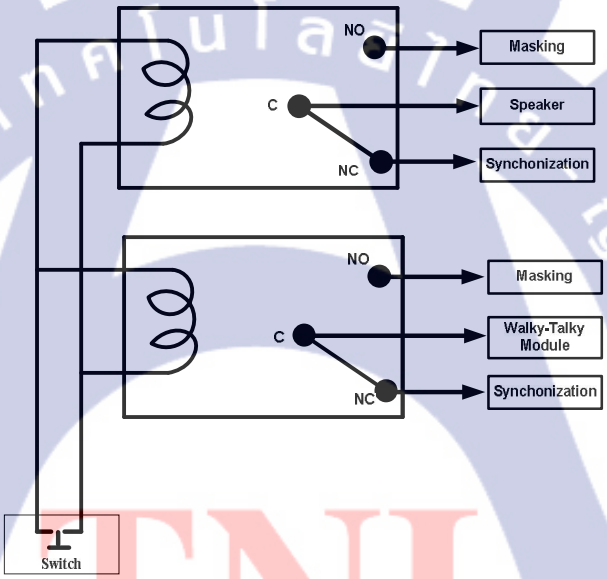

Figure 4.38 Switching control sending and receive circuit.

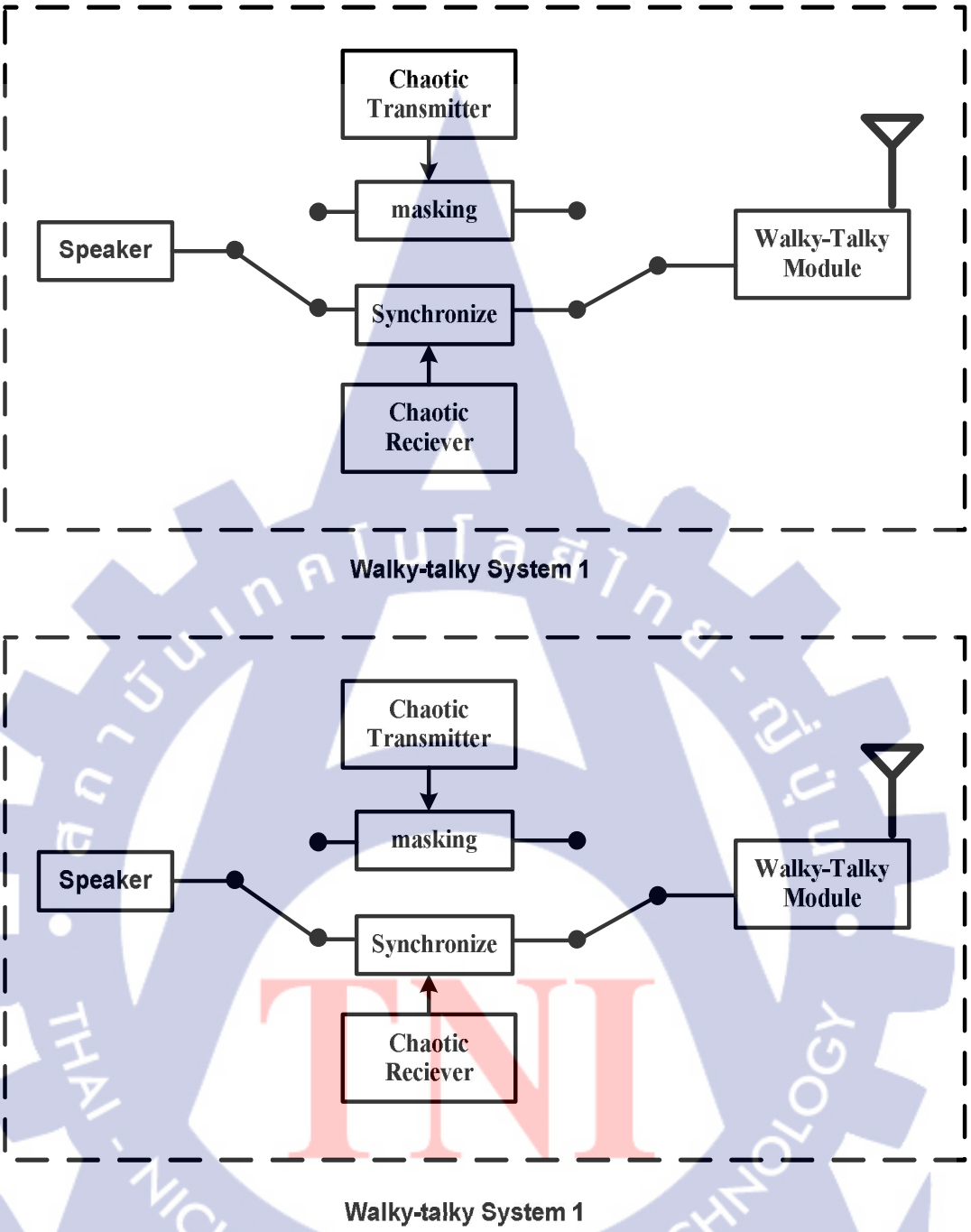

Figure 4.39 Design Schematic of chaotic communication application for walky-talky.

4.4.1 Experimental

This section, implemental real electronics circuit for includes chaotic communication application for walky-talky, consist of chaotic transmitter circuit, receiver circuit, chaotic masking circuit, chaotic synchronization circuit, switching control sending and receive circuit and walky-talky module.

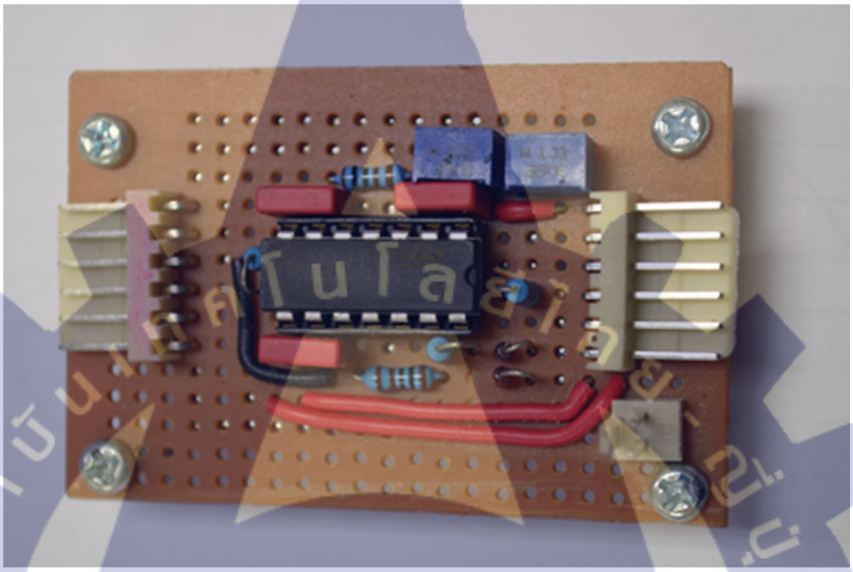

Figure 4.40 Real chaotic circuit transmitter.

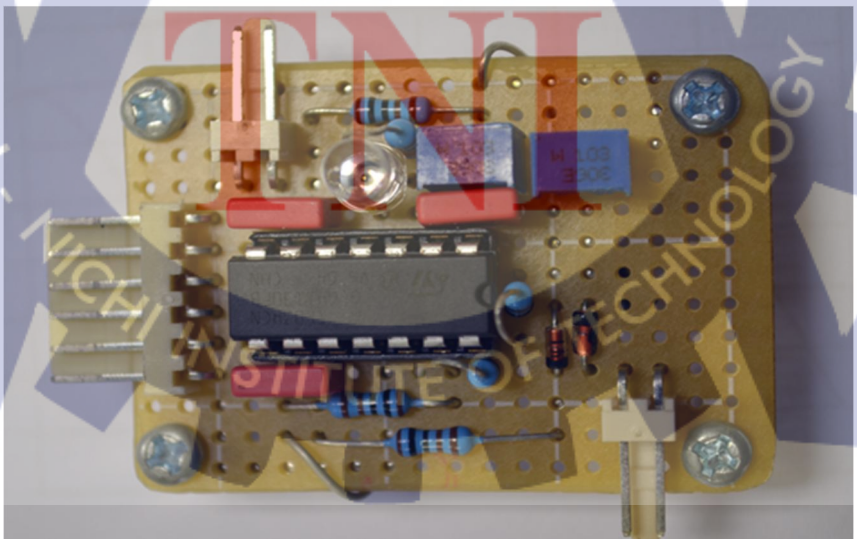

Figure 4.41 Chaotic circuit receivers.

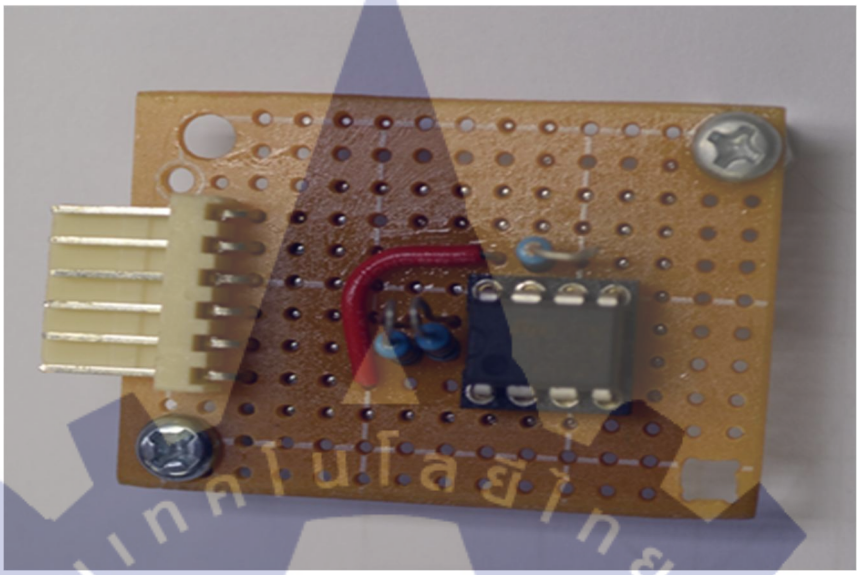

Figure 4.42 Chaotic masking and chaotic synchronization circuit.

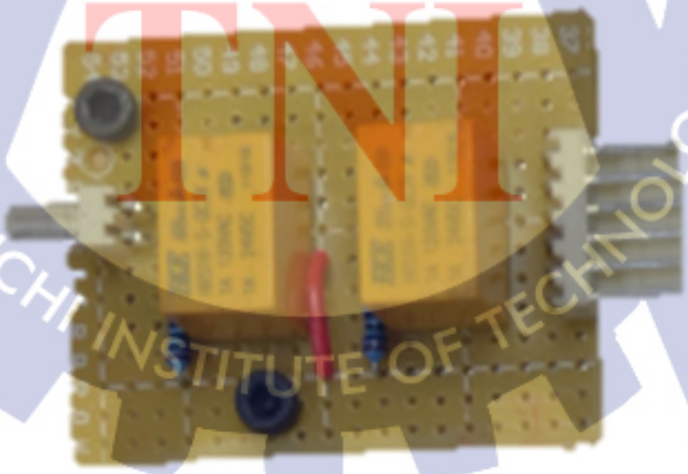

Figure 4.43 Real circuit switching control sending and receive circuit.

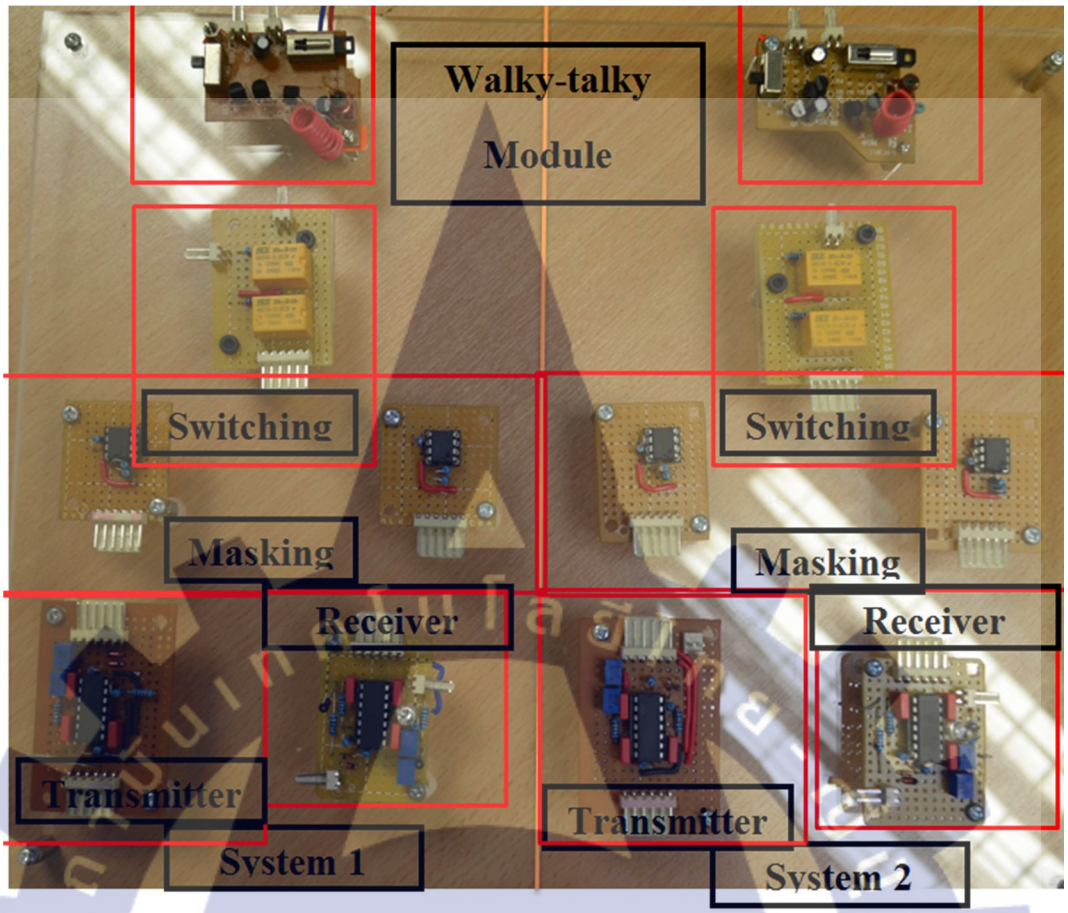

Figure 4.44 Real circuit chaotic communication application for walky-talky.

Chapter 5

Conclusion

5.1 Rössler Attractor using Diode Equation

This section focuses on the new Rössler chaotic Attractor's chaotic oscillator circuits is designed from Equation 4.1 and can be described by Bifurcation, Lyapunov Exponents, and Kaplan-Yorke Dimension, implement chaotic circuit and their applications in signal masking communications. New Rössler Attractor's chaotic oscillator circuits has were designed and simulated. Chaotic signal masking circuits were realized using Matlab-Simulink and real circuit. Related figures in Figure 4.12 point out that Matlab-Simulink and Real circuit outputs prove the same conclusions. We have demonstrated in simulations that Chaos can be synchronized and applied to secure communications. We suggest that this phenomenon of chaos synchronism may serve as the basis for little known new Rössler Attractor to achieve secure communication. Simulation results are used to visualize and illustrate the effectiveness of new Rössler chaotic system in signal masking. All simulations results performed on Rössler chaotic system are verified the applicable of secure communication.

Result experiment, we can implement chaotic circuit has high stability and application for two channel chaotic communication. The synchronization of chaotic systems offers an interesting possibility to send secure information via chaotic signals, generated it her by electronic circuit.

5.2 Chaotic jerk Attractor

This paper has presented a very simple autonomous RC chaotic jerk oscillator with nine electronic components. The nonlinearity required for chaos is implemented through the use of a well-known diode equation. Basic dynamical properties are described including Equilibria, eigenvalue of Jacobian matrix, chaotic attractors, time-domain waveforms and bifurcations. Potential application of such a simple autonomous RC chaotic jerk oscillator is presented in message-masking and synchronization for secure digital communications. The results show that the

chaotically masked message is fully synchronized at the receiver through the use of very simple circuit. Consequently, the proposed new paradigm on secure communication schemes offers not only a simple mathematical system, but also very cost-effective circuit and system implementations.

This system we can implement very cost-effective circuit but application for communication can be quite difficult because this circuit has been low stability.

5.3 A Back-to-Back Twisted Chaotic Jerk Attractor using Inherent Hyperbolic Sine Function

This section we implement electronics circuit form on chaotic Jerk attractor using Inherent hyperbolic sine function and synchronize of chaotic Jerk attractor using Inherent hyperbolic sine function and its application in signal masking and secure communications. The Pecora – Carroll identical cascading synchronizations method is used. The behavior of the response system depends on the behavior of the drive system, but is not invertible. We have demonstrated in simulations and also proved in real electronic circuits that chaos can be synchronized and applied to secure communications. We suggest that this phenomenon of chaos synchronicity may serve as the basis for little- known chaotic Jerk attractor using Inherent hyperbolic sine function to achieve secure communication. Chaos synchronizations and chaos masking were realized using Matlab – Simulink, real electronics circuit and also real electronic experimental applications. Related in Figures. 4.28 – 4.30 for synchronization and Figures. 4.31, 4.32 and 4.33 for masking communication show that Matlab – Simulink and also real electronic experimental application results prove the same conclusions.

5.4 Application for walky-talky communication

Section first, Design schematic for chaotic masking communication form chaotic Jerk attractor using Inherent hyperbolic sine function because chaotic Jerk attractor using Inherent hyperbolic sine function have simple circuit and high stability it's easy to create a secure communication system.

Section second, implement circuit for communication from general circuit op-amp such as summing amplifier, switching relay and buffer op-amp, consist of circuit application for chaotic communication walky-talky.

Reference

Reference

[1] Kathleen T. Alligood; et al. (2000). **Chaos: An Introduction to Dynamical Systems**. USA: California Institute of Technology.

[2] Edward Ott. (2002). **Chaos in Dynamical Systems**.USA: Cambridge University.

[3] Grebogi; et al. (1987). Unstable Periodic Orbits and the Dimension of Chaotic Attractors. **Journal of Physics Review A**. 36(7):3,522-3,524.

[4] Volodymyr Lynnyk (2010). **Chaos-basedCommunication Systems**. Czech:Prague university.

[5] Ken Kiers; and Dory Schmidt. (2004). **Precision Measurements of a Simple Chaotic Circuit.**USA.: Taylor University.

[6] Vinod Patidar; and K KSud. (2005**). Bifurcation and Chaos in Simple Jerk Dynamical Systems**. India: M.L.S. University.

[7] GuoboXie; Pinghua Chen; and Minghua Liu. (2008). Generation of Multidirectional Multiscroll Attractors under the Third-Order Jerk System**.8 th Conference of International Symposium on Information Science and Engieering.** pp. 385-379.

[8] Ljubiša M. Kocić; and Sonja Gegovska-Zajkova. (2009). On A Jerk Dynamical System. **Journal of Automatic Control and Robotics.** 8(1): 35-44.

[9] Wimol San-Um; Bancha Munmaungsan; and Banlue Srisuchinwong. (2011). An LC and RC Chaotic Jerk Oscillators Based on a Diode Equation. **3 th Conference of Thailand Computer Science.** pp. 325-329.

[10] Shihua Chen; JaHua; Changping Wang; and JinhuLü. (2003). Adaptive Synchronization of Uncertain Rössler hyperchaotic System Based on Parameter Identification. **Journal of Physics Letters B.** 321(2):50-55.

[11] Pehlivan; and Y. Uyaroglu. (2007). Simplified Chaotic Diffusionless Lorentz attractor and Its Aplication to Secure Communication Systems. **Journal of Institution of Engineering and Technology Communication.** 17(2): 473-488.

[12] GaoBingkun; Li Wenchao; and Hu Yue. (2009). The Application Research of Hyperchaos Encryption in Security Communications. **1st Conference of Chinese Control and Decision Conference**. pp. 1,278-1,281.

[13] Said Sadoudi; and Mohamed Salah Azzaz. (2009). Hardware Implementation of the Rössler ChaoticSystem for Securing Chaotic Communication. **5th Conference of Technologies of Information and Telecommunications.** pp. 22-27.

[14] IhsanPehlivan; YilmazUyaroglu; and M. Ali YalcinveSelçukCoskun. (2009). Design And Simulation Of The Arneodo Attractor's Chaotic OscillatorAnd Signal Masking Circuits. **5th Conference of International AdvancedTechnologies Symposium.** pp. 11-20.

[15] Sameer Al-Khawaja. (2010). Phase Synchronization in Mutually Coupled Chaotic Josephson Junctions: Effect Of Asymmetry And Incommensurate Frequencies. **Journal ofAtomic Energy Commission.** 41(3): 378-385.

[16] Dandan Zhao; Yuxia Li; Xuezhen Liu; and YongchaoCao. (2008). The Generation of a New Hyperchaos Based on Lorenz System. **Journal of Information Engineering Technology Communications.** 2(1): 67-75.

[17] R. May. (1976). Simple Mathematical Models with very Complicated Dynamics. **Journal of Nature.** 261(1): 459-467.

[18] M. W. Hirsch; and S. Smale. (1974). **Differential Equations Dynamical Systems and Linear Algebra Academic**. USA.: Academic Press.

[19] G. Duffing; et al. (1980). In New Approaches to Nonlinear Problems in Dynamics. **Journal of Applied Mechanics.** 78(1): 311.

[20] J. M. T. Thompson; and H. B. Stewart. (1986). **Nonlinear Dynamics and Chaos.** USA.:University of California.

[21] E. N. Lorenz. (1963). Deterministic Nonperiodic Flow.**Journal of the Atmospheric Sciences.** 20(2): 130-41.

[22] Tao Yang; and Leon O. Chua. (2000). Piecewise-Linear Chaotic Systems with a Single Equilibrium Point. **Journal of Bifurcation and Chaos.** 10(9): 2,015-2,060.

[23] J. C. Sprott. (2000). A New Class of Chaotic Circui. **Journal of Physics LettersA**. 266(1): 19–23.

[24] O. E. Rossler. (1976). An Equation for Continuous Chaos. **Journal of Physics Letters A.** 57(7):397–398.

[25] J. C. Sprott. (1994).Some Simple Chaotic Flows. **Journal of Physics Review E.** 50(1): 647–650.

[26] H. P. W. Gottlieb. (1996). What is the Simplest Jerk Function that gives Chaos. **American Journal of Physics.** 64(5): 525.

[27] S. H. Schot. (1978). Jerk: The Time Rate of Change of Acceleration. **American Journal of Physics.**46(11): 1,090–1,094.

[28] T. R. Sandin. (1990). The Jerk. **Journal of The Physics Teacher.** 28(6): 6-60

[29] S. Nose. (1991). Constant Temperature Molecular Dynamics Methods. **Program TheoryPhysics Supply.** 103: 1–46.

[30] W. G. Hoover. (1995). Remark on Some Simple Chaotic Fows. **Journal of Physics Review E.** pp. 759–760.

[31] J. C. Sprott. (1993). How Common is Chaos. **Journal of Physics Letters A.** 173(1): 21–24.

[32] A. Wolf; J. B. Swift; H. L. Swinney; and J. A. Vastano. (1985). Determining Lyapunov Exponents from a Time Series. **Journal of Physica D.** 16: 285–317.

[33] J. C. Sprott. (1993). **Strange Attractors: Creating Patterns in Chaos**. USA.: M&T Books.

[34] J. C. Sprott. (2006). Simplest Dissipative Chaotic Flow. **Journal of Physics Letters A.** 28(1): 271-274.

[35] V. I. Arnold. (1978). **Mathematical Methods in Classical Mechanics Springer.** USA.: Springer.

[36] A. Cromer. (1981). Stable Solutions using the Euler Approximation. **American Journal of Physics.** 49(5): 455–459.

[37] Simin Yu; Jinhu Lu; Leung; and Guanrong Chen. (2005). Design and Implementation of n-Scroll Chaotic Attractor from a General Jerk Equation. **Journal of IEEE Transactions on Circuits and Systems.** 52(7): 1,459–1,476.

[38] J. C. Sprott. (2010). Simple Autonomous Chaotic Circuit. **Journal of IEEE Transactions on Circuits and Systems**. 57 (7) : 240-243.

[39] B.Munmaungsan; B. Srisuchinwong; and J. C. Sprott. (2011). Generalization of the Simplest Autonomous Chaotic System.**Physics Letters A.** 375(12): 1,445-1,450.

[40] J. C. Sprott. (2011). A New Chaotic Jerk Circuit. **Journal of IEEE Transactions on Circuits and Systems.** 58(4): 240-243.

[41] S. Celikovsky; and C.Guanrong. (2005). On the Generalized Lorenz Canonical Form**. Journal of Chaos Solitons and Fractals.** 26(5): 1,271-1,276.

[42] J. Lu; G. Chen; and S. Zhang. (2002). The Compound Structure of a new Chaotic Attractor. **Journal of Chaos Solitons and Fractals.** 14(1): 669-672.

[43] J.C.Sprott. (1997). Some Simple Chaotic Jerk Functions. **American Journal of Physics.** 65(6): 537.

[44] G. Eason; B. Noble; and I.N. Sneddon. (1955). On Certain Integrals of Lipschitz-Hankel Type Involving Products of Bessel Functions. **Journal of Philosophical Transactions of the Royal Society of London. Series A Mathematical and Physical Sciences.** 247(293): 529-551.

[45] J. Clerk Maxwell. (1892**). A Treatise on Electricity and Magnetism.** USA.: Cambridge University.

[46] I.S. Jacobs; and C.P. Bean. (1963). **Fine Particles, Thin Films and Exchange Anisotropy**. USA.: New York Academic.

[47] Y. Yorozu; M. Hirano; K. Oka; and Y. Tagawa. (1982). Electron Spectroscopy Studies on Magneto-Optical Media and Plastic Substrate Interface**. Journal of IEEE Translation Magnetics in Japan**. 2(8): 740-741.

[48] M. Young. (1989). **The Technical Writer's Handbook.** USA.:Oxford University.

Appendix

Matlab Simulation Code

1. Matlab code for Bifurcations

```
function Bifurcation
        clear all
        t  = 0: 0.01: 100;
        y0 = [1.6 ; -1 ; 0.09];

        xmax        = 1;
        xmin = 0;
        Sample_Points = 10;
        Step_Size=(xmax-xmin)/Sample_Points;
        v  = zeros(Sample_Points+1,length(t));
        tp = zeros(Sample_Points+1,1);

globalgramma delta c
        delta = 0.4;
        c=1;

for i = 1: 1: Sample_Points+1;
        gramma = (i-1)*Step_Size+xmin;
          [t, y] = ode45(@ODE, t, y0);
          A = y(:,2)';
        for j = 1: 1: length(A)
        h(i, j) = A(1, j);
        end
        v(i,:) = feval('FindMax', h(i,:));
        v(i, 1: 15000) = 0;
        tp(i) = (i-1)*Step_Size+xmin;
        end

        subplot(2, 2, 1)
        plot(tp,v,'b.','MarkerSize',4.5)
        xlabel('Parameter a', 'FontSize', 16, 'FontName', 'Cordia New', 'FontWeight', 'bold')
```

```
ylabel(     'x max', 'FontSize', 16, 'FontName', 'Cordia New', 'FontWeight', 'bold')

function F = ODE(t, f)
        globalgramma delta c

        x = f(1);
        y = f(2);
        z = f(3);
        F = zeros(size(f));
        F(1) = -y-z;
        F(2) =x+a*y;
        F(3) = -z+b*exp(x);

function g = FindMax(h)
        g=zeros(1,length(h(1,:)));
        for k = 2: 1: (length(h(1,:))-1)
        if (h(1, k-1)<h(1, k))&&(h(1, k)>h(1, k+1))
        g(1, k) = h(1, k);
        end
        end
        function g = FindMax(h)
        g=zeros(1,length(h(1,:)));
        for k = 2: 1: (length(h(1,:))-1)
        if (h(1, k-1)<h(1, k))&&(h(1, k)>h(1, k+1))
        g(1, k) = h(1, k);
        end
        end
```

2. Matlab code for Poincare

```
function plotPoincareMap_3
        clearall
        Fs = 1e3;
        t  = (0: 1/Fs: 5000);
        y0 = [1; 0; 1];
global a b
        a = 0.2;
        b = 0.7e-3;
        [t, y] = ode45(@ODE, t, y0);
        L=length(y(:,1));
        x = y';

        C1_2=zeros(1,L);
        C1_3=zeros(1,L);
        k1=0;
        for i1=2: L
        if (x(1,i1)<(0+0.1))&&(x(1,i1)>(0-0.1))
            k1=k1+1;
            C1_2(k1)=x(2,i1);
            C1_3(k1)=x(3,i1);
        end
        end

        C2_1=zeros(1,L);
        C2_3=zeros(1,L);
        k2=0;
        for i2=2: L
        if (x(2,i2)<(0+0.1))&&(x(2,i2)>(0-0.1))
            k2=k2+1;
            C2_1(k2)=x(1,i2);
            C2_3(k2)=x(3,i2);
        end
```

```
end

C3_1=zeros(1,L);
C3_2=zeros(1,L);
k3=0;
for i3=2: L
if (x(3,i3)<(0+0.1))&&(x(3,i3)>(0-0.1))
    k3=k3+1;
    C3_1(k3)=x(1,i3);
    C3_2(k3)=x(2,i3);
end
end

subplot(2, 2, 2)
plot(C1_2(1:k1),C1_3(1:k1),'b.','MarkerSize',1)
xlabel('y', 'FontSize', 16, 'FontName', 'Cordia New', 'FontWeight', 'bold')
ylabel('z', 'FontSize', 16, 'FontName', 'Cordia New', 'FontWeight', 'bold')

subplot(2, 2, 3)
plot(C2_1(1:k2),C2_3(1:k2),'b.','MarkerSize',1)
xlabel('x', 'FontSize', 16, 'FontName', 'Cordia New', 'FontWeight', 'bold')
ylabel('z', 'FontSize', 16, 'FontName', 'Cordia New', 'FontWeight', 'bold')

subplot(2, 2, 4)
plot(C3_1(1:k3),C3_2(1:k3),'b.','MarkerSize',1)
xlabel('x', 'FontSize', 16, 'FontName', 'Cordia New', 'FontWeight', 'bold')
ylabel('y', 'FontSize', 16, 'FontName', 'Cordia New', 'FontWeight', 'bold')

function F = ODE(t, f)
    global a b
    x = f(1);
    y = f(2);
    z = f(3);
```

```
F = zeros(size(f));
F(1) = -y-z;
F(2) = x+a*y;
F(3) = -z+b*exp(x);
```

3. Matlab code for Power spectrum

```
function PowerSpectrum_3
    Fs = 1e3;
    t  = 0: 1/Fs: 500;
    y0 = [1.6; -1; 0.09];
global a
    a = 20;

    [t, y] = ode45(@run_Attractors, t, y0);
    f = y(50000:length(y),:);

    PS1 = (abs(fft(f(:,1)))/length(f(:,1))).^2;
    Hmss1 = dspdata.msspectrum(PS1, 'Fs', Fs);
    subplot(2, 2, 2)
    plot(Hmss1);
    ylabel('Power x (dB)', 'FontSize', 16, 'FontName', 'Cordia New', 'FontWeight',
    'bold');
    xlabel('Frequency (Hz)', 'FontSize', 16, 'FontName', 'Cordia New', 'FontWeight',
    'bold');

    PS2 = (abs(fft(f(:,2)))/length(f(:,2))).^2;
    Hmss2 = dspdata.msspectrum(PS2, 'Fs', Fs);
    subplot(2, 2, 3)
    plot(Hmss2);
    ylabel('Power y (dB)', 'FontSize', 16, 'FontName', 'Cordia New', 'FontWeight',
    'bold');
    xlabel('Frequency (Hz)', 'FontSize', 16, 'FontName', 'Cordia New', 'FontWeight',
    'bold');
```

```
PS3 = (abs(fft(f(:,3)))/length(f(:,3))).^2;
Hmss3 = dspdata.msspectrum(PS3, 'Fs', Fs);
subplot(2, 2, 4)
plot(Hmss3);
ylabel('Power z (dB)', 'FontSize', 16, 'FontName', 'Cordia New', 'FontWeight',
'bold');
xlabel('Frequency (Hz)', 'FontSize', 16, 'FontName', 'Cordia New', 'FontWeight',
'bold');

function F = run_Attractors(t, f)
    global a b
    x = f(1);
    y = f(2);
    z = f(3);
    F = zeros(size(f));
    F(1) = -y-z;
    F(2) = x+a*y;
    F(3) = -z+b*exp(x);
```

4. Matlab code for Attractor

```
function Attractors_3
    Fs = 1e3;
    t  = 0: 1/Fs: 500;
    y0 = [1.6; -1; 0.09];
global a
    a = 20;

    [t, y] = ode45(@run_Attractors, t, y0);
    f = y(50000:length(y),:);

    subplot(2, 2, 1)
    plot3(f(:,1), f(:,2), f(:,3));
```

```
xlabel('x', 'FontSize', 16, 'FontName', 'Cordia New', 'FontWeight', 'bold')
ylabel('y', 'FontSize', 16, 'FontName', 'Cordia New', 'FontWeight', 'bold')
zlabel('z', 'FontSize', 16, 'FontName', 'Cordia New', 'FontWeight', 'bold')

subplot(2, 2, 2)
plot(f(:,1), f(:,2));
xlabel('x', 'FontSize', 16, 'FontName', 'Cordia New', 'FontWeight', 'bold')
ylabel('y', 'FontSize', 16, 'FontName', 'Cordia New', 'FontWeight', 'bold')

subplot(2, 2, 3)
plot(f(:,1), f(:,3));
xlabel('x', 'FontSize', 16, 'FontName', 'Cordia New', 'FontWeight', 'bold')
ylabel('z', 'FontSize', 16, 'FontName', 'Cordia New', 'FontWeight', 'bold')

subplot(2, 2, 4)
plot(f(:,2), f(:,3));
xlabel('y', 'FontSize', 16, 'FontName', 'Cordia New', 'FontWeight', 'bold')
ylabel('z', 'FontSize', 16, 'FontName', 'Cordia New', 'FontWeight', 'bold')

function F = run_Attractors(t, f)
global a b
    x = f(1);
    y = f(2);
    z = f(3);
    F = zeros(size(f));
    F(1) = y-z;
    F(2) = x+a*y;
    F(3) = -z+b*exp(x);
```

5. Matlab code for Time Domain

```
function TimeDomainSignals_3
        Fs = 1e3;
        t  = 0: 1/Fs: 500;
        y0 = [1.6; -1; 0.09];
global a b
        a = 20;

        [t, y] = ode45(@run_Attractors, t, y0);
        f = y(50000:length(y),:);

        subplot(2, 2, 1)
        plot(t, y(:,1), t, y(:,2), t, y(:,3));
        xlabel('Time (s)', 'FontSize', 16, 'FontName', 'Cordia New', 'FontWeight', 'bold');
        ylabel('(V)', 'FontSize', 16, 'FontName', 'Cordia New', 'FontWeight', 'bold');

        subplot(2, 2, 2)
        plot(t, y(:,1));
        xlabel('Time (s)', 'FontSize', 16, 'FontName', 'Cordia New', 'FontWeight', 'bold');
        ylabel('x (V)', 'FontSize', 16, 'FontName', 'Cordia New', 'FontWeight', 'bold');

        subplot(2, 2, 3)
        plot(t, y(:,2));
        xlabel('Time (s)', 'FontSize', 16, 'FontName', 'Cordia New', 'FontWeight', 'bold');
        ylabel('y (V)', 'FontSize', 16, 'FontName', 'Cordia New', 'FontWeight', 'bold');

        subplot(2, 2, 4)
        plot(t, y(:,3));
        xlabel('Time (s)', 'FontSize', 16, 'FontName', 'Cordia New', 'FontWeight', 'bold');
        ylabel('z (V)', 'FontSize', 16, 'FontName', 'Cordia New', 'FontWeight', 'bold');

function F = run_Attractors(t, f)
```

```
global a b
    x = f(1);
    y = f(2);
    z = f(3);
    F = zeros(size(f));
    F(1) = -y-z;
    F(2) = x+a*y;
    F(3) = -z+b*exp(x);
```